Nonlinear Dynamics of Semiconductor Lasers: Control and Synchronization of Chaos

Rajesh S.

International School of Photonics
Cochin University of Science and Technology
Kochi
682 022, India

Thesis submitted to Cochin University of Science and Technology in partial fulfillment of the requirements for the award of the Degree of
Doctor of Philosophy

January 2005

Nonlinear Dynamics of Semiconductor Lasers:
Control and Synchronization of Chaos

Ph D Thesis in the field of Nonlinear Dynamics

Author:

Rajesh S.

Research Fellow

International School of Photonics,

Cochin University of Science and Technology,

Kochi, 682022, India

E-mail: rajeshsivan@gmail.com

Research Advisor:

Dr. V. M. Nandakumaran

Professor

International School of Photonics,

Cochin University of Science and Technology,

Kochi, 682022, India

E-mail: nandak@cusat.ac.in

International School of Photonics,

Cochin University of Science and Technology,

Kochi, 682022, India

www.photonics.cusat.edu

January 2005

To My Parents

CERTIFICATE

Certified that the research work presented in the thesis entitled "***Nonlinear Dynamics of Semiconductor Lasers: Control and Synchronization of Chaos***" is based on the original work done by Mr. Rajesh S. under my guidance in the International School of Photonics, Cochin University of Science and Technology, Kochi 682 022 and has not been included in any other thesis submitted previously for the award of any degree.

Kochi
27 January, 2005

Dr. V. M. Nandakumaran
(Supervising Guide)
International School of Photonics
CUSAT

DECLARATION

Certified that the work presented in the thesis entitled "***Nonlinear Dynamics of Semiconductor Lasers: Control and Synchronization of Chaos***" is based on the original work done by me under the guidance and supervision of Dr. V. M. Nandakumaran, Professor, International School of Photonics, Cochin University of Science and Technology, Kochi 682 022, India and has not been included in any other thesis submitted previously for the award of any degree.

Kochi

27 January, 2005 **Rajesh S.**

Acknowledgements

The first person I would like to thank is my supervising guide Prof. V. M. Nandakumaran. I am greatly indebted to him for his valuable guidance and suggestions for proper orientation and successful completion of this work.

I am greatful to Dr. P. Radhakrishnan, Professor and Director, International School of Photonics, Dr. C. P. Girijavallabhan, (Emeritus Professor, ISP and Director CELOS) and Dr. V. P. N. Nampoori (Professor, ISP), and Mr. M. Kailasnath (Lecturer, ISP) for their full hearted co-operation, support and valuable suggestions during the course of my work.

I would like to express my heartfelt thanks to Dr. A. Deepthy (Young Scientist Fellow) for her kind words, support and thoughtfulness that helped me very much.

I owe a lot to Prof. K. P. Rajappan Nair, Prof. K. Babu Joseph, Prof. M. Sabir, Dr. M. R. Anantharaman and Dr. T. Ramesh Babu of the department of physics for their encouragement and valuable suggestions which helped me very much in my career .

The discussions I had with Prof. Jurgen Kurths (University of Potsdam, Germany) was a great help for the timely completion of this work. I am truly grateful to him.

I owe very much to Manu, Vinu and Jijo for all the support and helps that they provided during my research work. I would not have finished my work in this time without their support. I also appreciate Abraham V. Scaria who encouraged me very much and helped me a lot. The joyful days that I spent with these people are really unforgettable in my life. I would like to express my deep sense of gratitude to them.

Thanks, my class mates, Thomas Lee, Pravitha and Robin Francis for helping me in whatever ways they can. The heated discussions and funny moments I had with them are really unforgettable.

I am greatly thankful to Rajesh M for timely helps and support that I received from him during the course of my research work.

Thanks, Radhakrishnan and Chithra, my friends in department of physics who did great helps in completing this thesis.

I am thankful to all my friends in ISP, Pramod, K. P. Unnikrishnan, Binoy, Jibu Kumar, Suresh Kumar, Jayashree, Achamma Kurien, Sajan D. George, Santhi, Rekha, Sr. Ritty, Bindu V, Bindhu Krishnan, Geetha, Dilna, Sreeja, Aneesh, Prasanth, Saritha, Dann, Lyjo,

Litty, Thomas, Sheeba, Hrebesh, Anwar, Ambika and K. T. Unnikrishnan for their helps and support throughout the period of my work.

Finally, I would like to express my sincere thanks to my loving parents and my dearest sister for their constant encouragement, selfless support and patience which are the major factors behind the successful completion of my work. It is difficult to express my gratitude to my father who always encouraged my interest in science and my quest to study.

Rajesh S.

Preface

Nonlinear dynamics of laser systems has become an interesting area of research in recent times. Lasers are good examples of nonlinear dissipative systems showing many kinds of nonlinear phenomena such as chaos, multistability and quasiperiodicity. The study of these phenomena in lasers has fundamental scientific importance since the investigations on these effects reveal many interesting features of nonlinear effects in practical systems. Further, the understanding of the instabilities in lasers is helpful in detecting and controlling such effects.

Chaos is one of the most interesting phenomena shown by nonlinear deterministic systems. It is found that, like many nonlinear dissipative systems, lasers also show chaos for certain ranges of parameters. Many investigations on laser chaos have been done in the last two decades. The earlier studies in this field were concentrated on the dynamical aspects of laser chaos. However, recent developments in this area mainly belong to the control and synchronization of chaos. A number of attempts have been reported in controlling or suppressing chaos in lasers since lasers are the practical systems aimed to operated in stable or periodic mode. On the other hand, laser chaos has been found to be applicable in high speed secure communication based on synchronization of chaos. Thus, chaos in laser systems has technological importance also.

Semiconductor lasers are most applicable in the fields of optical communications among various kinds of laser due to many reasons such as their compactness, reliability modest cost and the opportunity of direct current modulation. They show chaos and other instabilities under various physical conditions such as direct modulation and optical or optoelectronic feedback. It is desirable for semiconductor lasers to have stable and regular operation. Thus, the understanding of chaos and other instabilities in semiconductor lasers and their

control is highly important in photonics.

We address the problem of controlling chaos produced by direct modulation of laser diodes. We consider the delay feedback control methods for this purpose and study their performance using numerical simulation. Besides the control of chaos, control of other nonlinear effects such as quasiperiodicity and bistability using delay feedback methods are also investigated.

A number of secure communication schemes based on synchronization of chaos semiconductor lasers have been successfully demonstrated theoretically and experimentally. The current investigations in these field include the study of practical issues on the implementations of such encryption schemes. We theoretically study the issues such as channel delay, phase mismatch and frequency detuning on the synchronization of chaos in directly modulated laser diodes. It would be helpful for designing and implementing chaotic encryption schemes using synchronization of chaos in modulated semiconductor lasers.

The thesis consists of seven chapters. The content of each chapter is described briefly as follows.

Chapter 1 is an introductory chapter, which describes the basic concepts of nonlinear dynamics and chaos. A short description of the development of chaos theory is given. The fundamental properties and necessary conditions for the existence of chaos are described and chaotic behavior of discrete and continuous dynamical systems is illustrated for the logistic map and the Lorenz system respectively. The main routes to chaos are also discussed. The necessary computational tools used in numerical studies of chaotic system are presented. A brief outline of laser chaos is also presented. The concepts of control and synchronization of chaos are also given.

Chapter 2 is a review on the chaotic behavior in directly modulated semiconductor lasers, reported in the last two decades. Two different types of laser diodes are considered, i.e. the InGaAsP lasers and the self pulsating laser diodes. The transitions from periodicity to chaos are illustrated with numerical simulation. The periodic, quasiperiodic and chaotic behaviours are characterized using the computational tools such as time series plots, phase portraits, Poincare section, bifurcation diagrams and power spectra. In addition to chaos, the phenomena like formation of double peaked pulses and bistability are also discussed.

Chapter 3 describes the application of delayed optoelectronic feedback for controlling

chaos in directly modulated InGaAsP laser diodes. Such lasers are most important in optical fibre communications. The effect of two different delay feedbacks have been studied, the self adjusting delayed optoelectronic feedback based on Pyragas method and a direct delayed optoelectronic feedback. The performance of these methods is compared using numerical simulations. The chaotic and periodic states are characterized using time series plots, phase portraits and power spectra .

Chapter 4 contains the results of the numerical studies on the effect of delayed optoelectronic feedback in directly modulated self pulsating AlGaAs semiconductor lasers. As done in the case of modulated InGaAsP lasers, the effect of two different delayed optoelectronic feedback schemes (self adjusting feedback and direct feedback) are considered. In addition to the control of chaos, control of quasiperiodicity is also investigated. The periodic, quasiperiodic and chaotic states are studied using Poincare sections, time series plots, phase portraits and power spectra.

Chapter 5 deals with the control of bistability in directly modulated semiconductor lasers using delay feedback techniques. The suppression of hysterisis and bistability is numerically demonstrated using the bifurcation diagrams drawn by the method of continuous-time simulation. The area of the hysteresis loops with the change of delay and feedback strength is calculated for a wide range of delay and feedback strength and the possible regimes of suppression of hysteresis and bistability are globally classified. Variation of the area of hysteresis loop with the increase of feedback strength is presented. The significance of feedback delay time in the suppression of bistability is also discussed

Chapter 6 presents the results of the theoretical investigations on the effects of phase mismatches, delay and frequency detuning on synchronization of chaos in directly modulated self pulsating laser diodes and nonlinear oscillators. Synchronization of chaos in two unidirectionally coupled remote directly modulated self pulsating semiconductor lasers is considered. Synchronization of such lasers has been shown to be useful in chaotic secure communications. The initial phase difference of the modulating signals and the delay produced by the light signal through the optical fiber channel are incorporated in the model describing the coupled laser system. The loss of synchronization due to these effects is demonstrated. The extent of synchronization is quantitatively studied using the similarity function. A general coupled non autonomous system with channel delay and detuning

were considered and analytically verified these results. The results are further illustrated numerically with coupled Duffing oscillator- a very familiar system.

Chapter 7 summarizes the results obtained. A brief discussion on the possible future works in the area of nonlinear dynamics of semiconductor lasers are also discussed in this chapter.

List of Publications

- **S Rajesh** and V M Nandakumaran ***Suppression of chaos in a directly modulated semiconductor laser with delayed optoelectronic feedback***, Phys. Lett. A **319** (2003) 340-347
- **S Rajesh** and V M Nandakumaran ***Effects of channel delay and frequency detuning in synchronization of chaos in two unidirectionally coupled driven nonlinear oscillators***, communicated.
- **S Rajesh** and V M Nandakumaran , ***Stabilization of Quasiperiodic and Chaotic Pulses from a Directly Modulated Self Pulsating Semiconductor Laser***, Proc. of Photonics-2004, International Conference on Fiber optics and Photonics, Cochin, December 2004
- **S Rajesh** and V M Nandakumaran ***Synchronization of chaos in unidirectionally coupled modulated self pulsating semiconductor lasers: effects of delay and detuning***, Proc. of the international conference, Perspectives in Nonlinear Dynamics (PNLD 2004), IIT Madras Chennai, July 2004
- **S Rajesh** and V M Nandakumaran ***Control of chaos in directly modulated semiconductor lasers***, Proc.of Photonics-2002, International Conference on Fiber optics and Photonics, Tata Institute of Fundamental Reasearch, Bombay, December 2002
- **S Rajesh** and V M Nandakumaran, ***Quasiperiodicity and chaos in directly modulated semiconductor lasers***, Proc.of National Laser Symposium (NLS 2002), Sree Chitra Thirunal Institute of Medical Science, December, 2002
- V M Nandakumaran and **S Rajesh**, ***Synchronization of non autonomous systems: effects of delay and detuning***, Proc. of the international conference, Perspectives in Nonlinear Dynamics (PNLD 2004), IIT Madras Chennai, July 2004
- P U Jijo, M P John, **S Rajesh**, and V M Nandakumaran, ***Control of chaos and noise induced instabilities in Duffing oscillator with amplitude modulated feedback***, Proc. of the international conference, Perspectives in Nonlinear Dynamics (PNLD 2004), IIT Madras Chennai, July 2004

Table of Contents

Chapter 1

Introduction

Nonlinear dynamics is one of the branches of science in which extensive research activities have been done in the last few decades [1]. Basically, this is an interdisciplinary area of science, which deals with the study of the systems described by nonlinear mathematical equations. Since most of the natural and engineering systems are nonlinear, the study of nonlinear dynamics has fundamental importance in science and technology. Nonlinear systems show a rich variety of phenomena such as self sustained oscillations [2], multistability [2, 4, 5], quasiperiodicity [6], pattern formation [7] and chaos [8]. A proper understanding of such effects is helpful in their control in technology, where such effects may cause unwanted results. On the other hand, the nonlinearities have been found sometimes to be applicable in technology and they can be applied for practical purposes such as chaotic cryptography [15] and soliton-based optical communications [10].

1.1 Chaos: The fundamental concepts

Chaos is one of the most widely discussed and fascinating phenomena in nonlinear dynamics. Literally, the word 'chaos' means the total disorder or utter confusion. However, in nonlinear dynamics, it has a different meaning. The unpredictable and complex evolution of deterministic systems is commonly referred to as chaos. The randomness associated with a chaotic system comes from the intrinsic dynamics of the system and it is entirely different from the randomness one encounters in systems with the stochastic external forces. The fundamental characteristic of a chaotic system is its extreme sensitivity to the initial conditions, i.e., the phase space trajectories started with slightly different initial conditions will diverge exponentially and they will become totally uncorrelated after a finite time. Thus a very small variation in the initial condition produces an infinitely large effect on the long term behavior of the system. For the same reason, the long term prediction of a chaotic

system is practically impossible.

The first numerical evidence of chaos was given by Edward Lorenz in 1963 [11]. He observed certain non repeating solutions while simulating a truncated version of atmospheric convection. However, the history of chaos theory starts from the time of the renowned French mathematician Henry Poincaré. There was a belief that the complete evolution of a physical system can be predicted if its dynamical equations and the corresponding initial conditions are given. However, no physical quantity can be measured with infinite precision and there will be certain amount of error associated with each dynamical variable. The predictability of the dynamical system definitely depends on the evolution of this error in computations. Poincaré pointed out that, the errors will grow exponentially in certain nonlinear systems and hence the long term prediction of such system becomes practically impossible. This issue is currently known as the sensitive dependence on initial conditions and it is the fundamental property of chaotic systems. Even though Poincaré had predicted the possibility of chaotic solutions, it has taken a long time for the discovery of chaos in many of the physical systems. One of the reasons for this delay was the lack of sophisticated computational systems. After Lorenz' discovery of chaos in the convection model, chaos has been observed in many nonlinear systems such as lasers [31], population models [13] and electronic circuits [14] . The realm of chaos has now been extended to the diverse branches of science such as chemistry [15] and biology [16]. The field of applications of chaos theory include the study of turbulence [17], pattern formation [18], secure communication [19], EEG data analysis [20, 21] and the study of ECG signals of arrhythmic heart [22].

A remarkable development of chaos theory is the universality of chaotic systems established by Feigenbaum [21]. He showed that there are certain universal constants associated with the transitions of the systems to chaos irrespective of the details of the systems. Further, there are certain universal categories of chaotic systems and most of the fundamental characteristics of the chaotic systems belonging to each category does not vary within them.

Chaos is common even in very simple deterministic systems. Very simple dynamical models of nonlinear systems have been found to behave chaotically. For a continuous dynamical system, the necessary number of degree of freedom for observing chaos is 3 or more. If it is a non-invertible discrete mapping (a dynamical system represented by discrete-time difference equations), there is no such restriction. For example, one dimensional maps such as logistic map and tent map are known to exhibit chaotic evolutions. The mechanism behind the complex nature of chaotic trajectories is the so-called stretching and folding of the trajectories in the phase space. The trajectories may experience stretching and folding in different directions and the exponential sensitivity is an outcome of these effects. The

sensitive dependence on initial conditions is quantitatively described by the logarithmic average of divergence of the trajectories which are commonly known as Lyapunov exponents. There are N Lyapunov exponents associated with an N-dimensional deterministic system. A system is said to be chaotic if at least one of these exponents is positive.

Both the conservative and dissipative physical systems show chaos under various conditions. Hamiltonian systems are certain conservative systems, the dynamical behavior of which can be completely described by the so-called Hamiltonian function [24]. Kolmogorov Arnold Moser (KAM) theorem is known to be a paradigm for Hamiltonian chaos [25]. Plasma physics [26], mixing of fluids [27] and celestial mechanics [28] are some of the fields wherein the concepts of Hamiltonian Chaos can be applied. The fundamental issues in physics such as ergodicity have been discussed within the framework of Hamiltonian chaos [29]. Most of the natural and engineering systems are dissipative. The phase space trajectories of the dissipative systems asymptotically approaches some limit sets called attractors. The attractors associated with chaotic systems have non-integer dimensions and they are known as strange attractors. It should be noted that the Hamiltonian chaotic systems do not have attractors because of the phase-volume preservation.

1.2 Necessary computational tools

Dynamical aspects of the nonlinear systems are usually investigated with a number of numerical techniques. In this section, we give a brief account of the computational techniques which are used for characterizing different dynamical states of semiconductor lasers and the nonlinear oscillators.

1.2.1 Poincaré section

Poincaré section is a method used to construct a discrete mapping of a deterministic dynamical system that is originally described by a system of nonlinear differential equations [24]. For example consider a three dimensional flow described by a system of autonomous differential equations. We consider a two dimensional surface in the three dimensional phase space and mark every crossing of the trajectories in the same direction. The points obtained by this method constitute the Poincaré section. Since the system is deterministic, there will be certain definite relation (mapping) between the points obtained by two successive crossings i.e, $P_{n+1} = f(P_n)$, where f is a nonlinear function. Hence the three dimensional flow is reduced to a two dimensional map. Fig.1.1 shows the construction of Poincaré section for a three dimensional flow. Similarly, for obtaining the Poincaré section of an N dimensional continuous dynamical system we should take the crossings of the trajectories on an $N-1$

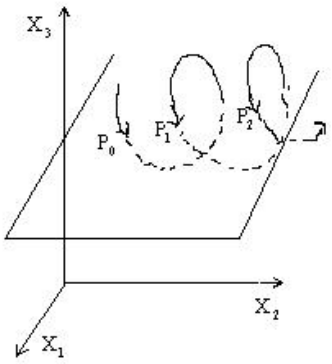

Figure 1.1: Poinacaré section

dimensional hyperplane of the N-dimensional phase space. The dimensionality reduction is an additional advantage since it is very difficult to visualize the attractors in higher dimensions. The dimension of the attractor can further be reduced by taking first return map $(X_{n+1}\, vs\, X_n)$ of just one variable of the section obtained. This type of maps can be used in bifurcation diagrams.

1.2.2 Bifurcation diagrams

Bifurcation is the event in which the qualitative properties of attractor of a dynamical system is changed as a control parameter of the system is varied. In the bifurcation phenomena, attractor may appear, disappear or an attractor is replaced by another one. Bifurcation diagrams helps us to visualize these transitions. They are the plot of the attractor points versus the control parameter. Period doubling in logistic map is a good example for bifurcations [8]. In each period doubling of the map, a period n orbit becomes unstable and a stable period $n+1$ orbit appears. After an infinite number of period doublings, the map becomes chaotic. Actually a number of continuous and discrete systems follow the period doubling route to chaos. For plotting the bifurcation of continuous dynamical systems, a set of values of a single variable representing the attractor must be obtained. This is usually done by the return map obtained from the Poincaré section [21]. There is another method for obtaining discrete mappings from the flows. Lorenz has constructed a one dimensional

map from the three dimensional flow (X, Y, Z) by taking consecutive maxima of the single variable Z [11]. Such methods also can be used for plotting bifurcation diagrams.

1.2.3 Power spectrum

Fourier techniques are commonly used in nonlinear dynamics for characterizing periodic, quasiperiodic and chaotic states of a system. Fourier spectra give the power distribution of the observed signal as a function of frequencies. Consider a signal $y(t)$ which has N discrete values sampled at intervals of Δt. The discrete fourier transform of this signal is

$$Y(f_k) = \sum_{l=0}^{N-1} y(t_l) e^{-2\pi i l k/N}, k = 0, 1..N-1, i = \sqrt{-1}, \tag{1.2.1}$$

where the discrete frequency components are given by

$$f_k \; = \; k/(N\Delta t) \tag{1.2.2}$$

and the coefficients

$$t_l = l\Delta t \tag{1.2.3}$$

The separation Δt of sampled points determines the maximum frequency component of $y(t)$ and the total time span $N\Delta t$ determines the minimum frequency. The squares of the Fourier coefficients given in the Eq. (1.2.1) is referred to as power spectrum.

Fast Fourier Transform (FFT) is a convenient algorithm for obtaining the power spectrum of a time series[33]. In this method, the number of numerical calculation are considerably reduced using the recurrence properties of the fourier series.

The expression given in Eq.(1.2.1) can be written as

$$Y_k = \sum_{l=0}^{N-1} y_l W^{kl}, \tag{1.2.4}$$

where, $W = e^{-2\pi i l k/N}$

There exist certain simple relations between the terms appearing in the series represented by Eq.(1.2.4) and hence the total number of steps needed for calculating power spectra reduces significantly. (For instance, suppose we have a time series of 8 samples, we require all the terms from W^0 to W^{49}. However the number of terms can be conveniently reduced to eight W's from W^0 to W^7. Further more, $W^7 = -W^3$, $W^6 = -W^2$, $W^5 = -W^1$ and $W^4 = -W^0$.) The FFT algorithm utilize this opportunity to complete the computation of power spectra with in a relatively short time.

The power spectrum of a time series gives us the information about its periodicity. If the system is periodic, the spectrum is peaked at a single point and at its higher harmonics. If it is quasi periodic, the peaks will be at all linear combinations of two (or three) fundamental incommensurate frequencies. If the system is chaotic, we will get broadband power spectra.

1.2.4 Lyapunov exponents

Lyapunov exponents are the widely accepted tools for characterizing chaotic and periodic states of a system. They quantify the exponential divergence of phase space trajectories of the systems which is the fundamental property of chaotic system by definition. Lyapunov exponents can also be used for determining the stability of periodic orbits of a dynamical system. In this section, we discuss briefly the definition and computational aspects of the Lyapunov exponents of the continuous and discrete dynamical systems.

Consider a continuous system represented by the following nonlinear differential equation

$$\frac{d\mathbf{X}(t)}{dt} = F(\mathbf{X}(t)),\ \mathbf{X} \in \mathbf{R^N}, \tag{1.2.5}$$

where $\mathbf{F}(X(t))$ is a nonlinear function of the vector $\mathbf{X}(t)$ representing the state variables, given by

$$\mathbf{X}(t) = \begin{pmatrix} X_1 \\ X_2 \\ . \\ . \\ X_N \end{pmatrix} \tag{1.2.6}$$

Assume that a solution $\mathbf{X}(t)$ of the equations exists for a particular initial condition $\mathbf{X}(0)$. This solution can be obtained using numerical integration of the above system of differential equations. Consider another trajectory starting from a slightly different point $\mathbf{X}(0) + \delta\mathbf{X}(0)$. Let $\delta\mathbf{X}(t)$ be the vector representing the separation between the trajectories after a time t.

Lyapunov exponent of the system (corresponding to these initial conditions) is defined as [8]

$$\lambda(\mathbf{X}(0), \delta\mathbf{X}(0)) = \lim_{t\to\infty} \frac{1}{t} log \frac{||\delta\mathbf{X}(t)||}{||\delta\mathbf{X}(0)||} \tag{1.2.7}$$

The Lyapunov exponent defined by Eq.1.2.7 depends on the initial values $\mathbf{X}(0)$ and $\delta\mathbf{X}(0)$ and hence it is no longer an invariant measure of the attractor of the system. Totally,

there are N Lyapunov exponents for an N dimensional system and they are independent of the initial conditions chosen for calculations. Secondly, the long term integration of the trajectories does not assure the smallness of separation vectors. In order to overcome these issues, the calculation of Lyapunov exponents are usually done using a different technique where a reference trajectory is obtained by the integration of nonlinear equations and the evolution of small deviations from this trajectory (separation vectors) is determined by integrating a set of linearized equations of the corresponding nonlinear equations. The vectors are normalized frequently using the Gram Schmidt Orthoginolization (GSR) procedure. The eigen values obtained by this process are averaged throughout the attractor in order to find the Lyapunov exponents. The Wolf's algorithm is one of the commonly used scheme for calculating the complete set of Lyapunov exponents of a system [34]. To find the Lyapunov exponents of a system described by the delay differential equations (Eg.,Laser with delayed feedback), the Farmer's algorithm can be used [35]. In this algorithm, the infinite dimensional delay differential equations are approximated to finite dimensional maps for the convenience of computation.

1.3 Simple examples of chaotic systems

We illustrate the general characteristics of chaotic systems using two well known dynamical systems. The former is the logistic map, which is a discrete system derived from a model of insect population. The latter is the Lorenz system, which is a continuous model obtained by the Raleigh Benard thermal convection model. Even though these models are represented by very simple and deterministic mathematical equations, their solutions are very complex and unpredictable for certain regimes of parameters.

1.3.1 Logistic map

Logistic map is a simple mathematical model proposed by R. M. May for studying the yearly variations in population of an insect species living with limited resources [13]. The map is given by

$$X_{n+1} = f(X_n), \tag{1.3.1}$$

where X_n represents the normalized population of insects in the n^{th} generation and the nonlinear function $f(X) = \lambda X(1 - X)$. λ is the control parameter depends on the reproduction rate of insects. The above function can be represented graphically by a parabola as shown in Fig.1.2 ($\lambda = 4$). The domain of the map is the interval [0,1].

The dynamical behavior of the map depends on the control parameter λ which can be varied from 0 to 4. For $\lambda > 4$ the values in the interval $[0, 1]$ are not mapped into itself. Let

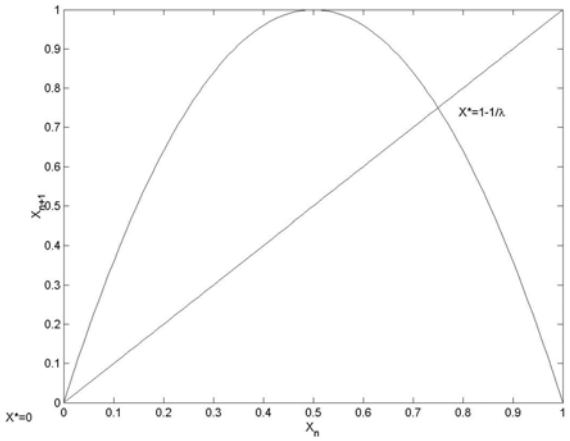

Figure 1.2: Logistic map

us consider the fixed points of the map and their stability. A point X^* is said to be a fixed point of the map if it satisfy the condition

$$f(X^*) = X^* \tag{1.3.2}$$

Since the function is quadratic, there will be two fixed points for the map.

The first fixed point is

$$X^* = 0 \tag{1.3.3}$$

and the second one is,

$$X^* = 1 - 1/\lambda \tag{1.3.4}$$

The map shows a sequence of period doubling bifurcations when the control parameter λ is varied from 0 to 4. For all the value of $\lambda < 1$, the fixed point at 0 is stable and attracting the trajectories originating from the domain of the map. If λ is increased beyond 1, the attractor at 0 becomes unstable and the other fixed pint becomes stable. This fixed point becomes unstable at the value $\lambda = 3$ and a stable period 2 cycle is formed. This is the first period doubling bifurcation of the map. On increasing λ further, a sequence of period doubling bifurcations take place and finally the map becomes chaotic for a limiting value $\lambda = \lambda_\infty = 3.57....$ The bifurcation diagram of the logistic map is shown in Fig.1.3. The parameter regime ranging from λ_∞ to 4 is mainly chaotic domain where certain periodic windows are also present.

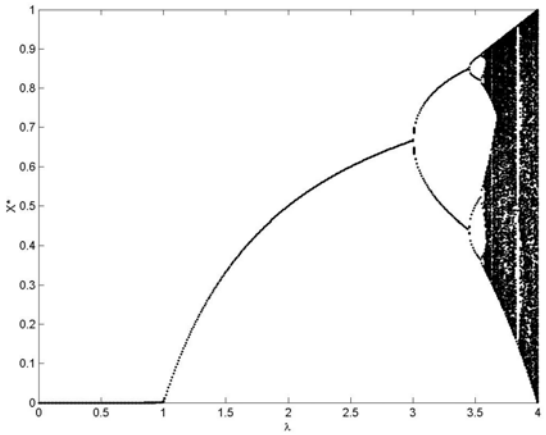

Figure 1.3: Bifurcation diagram of the logistic map

Feigenbaum has shown that there exist certain universal constants associated with the bifurcation phenomena [21]. It has been found that these constants apply not only to the logistic map, but to many of the chaotic systems following a period doubling route [8].

1.4 Lorenz system: A typical chaotic flow

Lorenz model is a well known example for continuous dissipative dynamical system showing chaos. The model was derived by E. N. Lorenz in 1963 [11]. It is a highly simplified model of Raleigh - Benard convection [36]. The original model considers the convection of a fluid contained between two rigid plates placed horizontally and kept with a temperature difference in between them. The importance of the Lorenz model was not in quantitatively describing the convection, but it illustrates how a simple deterministic model can show a rich variety of complex phenomena depending on the values of parameters. The model is described by a system of three nonlinear differential equations, which is a truncated version of Navier-Stokes equations

$$\begin{aligned} \frac{dX}{dt} &= -\sigma(X-Y) \\ \frac{dY}{dt} &= -XZ + rX - Y \\ \frac{dZ}{dt} &= XY - bZ, \end{aligned} \tag{1.4.1}$$

where σ, r and b are dimensionless parameters. The variable X is a quantity proportional to the circulatory fluid flow velocity, Y represents the temperature difference and Z is the deviation of the vertical temperature profile from linearity. Lorenz numerically studied the case for $\sigma = 10$, $b = 8/3$ and $r = 28$. The system has two fixed points where $\frac{dX}{dt} = \frac{dY}{dt} = \frac{dZ}{dt} = 0$. For the parameters specified above, these fixed points are unstable. The trajectories near to a fixed point spirals outward then switches to spiraling outward from the other fixed point. The projection of Lorenz attractor in the $Y - Z$ plane is shown in Fig.1.4(a). The patterns repeat forever and the jump from one wing to other is in an erratic manner. Lorenz obtained a sequence m_n by giving the n_{th} maxima of the variable $Z(t)$ and plotted m_{n+1} versus m_n. The plot is shown in Fig.1.4(b). It is an approximate one-dimensional map and resembles the tent map. The magnitude of the slope of the plot is always greater than unity indicating that all the points are unstable similar to the case of tent map.

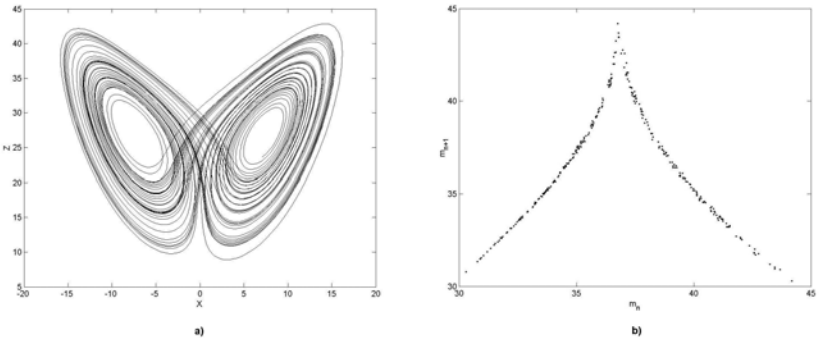

Figure 1.4: Lorenz attractor: (a) projection in the $X - Z$ plane (b) return map obtained from the maxima of $Z(t)$

1.5 Attractors and dimensions

Attractors are the limit sets of points to which the phase space trajectories of different dynamical systems converge asymptotically. These attractors are usually characterized by their dimensions. The important dimensions are the capacity dimension, information dimension and the correlation dimension. The capacity dimension or the fractal dimension is related to the scaling properties of the attractor [37]. The information dimension quantify the extra information required to specify an initial condition on the attractor [38]. The

correlation dimension[39] is useful for describing the local inhomogeneity of the attractor i.e., the small scale variations of density of fractal objects over small scales.

A fixed point is considered as a zero dimensional attractor. The dimension of the periodic limit cycles is 1. A bi-periodic torus is the attractor of a two-frequency quasiperiodic system and it is having a dimension 2. The attractors having non-integer dimensions are called strange attractors and they are often associated with the chaotic states.

1.6 Different routes to chaos

In section 1.3, we have discussed about the period doubling route to chaos. Besides the logistic map many dissipative systems follow the period doubling scenario[14, 31]. For a continuous dissipative system, usually there will be a stable fixed point (dimension 0) which bifurcates in to a limit cycle (dimension 1) when varying the control parameter. This process is called a Hopf bifurcation [40]. This period 1 cycle then bifurcates into a period 2 cycle. This period doubling process continues as the control parameter is again varied and the system finally reaches at a chaotic state. The other important route is the quasi periodic route to chaos [41]. The Hopf bifurcation is followed by a transition of singly periodic limit cycle into a doubly periodic torus (dimension 2) and this torus bifurcates into a chaotic attractor having fractal dimension. In certain systems, the three frequency quasi periodicity route has also been reported [42]. The third route is the intermittency route which has no relevance to our work and it is not discussed here. A schematic description of period doubling and quasi periodic routes are given in the Fig.1.5.

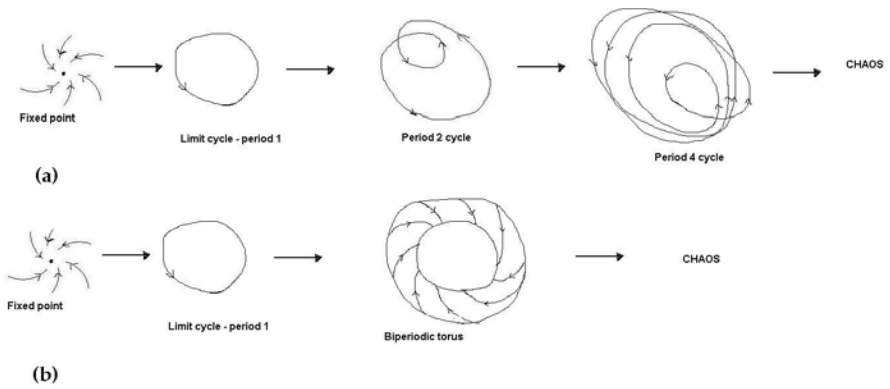

Figure 1.5: Two main routes to chaos: (a) period doubling route (b) quasiperiodicity route

1.7 Chaos in laser systems

Lasers are good examples of nonlinear systems which show many complex phenomena. Actually, lasers are the earlier experimental systems wherein chaos has been observed. Haken [43] formulated Lorenz like model of lasers by applying the Rotating Wave Approximation (RWA) and the Slowly Varying Envelope Approaximation (SVEPA) to Laser equations. However the first experimental observation of chaos in a quantum - optical molecular system was reported by Arecchi *et. al.* in 1982 [31]. They observed subharmonic bifurcations, chaos and multistability in a Q - Switched CO_2 laser modulated by an electro optical modulator.

Later, chaos has been reported in laser systems such as single mode inhomogeneously broadened xenon laser [44], NdP_5O_{14} tunable laser with modulated pump [45], NH_3 laser [47], Nd:YAG [48] and semiconductor lasers. The chaotic behavior observed in the far infra red NH_3 lasers are good example of Lorenz type chaos in lasers [49].

Chaos and other instabilities in the semiconductor lasers are particularly important since such lasers are widely used in optical communications and optical data processing. Semiconductor lasers show chaos under various physical conditions such as high speed modulation [50, 51, 20, 53], external optical injection [54] and optical or optoelectronic feedback [55, 56]. The feedback systems are usually delay systems and hence infinite dimensional. The high dimensional chaotic attractors shown by the external cavity laser diode have been widely studied [57, 58, 59].

In addition to the fundamental importance in nonlinear dynamics, study of chaotic laser systems have good practical importance. Study of chaotic dynamics in lasers help us to control chaos in laser systems and ensure their stable operation. On the other hand, chaos in lasers has an important application in technology. Synchronization of various types of chaotic laser systems have been successfully used for the optical data encryption. Hence, the study of nonlinear dynamics of lasers is helpful in the generation of chaos also.

1.8 Control of chaos

Since most of the engineering systems are expected to be operated in a steady or stable periodic state, chaos is an unwanted phenomenon in these systems. Hence, a number of methods have been developed for controlling chaos [14]. Most of these schemes are based on the fact that an infinite number of unstable periodic orbits (UPO) are embedded with in the chaotic attractors. These unstable orbits can be stabilized by applying small perturbations to an accessible system-parameter or a state variable. In this section some important

methods those are employed for controlling chaos are briefly discussed.

1.8.1 Unstable periodic orbits

It is well known that an infinite number of unstable periodic orbits (UPO) are embedded within the chaotic attractor. The presence of the UPOs can be easily understood by the bifurcation sequence through which the chaos is developed in the systems [61]. For example, on every period doubling bifurcation, one period n orbit becomes unstable and a stable period $2n$ orbit is formed in the place of them, where n is any integer. The system becomes chaotic through an infinite number of such bifurcations and that much UPOs are formed on the attractor. The presence of UPOs can be determined by time delay reconstruction of a chaotic system [14]. Many characteristic features of the attractors such as fractal dimensions and entropy can be extracted from the UPOs [62].

1.8.2 Ott, Grebogy and Yorke (OGY) method

The first attempt to control chaos by stabilising UPOs was done by Ott, Grebogy and Yorke [6] in 1990. They proposed that the UPOs of a chaotic system can be stabilized by applying small discrete perturbations to an accessible and suitable parameter. The UPOs can be located by time delay reconstruction of the considered system. This is possible even if we don't know the model equations of the system. The second step is to choose the specific periodic orbits to be stabilized. The eigen values of the unstable fixed points in the Poincaré section is determined from the reconstructed time series of the system. The perturbation required to stabilize the particular UPO can be obtained from these eigen values. The major advantage of this control scheme is that no detailed information of the dynamical model of the system is required to implement it. Ditto *et. al.* have successfully applied the OGY method for a magneto elastic ribbon working in chaotic domain [7]. Roy and coworkers used a modified version of OGY method for controlling a chaotic Q-switched Nd YAG laser [15]. Even though it was successful in controlling chaos, it had two main disadvantages; 1) The implementation of the control scheme requires time delay reconstruction of the measured time series and hence computer assistance is needed for OGY method. 2) The controlled systems do not have good tolerance to the presence of noise. The effect of noise causes intermittent bursts in the output. In spite of these difficulties, OGY method attracted a wide attention and was implemented in a number of practical systems.

1.8.3 Targeting

The first targeting algorithm was proposed by Huberman and Lumer [8]. The method is based on an adaptive feedback aimed at bringing the chaotic systems to a desired state. The parameter would be adjusted in such a way that the system gives the required output. The desired state may be one of the periodic orbits or another chaotic state . Ramaswamy, Sinha and Rao have extended the targeting algorithm to multi parameter and higher dimensional systems [9]. They found that if a sudden perturbation is applied to the controlled system, the system will recover the controlled state after a short while and the recovery time is always proportional to the inverse of control stiffness.

1.8.4 Periodic parametric perturbation

It was theoretically shown by Lima and Pettini that a small, periodic perturbation to a parameter of a chaotic system may suppress chaos [10]. They applied a periodic perturbation to the amplitude of the cubic term in the Duffing-Holmes equation describing the chaotic oscillator and found that the regular periodic behavior was achieved by perturbations of small strength. Colet and Braiman have shown that chaos in a multimode solid state laser could be controlled by using periodic parametric perturbations [11].

1.8.5 Delay feedback control

K. Pyragas introduced a control scheme for chaotic systems [26, 27]. It was based on the synchronization of unstable periodic orbits to their past states. For controlling a particular UPO, a continuous feedback is applied to an accessible state variable of the system with a time delay equal to the period of the specific periodic orbit. Consider a chaotic system described by the ordinary differential equations,

$$\dot{\mathbf{X}} = \mathbf{F}(\mathbf{X}) \tag{1.8.1}$$

Where $\mathbf{X} = (X_1, X_2..X_N)^T$ represents the state variables of the N dimensional phase space. Let us assume that a state variable X_k can be measured. For controlling a UPO of period τ, a feedback proportional to the difference between the value of X_k delayed by τ units of time and the current value of X_k is applied to the system.

The modified dynamical equation of the system is given by,

$$\dot{\mathbf{X}} = \mathbf{F}(\mathbf{X}) + C[X_k(t-\tau) - X_k(t)], \tag{1.8.2}$$

where C is the feedback strength. If the control is achieved the feedback term will vanish and the system becomes periodic. The delay feedback control has many advantages

over earlier methods. It does not require any computation since no delay reconstruction is needed for implementing the control. No external signal is required to apply the perturbation. In contrast to the OGY method, the Pyragas method is very much robust to noise. The delay feedback control scheme is currently known as the Time Delay Auto Synchronization (TDAS). It has been successfully applied for controlling chaos in several nonlinear systems such as electronic circuits [72], glow discharge [24], magneto-elastic ribbon [74], and periodically driven yttrium iron garnet film [75]. Recently, Arecchi *et al.* have employed this technique for stabilizing high period orbits in a CO_2 laser [76]. The TDAS scheme also has some limitations. It is difficult to control high period orbits and the period orbits of the attractors with large positive Lyapunov exponents. Multistabilty of controlled orbits is another problem [26]. In spite of these limitations, delay feedback is known to be one of the most efficient and simple methods for controlling chaos.

1.9 Synchronization of chaos

Synchronization of chaos is a novel area of research in nonlinear dynamics which has emerged in 1980s. Chaotic systems are known to show extreme sensitivity to the initial conditions. The phase space trajectories of two identical chaotic systems diverge exponentially and they will become totally uncorrelated after a finite time. Hence it is impossible to construct two independent chaotic systems with the same temporal evolution. However, certain techniques have been developed for synchronizing chaotic systems. Yamada and Fujisaka have shown that two identical chaotic systems are synchronized when they are coupled together by sending information between them [1]. Afraimovich, Verichev and Rabinovich have studied the features of synchronized chaos in detail [2]. In 1990, Pecora and Caroll introduced a new synchronization scheme based on the complete replacement a variable of one of the two identical subsystems (response) by the corresponding variable of the other subsystem (drive) for synchronizing chaotic systems [3]. This method has been shown to be efficient in synchronizing many types of analogue electronic circuits [80]. However, coupling is commonly used for synchronizing other types of chaotic systems including the chaotic lasers operating in very high frequency regime.

1.9.1 Coupling of chaotic systems

Consider two identical chaotic systems described by the following differential equations

$$\frac{d\mathbf{X}}{dt} = \mathbf{F}(\mathbf{X}) \tag{1.9.1}$$
$$\frac{d\mathbf{Y}}{dt} = \mathbf{F}(\mathbf{Y}) \tag{1.9.2}$$

where, $\mathbf{X}$ and $\mathbf{Y}$ represent the vectors representing state variables of two systems given as

$$\mathbf{X}(t) = \begin{pmatrix} X_1 \\ X_2 \\ . \\ . \\ X_N \end{pmatrix} \tag{1.9.3}$$

and

$$\mathbf{Y}(t) = \begin{pmatrix} Y_1 \\ Y_2 \\ . \\ . \\ Y_N \end{pmatrix} \tag{1.9.4}$$

and

$$\mathbf{F}(\mathbf{X}) = \begin{pmatrix} f_1(X_1, X_2..X_N) \\ f_2(X_1, X_2..X_N) \\ . \\ . \\ f_N(X_1, X_2..X_N), \end{pmatrix} \tag{1.9.5}$$

where, $f_1, f_2..f_N$ are some nonlinear functions.

Coupling of these systems can be done by sending the variables of each individual system to the other and applying feedbacks proportional to the difference of similar variables of the systems. A general expression for the dynamical equations for a coupled system is

$$\begin{aligned} \frac{d\mathbf{X}}{dt} &= \mathbf{F}(\mathbf{X}) + \mathbf{C}_{\mathbf{X}}(\mathbf{Y} - \mathbf{X}) \\ \frac{d\mathbf{Y}}{dt} &= \mathbf{F}(\mathbf{Y}) + \mathbf{C}_{\mathbf{Y}}(\mathbf{X} - \mathbf{Y}), \end{aligned} \tag{1.9.6}$$

where

$$C_X = [C_{X1}, C_{X2}, ...C_{XN}]^T \tag{1.9.7}$$

$$C_Y = [C_{Y1}, C_{Y2}, ...C_{YN}]^T \tag{1.9.8}$$

are matrices representing the strength of perturbations applied to the first and second systems respectively. The coupling described by Eq.1.9.6 involves the measurement of all the variables of individual systems and the feedback is assumed to be given to all the variables. This is difficult to implement in practice. Usually, a single variable is measured and the feedback is applied to anyone of the accessible variables of the systems.

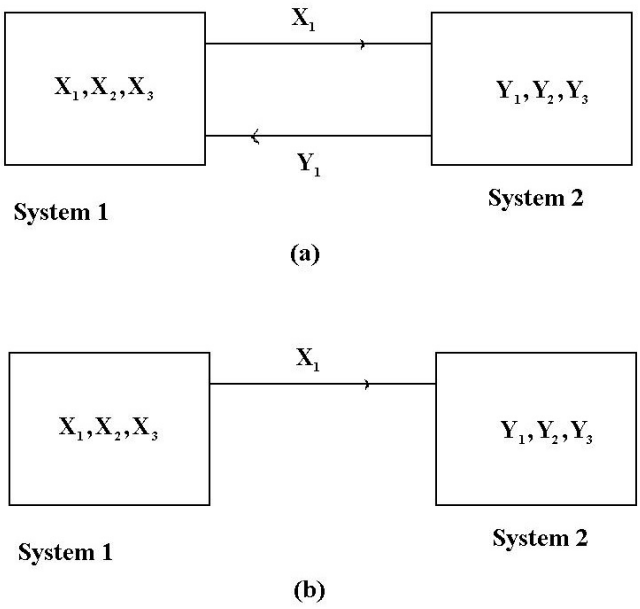

Figure 1.6: Schematic diagram of the coupling schemes (a) bidirectional and (b) unidirectional coupling.

The coupling scheme may be bidirectional or unidirectional depending on the specific situations. In bidirectional coupling, the measured signal corresponding to one of the variables are sent mutually in between the system. The schematic diagram of such a coupling scheme is given in Fig.1.6 (a). In the unidirectional method, the signal is sent in one direction only and all the coefficients of one of the matrices (say $\mathbf{C_X}$) are assumed to be zero. The schematic diagram of the unidirectional scheme is given in the Fig. 1.6(b). This

coupling scheme is widely used for developing the secure communication schemes using synchronization of chaos.

1.9.2 Pecora and Caroll method: The replacement synchronization

This method was proposed by Pecora and Caroll in 1990 [3]. The basic criteria of this scheme is to construct two identical subsystems (drive and response) of a chaotic system and replacing one of the variables of the response completely with the corresponding variable of the drive.

Consider a chaotic system described by an m dimensional state vector

$$\mathbf{W}(t) = \begin{pmatrix} \mathbf{X}(t) \\ \mathbf{Y}(t) \end{pmatrix} \tag{1.9.9}$$

where $\mathbf{X}$ and $\mathbf{Y}$ are the subsystems of $\mathbf{W}$ and they are having dimensions m_1 and m_2 ($m_1 + m_2 = m$). The evolution of the system $\mathbf{W}$ can be described by

$$\frac{d\mathbf{W}}{dt} = \mathbf{F}(\mathbf{W}) \tag{1.9.10}$$

where the nonlinear function,

$$\mathbf{F}(W) = \begin{pmatrix} \mathbf{G}(\mathbf{X}, \mathbf{Y}) \\ \mathbf{H}(\mathbf{X}, \mathbf{Y}) \end{pmatrix} \tag{1.9.11}$$

Thus the m dimensional system can be decomposed into two subsystems

$$\frac{d\mathbf{X}}{dt} = \mathbf{G}(\mathbf{X}, \mathbf{Y}) \tag{1.9.12}$$

$$\frac{d\mathbf{Y}}{dt} = \mathbf{H}(\mathbf{X}, \mathbf{Y}) \tag{1.9.13}$$

The next step is to construct another subsystem in such a way that its dynamics can be described as

$$\frac{d\hat{\mathbf{Y}}}{dt} = \mathbf{H}(\mathbf{X}, \hat{\mathbf{Y}}) \tag{1.9.14}$$

This system is identical to the subsystems $\mathbf{Y}$ and it is called the driven replica subsystem. The schematic diagram of the replacement synchronization is given in Fig.1.7. One of the variable of the response sub system is completely replaced by the time series $\mathbf{Y}$ received from the drive system. The subsystems $\mathbf{Y}$ and $\hat{\mathbf{Y}}$ are said to be synchronized if

$$\lim_{t\to\infty} |\mathbf{Y}(t) - \hat{\mathbf{Y}}| = 0 \tag{1.9.15}$$

The synchronization of subsystems described by the above equations can be realized by analogue electronic circuits and it is one of the practical ways of chaotic data enchryption

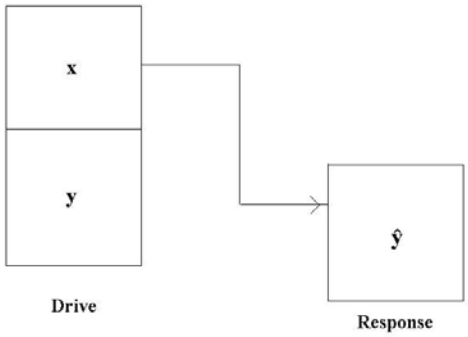

Figure 1.7: Schematic diagram of Pecora-Caroll method

1.9.3 Stability of the Synchronized State

A coupled system can be considered as a higher dimensional dynamical system. When the systems are synchronized, the phase space trajectories of the combined system are confined to a low dimensional hyperplane called synchronization manifold. The synchronization manifold of the coupled system described by Eq.1.9.6 is the hyperplane $X = Y$. The stability of synchronized state can be determined by calculating the so-called Transverse Lyapunov Exponents (TLE) introduced by Pecora and Caroll [3]. They are the Lyapunov Exponents in the direction normal to the synchronization manifold. The synchronization is said to be stable if all the TLEs are negative.

1.9.4 Perfect synchronization and partial synchronization

Two chaotic systems are said to be perfectly synchronized if the variables of one system exactly coincide with the corresponding variables of the other [80]. There are many factors such as parameter mismatches, noise and improper coupling which may lead to the loss of perfect synchronization. Since these factors are common in real physical systems, perfect synchronization is only an ideal case and we can achieve only a practical or almost synchronization in coupled chaotic systems. If there is strong mismatch in parameters or asymmetry in coupling, different types of partial synchronization is obtained. The study of such phenomena is significant as much as the study of perfect synchronization. In the next sections, we discuss briefly the concept of well known phase and lag synchronization.

1.9.5 Phase synchronization

Phase synchronization is a weak entrainment between the weekly coupled chaotic systems [33]. We can define a phase of chaotic oscillations which is analogous to the phase angle of the periodic oscillations by various methods such as Hilbert transform. Two chaotic systems are said to be phase synchronized if there exists a constant relationship between the phases of the oscillators while their amplitudes are varying chaotically. Phase synchronization is analogues to the phase locking in coupled periodic systems. It is generally a natural phenomena while perfect synchronization is possible only in the laboratory.

1.9.6 Lag synchronization

This type of synchronization is observed in the mutually coupled chaotic oscillators when the coupling strength is increased to relatively higher values. In this case the individual systems would have almost the same chaotic evolution. However one of the system lags from the other by constant amount of time. This phenomenon was first reported by Rosenblum, Pikovski and Kurths [33]. They have characterized the extent of synchronization using statistical measures such as the similarity function.

1.9.7 Generalized synchronization

It is the entrainment between two coupled non-identical chaotic oscillators [83]. Generalized synchronization is possible between two similar chaotic systems with large parameter mismatches or even between two chaotic systems belonging to entirely different classes. As the result of this entrainment, a new chaotic attractor is formed in which the evolution of the response system is uniquely determined by that of the drive system.

1.9.8 Secure communication using synchronization of chaos

Some novel secure communications schemes based on chaotic synchronization have been developed recently. The basic criteria behind these methods are given as follows. Two identical chaotic systems are synchronized by unidirectional coupling or replacement. The secure communication is possible between these systems. In one of the encryption schemes, the encrypting message is added with the output of the drive and this message can be recovered by taking the difference of the outputs of the drive and response [19] In the other method called Chaos Shift Keying (CSK), one of the parameter is slightly varied in proportion to the message and this variation produce the loss of synchronization. The encrypted signal can be recovered in the terms of synchronization errors [12].

1.10 Present work

Direct current modulation of semiconductor lasers has enormous applications in photonics technology. The modulation is usually done in the GHz frequency domain where the the nonlinear effects such as subharmonic generation, quasiperiodicity and chaos are produced as a result of the nonlinear interaction of charge carriers and photons in the laser cavity. The main objective of our work is to theoretically study the nonlinear dynamics of high speed modulated lasers with a particular emphasis to the control and synchronization of chaos. We expect that the numerical investigations on the possible methods for controlling chaos in directly modulated lasers would be helpful for the practical implementation of such schemes. The delay produced by the external transit of the optical signal, phase mismatches and frequency detuning of the modulating signal etc. are some of the practical issues in synchronizing modulated laser diodes. We address these issues while considering the application of these laser systems in chaotic secure communications.

1.11 Conclusion

A general introduction to the chaos theory and its applications is presented in this chapter. Fundamental concepts of chaos are explained and illustrated using two well known dynamical systems- the logistic map and the Lorenz model. The numerical techniques necessary for the study of chaotic semiconductor lasers are presented. The different methods used for controlling chaos are described. The concept of synchronization and its application in secure communications are explained in brief. The motivation behind the present work is also discussed.

Bibliography

[1] E. Atlee Jackson, *Perspectives of Nonlinear Dynamics*, Cambridge University Press, New York (1991)

[2] J. Guckenheimer and P. Holmes, *Nonlinear Oscillations, Dynamical System, and Bifurcations of Vector Fields,* Springer - Verlag, New York (1983)

[3] U. Feudel,C. Grebogi, B. R. Hunt and J. A. Yorke, Phys. Rev. E **54** (1996) 71

[4] U. Feudel and C. Grebogi, CHAOS **7**(1997) 597

[5] A. P. Kanjamala and A. F. J. Levi, Appl. Phys. Lett **72** (1998) 2214

[6] V. I. Arnold ,Trans. Amer. Math. Soc. 2nd series **46** (1965) 213

[7] R. Kapral, Phys. Rev. A. **31** (1985) 3868

[8] E. Ott, *Chaos in dynamical system,* Cambridge University Press (2002)

[9] Lj. Kocarev, K.S. Halle, K. Eckert, L.O. Chua and U. Parlitz *Int. J. Bifurcation Chaos* **2** (1992) 709

[10] G. P. Agrawal, *Nonlinear Fiber Optics*, Academic Press, San Diago (1989)

[11] E. N. Lorenz, J. Atmos. Sci. **20** (1964) 33

[12] F. T. Arecchi, R. Meucci, G. Puccioni and J. Tredicee, Phys. Rev. Lett. **49** (1982) 1217

[13] R. M. May, Nature **261** (1976) 459

[14] P. S. Linsay, Phys. Rev. Lett. **47** (1981) 1349

[15] B. P. Bolosov, *Sb. Ref. Radiats. Med.* Medgiz, Moscow (1958)

[16] F. A. Hopf. and F. W. Hopf, in *Frontiers of Nonequilibrium Statisical Physics.* eds. G. T. Moore and M.O.Scully, Plenum Press, New Yorke. (1986)

[17] F. Takens, *Detecting Strange Attractors in Turbulence*, Lecture Notes in Math. **898**, Springer, New York (1981)

[18] R. Kapral, Phys. Rev. Lett. **46** (1996) 922

[19] K. Cuomo and A. V. Oppenheim, Phys. Rev. Lett. **71** (1993) 65

[20] A. Babloyantz, J. M. Salazar, C. Nicolis, Phys. Lett. A, **111** (1985) 152

[21] S. P. Layne, G. Mayer-Kress, J. Holzfuss , *Problems associated with dimen- sional analysis of electroencephalogram data, In: Dimensions and entropies in chaotic systems,* Springer-Verlag, Berlin (1986)

[22] L. Glass, M. R. Guevara, A. Shrier and R. Perez, Physica D **7** (1983) 89

[23] M. J. Feigenbaum, J. Stat. Physics **19** (1979) 25

[24] H.Goldstein, *Classical Mechanics* Addison Wesley (1990)

[25] A. N. Kolmogorov, *Dokl. Akad. Nauk. SSR.* **98** (1954) 527 English Translation: Hao Bai-Lin, Chaos , World Scientinfic, Singapore (1984)

[26] P. Bryant, and C. Jefferies , Phys. Rev. Lett. **53** (1984) 250

[27] H. Aref, J. Fluid Mech. **143** (1984) 1

[28] C. L. Siegel and J. K. Moser *Lecture Notes on Celestial Mechanics* Springer - Verlag, New York (1971)

[29] V. I. Arnold and A. Avez, *Ergodic Problems in Classical Mechanics, Benjamin*, New York (1968)

[30] G. L. Baker, J. P. Gollub - *Chaotic Dynamics*, Cambridge Univ. Press (1990)

[31] T. S. Parker and L. O. Chua, *Practical numerical algorithms for chaotic systems*, Springer-Verlag, New York (1989)

[32] L. C. Andrews and Rolald L. Phillips, *Mathematical techniques for engineers and scientists* ,SPIE press, Bellingham, Washington (2003)

[33] W. H. Press, S. A. Teukolsky, W. T. Vettering and Brian P. Fianny,*Numerical recipes in C++, The art of Scientific computation*, Cambridge University Press (2002)

[34] A. Wolf, J. B. Swift, H. L. Swinney and J. A. Vatsano Physica D **16** (1985) 285

[35] J. D. Farmer, Physica D **4** (1982) 366

[36] P. Berge and M. Dubois, Contemp. Phys. **25** (1984) 535

[37] H. O. Peitgen H. Jürgens and D. Saqupe, *Chaos and Fractals: New Frontiers of Science*, Springer- Verlag, New York (1992)

[38] J. P. Eckmann and D. Ruelle, Ergodic theory of chaos and strange attractors, Rev. Mod. Phys. **57** (1985) 617

[39] H.G.F. Hentschel and I. Procaccia, Physica D **8** (1983) 435

[40] E. Hopf, Commun. Pure Appl. Math **1** (1948) 303

[41] D. Reulle and F. Takens, Commun. Math. Phys. **20** (1971) 167

[42] D. J. Bishwas and R. G. Harrison, Phys. Rev. A **32** (1985) 3835

[43] Phys. Lett. A **53** (1975) 77

[44] R. S. Gioggia and N. B. Abraham Phys. Rev. Lett. **51** (1983) 650

[45] W. Klische and C. O. Weiss, Opt. Lett. **9** (1984) 561

[46] D. Y. Tang, M. Y. Li, N. R. Heckenberg and J. Huebner, J. Opt . Soc. Am. B **13** (1996) 2055

[47] W. Klische and C. O. Weiss, Phys. Rev. A **31** (1985) 4049

[48] Bracikowski and R. Roy, Chaos **1** (1991) 49

[49] C. O. Weiss, and W. Klische, Opt. Commun. **51** (1984) 47

[50] F. Liu and W. F. Ngai, IEEE J. Quantum Electron., **29** (1993) 1668

[51] M. Tang and S. Wang, Appl. Phys. Lett. **48** (1986) 900

[52] G. P. Agrawal, Appl. Phys. Lett. **49**(1986) 1013

[53] Y. Hori, H. Serizawa, and H. Sato, J. Opt. Soc. Amer. B **5** (1988) 1128

[54] V.Kovanis, A.Gavrielides, T.B.Simpson, J.M.Liu, Appl.Phys.Lett. **67** (1995) 2780

[55] C. H. Lee and S. Y. Shin, Appl. Phys. Lett. **62** (1993) 922

[56] S. Tang and J. M. Liu, IEEE J. Quant. Electron. **37** (2001) 329

[57] J. Mork, B. Tromberg , J. Mark, IEEE J. Quantum Electron. **28** (1992) 93

[58] Y. Cho and T. Umeda, Opt. Commun. **59** (1986) 131

[59] L. Goldberg, H. F. Taylor, A. Dandridge, H. F Weller, R. O. Miles, IEEE J. Quantum Electron. **18** (1982) 555 IEEE J. Quant. Electron. **30** (1994) 1537

[60] M. Ding, E. J. Ding, W. L. Ditto B. Gluckman, V. In, J. H. Peng M. L. Spano and W. Yang, Chaos **7** (1997) 644

[61] M. C. Gutzwiller, *Chaos in Classical and Quantum Mechanics* (Springer, New York (1990)

[62] D. Auerbach, P. Cvitanovic, J. P. Eckmann , G. Gunaratne and I. Procaccia Phys. Rev. Lett. **58** (1987) 2387

[63] E. Ott, C. Grebogi, and J. A. Yorke, Phys. Rev. Lett. **64** (1990) 1196

[64] W. L. Ditto, S. N. Rouso and M. L. Spano, Phys. Lev. Lett. **65** (1990) 3211

[65] R. Roy, T. W. Murphy Jr., T. D. Maier, Z.Gills, E. R. Hunt, Phys. Rev. Lett. **68** (1992) 259

[66] B. Huberman and H. L. Lumer, IEEE Trans. Circuits Syst. **37**, (1990) 547

[67] S. Sinha, R. Ramaswamy and J. Subba Rao, Physica D **43** (1990) 118

[68] R. Lima. and M. Pettini, Phys. Rev. A **41** (1990) 726

[69] P.Colet, Y.Braiman, Phys. Rev. E **53** (1996) 200

[70] K. Pyragas, Phys. Lett. A **170** (1992) 421

[71] K. Pyragas, Phys. Lett. A **181** (1993) 99

[72] C. Batlle, E. Fossas, G. Olivar, Int. J. Circuit Theory and Applications **27** (1999) 617

[73] Th. Pierre, G. Bonhomme, A. Atipo, Phys. Rev. Lett. **76** (1996) 2290

[74] T. Hikihara and T. Kawagoshi, Phys. Lett. A **211** (1996) 29

[75] M. Ye, D.W. Peterman and P.E. Wigen, Phys. Lett. A **203** (1995) 23

[76] F. T. Arecchi, R.Meucci, E.Allaria, A.DiGarbo and L.S.Tsimring, Phys.Rev.E **65** (2002) 046237

[77] T. Yamada and H. Fujisaka Prog. Theor. Phys. **70** (1983) 1240

[78] V. S. Afraimovich, N. N. Verichev, and M. I. Rabinovich, Inv. VUZ Rasiofiz. RPQAEC **29** (1986) 795

[79] L. M. Pecora and T. L. Carroll, Phys. Rev. Lett. **64** (1990) 821

[80] L. M. Pecora, T. L. Carroll, G. A. Johnson, D. J. Mar, Chaos, **7** (1997) 520

[81] M. G. Rosenblum, A. S. Pikovsky, and J. Kurths, Phys. Rev. Lett., **76** (1996) 1804

[82] M. G. Rosenblum, A. S. Pikovsky, and J. Kurths, Phys. Rev. Lett., **78** (1997) 4193

[83] N. F. Rulkov, M. M. Sushchik, L. S. Tsimring and H. D. I. Abarbanel, Phys. Rev E **51** (1995) 980

[84] T. Yang, C. W. Wu , and L. O. Chua, IEEE Trans. Circuits. Syst. I **44** (1997) 469

Chapter 2

Chaos in directly modulated semiconductor lasers

In this chapter, we present a review of the investigations on the chaotic behavior of directly modulated semiconductor lasers. The different dynamical features associated with the period doubling and quasiperiodicity routes to chaos are illustrated by numerical simulations. The fourth order Runge-Kutta algorithm is used for solving the nonlinear differential equations.

2.1 Semiconductor lasers: Basic concepts

Semiconductor lasers are the essential elements in optical fibre communication systems [4]. They were developed in 1962. The early semiconductor laser consisted of a single forward biased p-n junction of GaAs polished at both ends. Such lasers are known as homostructure laser diodes [2]. The performance of semiconductor lasers has been later improved by adopting the heterostructure which is the commonly accepted structure. The simplest model of a heterostructure semiconductor laser (Fig.2.1) consists of a thin active layer of thickness $\sim 0.1\mu m$ sandwiched between p and n type cladding layers of another semiconductor with higher band gap and lower refractive index. The resulting p-n junction is forward biased through metallic contacts. The laser light is emitted through an elliptic spot of dimensions $\sim 1 \times 100\mu m^2$. The main drawback of the homostructure lasers was the large values of threshold current (the minimum value of injection-current needed to start lasing). The use of heterostructure [3] has reduced the value of threshold current of laser diodes because of two reasons. The band gap difference between the layers helps to confine the electrons and holes to the active layer where they recombine to produce optical gain. The refractive index difference helps to confine the optical mode close to the active layer which acts as a

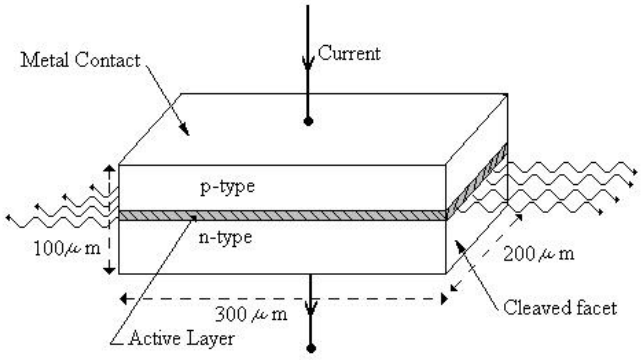

Figure 2.1: Structure of a heterostructure semiconductor laser.

dielectric waveguide. Many modifications have been applied to semiconductor lasers for the convenience of different applications. In the place of GaAs used in the early laser diodes, a variety of semiconductor materials such as, AlGaAs [4], InP [5] and InGaAsP [6] have been used for the purpose of fabricating semiconductor lasers. The emission wavelengths of these semiconductors vary up to about $100\mu m$. The InGaAsP lasers have particular importance in optical fibre communications. Their emission wavelength ranges from $1.3\mu m$ to $1.6\mu m$. The optical fibres yield minimum transmission loss to the light emitted in these wavelength region [4].

2.2 Laser rate equations

The dynamical behavior of semiconductor lasers can be well described by a set of differential equations called rate equations . They are derived from Maxwell's equations together with a quantum mechanical approach for induced polarization [2]. The single mode rate equations [20] are given by

$$\frac{dn}{dt} = \frac{I}{qV} - \frac{n}{\tau_e} - A(n - n_0)p \tag{2.2.1}$$

$$\frac{dp}{dt} = \Gamma A(n - n_0)(1 - \epsilon_{NL}p) - \frac{p}{\tau_p} - \Gamma\beta\frac{n}{\tau_e} \tag{2.2.2}$$

where n and p are the carrier and photon densities, τ_e and τ_p are the carrier and photon life times, I is the injection current, q is the electronic charge, V is the volume of active region, n_0 is the carrier density for transparency (the electron density above which the lasing gain becomes positive), A is the gain constant, β is the spontaneous emission factor, Γ is the confinement factor and ϵ_{NL} is the constant governing the nonlinear gain reduction occurring with an increase in p due to the nonlinear effects such as spectral hole burning.

For the convenience of numerical studies, the normalized carrier density N and the normalized photon density P can be used [20]. They are defined by

$$N = n/n_{th},\ P = p/p_0 \tag{2.2.3}$$

where $n_{th} = n_0 + (\Gamma A \tau_p)^{-1}$, the threshold carrier density and $p_0 = \Gamma(\tau_p/\tau_e)n_{th}$. The rate equations then become

$$\frac{dN}{dt} = \frac{1}{\tau_e}\left(\frac{I}{I_{th}} - N - \frac{N-\delta}{1-\delta}P\right) \tag{2.2.4}$$

$$\frac{dP}{dt} = \frac{1}{\tau_p}\left(\frac{N-\delta}{1-\delta}(1-\epsilon P)P - P - \beta N\right), \tag{2.2.5}$$

where

$$\delta = n_0/n_{th}, \epsilon = \epsilon_{NL}p_0 \tag{2.2.6}$$

are the two dimensionless parameters and

$$I_{th} = qVn_{th}/\tau_e, \tag{2.2.7}$$

the threshold current of the laser. The parameters for InGaAsP semiconductor lasers used for numerical simulation are given in Table 2.1.

τ_e	$3ns$
τ_p	$6ps$
β	5×10^{-5}
δ	0.692
ϵ	10^4
I_{th}	$26mA$

Table 2.1: Parameter values of InGaAsP semiconductor laser.

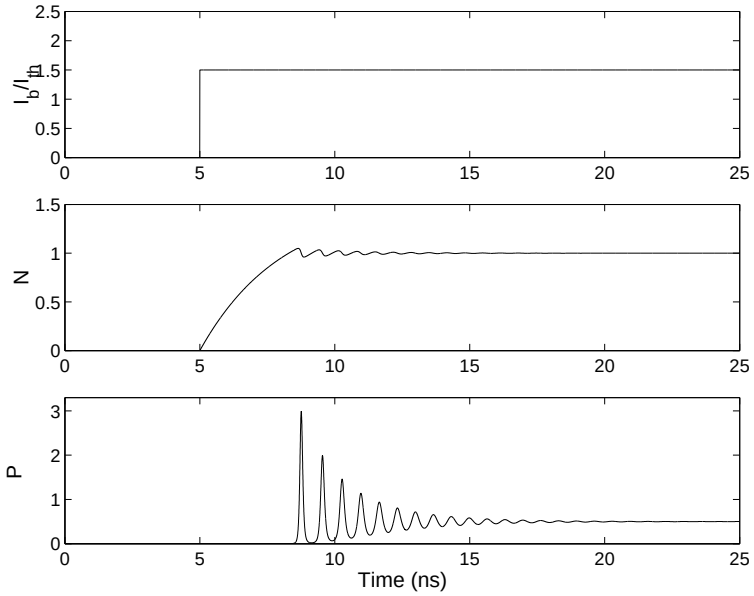

Figure 2.2: Relaxation oscillations of an InGaAsP semiconductor laser: time series plots of (a) injection current (normalized by the thresholds current), (b) normalized carrier density and (c) normalized photon density. The current is switched from 0 to $1.5I_{th}$ at t= 5 ns .

2.3 Static characteristics

A simple physical description of the variation of laser output with respect to the change in injection current can be obtained by the single mode rate equations. There will be no lasing action and hence practically no optical emission for the values of $I < I_{th}$. The light emitted in this situation is totally due to the contribution from spontaneous emission. At the point $I = I_{th}$, the output power would vary abruptly if the spontaneous emission is not present. However due to the amplified spontaneous emission, a gradual transition around the threshold takes place. The carrier density varies linearly up to the threshold current value and approaches the threshold carrier density as the current is increased beyond I_{th}.

2.4 Transient characteristics: Relaxation oscillation

The semiconductor laser exhibits damped periodic oscillations before settling down to a stable state . These oscillations are called relaxation oscillations and they are the result of an intrinsic resonance in the nonlinear laser system. The oscillations that occur when the current is switched from 0 to $1.5I_{th}$ is shown in Fig.2.2(c).

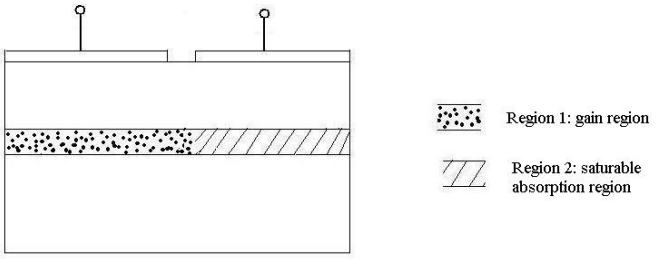

Figure 2.3: Structure of a self pulsating semiconductor laser.

2.5 Self pulsation in semiconductor lasers

It is not necessary for a semiconductor laser to have stable continuous output for all parameter values. For many practical conditions, they show self sustained pulsations. A good example for this behavior is the self pulsation in laser diodes having an unpumped region in their cavity, which acts as a saturable absorber. A saturable absorber is a material whose absorbtion decreases with the increase in incident radiation density. The structure of such a laser is given in Fig.2.3. The gain region and the saturable absorption region are labelled as region 1 and region 2 respectively.

The rate equation of the self pulsating laser diode is given by [1]

$$\frac{dp}{dt} = \left[a_1\xi_1(n_1 - n_{g1}) + a_2\xi_2(n_2 - n_{g2}) - G_{th}\right]p + b\frac{n_1 V_1}{\tau_s} \tag{2.5.1}$$

$$\frac{dn_1}{dt} = -\frac{a_1\xi_1}{V_1}(n_1 - n_{g1})p - \frac{n_1}{\tau_s} - \frac{n_1 - n_2}{T_{12}} + \frac{I}{qV_1} \tag{2.5.2}$$

$$\frac{dn_2}{dt} = -\frac{a_2\xi_2}{V_2}(n_2 - n_{g2})p - \frac{n_2}{\tau_s} - \frac{n_2 - n_1}{T_{21}} \tag{2.5.3}$$

where, a_i is the proportionality constants between gain coefficient and the electron density in the region i (i=1,2), b is the coefficient of spontaneous emission, q is the charge of the electron, V_i is the volume of region i, T_{ij} is a time constant to characterize the diffusion from region i to region j, ξ is the distribution ratio of the optical power in the

region i, N_{gi} is the electron density for transparency in the region i, G_{th} is the threshold gain level and τ_s is the electron life time due to the spontaneous emission. The parameters of GaAs self pulsating lasers used for numerical simulation is given in the Table.2.2

Quantity	Value	Unit
a_1	3.08×10^{-12}	$m^3 s^{-2}$
a_2	1.232×10^{-11}	$m^3 s^{-2}$
ξ_1	0.2034	-
ξ_2	0.1449	-
n_{g1}	1.4×10^{24}	m^{-3}
n_{g2}	1.6×10^{24}	m^{-3}
V_1	72	μm^{-3}
V_2	102.96	μm^{-3}
T_{12}	2.65×10^{-9}	ns
T_{21}	4.452×10^{-9}	ns
G_{th}	4.41×10^{11}	$s{-}1$
C	1.573×10^{-5}	μm^{-3}
τ_s	3	ns

Table 2.2: Parameter values of a self pulsating GaAs semiconductor laser

The time series plot of the photon density of the laser diode is shown in Fig.2.4. The bias current is 30mA. The continuous state is unstable here and the laser shows stable pulsating behavior. The frequency of pulsation is 2.06 GHz and that is shown in the power spectrum.

2.6 Modulation response

One of the advantages of the semiconductor lasers over the other lasers is the possibility of direct current modulation. The short optical pulses required for optical communications can be generated by the modulation of input current [4]. The sinusoidal modulation of a semiconductor laser is commonly used for many applications and that can be done by injecting a current signal in the form

$$I = I_b + I_m sin(2\pi f_m t), \tag{2.6.1}$$

where, I_b is the bias current, I_m is the amplitude and f_m is the frequency of modulation.

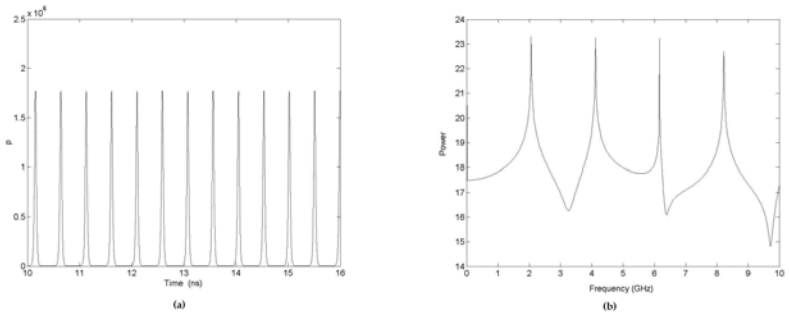

Figure 2.4: Self pulsation: (a) time series (b) power spectrum.

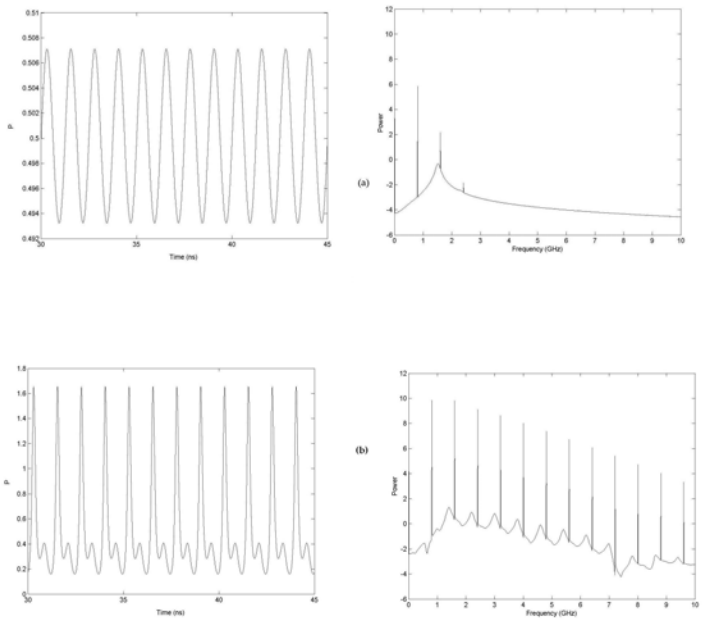

Figure 2.5: Period 1 pulses : Time series plots and power spectra of normalized photon density are given in the left column and the right column respectively. (a) Small signal modulation (m=0.002) (b)large signal modulation (m=0.2).

The modulation response of laser diodes has been studied from early days [8, 9]. The relaxation-oscillation frequencies of semiconductor lasers usually fall in the GHz frequency domain and they show maximum response to modulation in these regime [9]. Hence the direct modulation is usually done in the GHz frequencies for communication purposes [10]. Semiconductor lasers have a good modulation bandwidth in the order of 10GHz which makes them useful in the optical communication of ultra high bit rates.

Besides the applications in optical fiber communication, the short pulses generated by semiconductor lasers are useful in various other fields such as ultra fast optical signal processing [5]. The optoelectronic devices based on laser diodes provides as tunable microwave sources also [12]. Self pulsation in laser diode can be utilized for the above purposes. However the repetition rates of pulses produced in this way are usually determined by the intrinsic parameters of semiconductor material and hence modulation is the better way for the generation of short optical pulses with required frequencies. Usually it is expected that the direct modulation of semiconductor laser yields regular periodic pulses with a frequency (repetition rate) that is equal to the frequency of modulation . For small signal sinusoidal modulation, this is possible for a wide range of frequencies and modulation amplitudes. However, in practical situations large signal modulation is generally applied to the laser and then the nonlinear effects will come into play. Directly modulated InGaAsP laser diodes described by the Eqns.2.2.4, 2.2.5, and 2.6.1 have been found to follow a period doubling route to chaos [16]. Many theoretical [20, 14, 19] and experimental [19] investigations have been done on the period doubling and chaos in such lasers. The modulation of self pulsating lasers produce another class of interesting phenomena which are associated with the quasiperiodicity route to chaos.

We simulate the dynamics of an InGaAsP laser diode that is directly modulated by a sinusoidal current signal with an amplitude I_m and a constant bias current $I_b = 1.5I_{th}$, where I_{th} is the threshold current defined by Eqn.2.2.7. The depth of modulation can be described by the quantity $m = I_m/I_{th}$. The frequency of modulation is chosen as 0.8GHz since the direct modulation of semiconductor laser are commonly done with the signals of frequencies in this order and the nonlinear effects are predominant in such conditions[20]. The output time series plots and power spectra of the laser for two different modulation strengths are given in Fig.2.5. In the time series plots, the normalized photon density is plotted versus time in nanoseconds. Power spectra are calculated numerically from these time series using FFT algorithm described in the section 1.2.3 and it is given in the semi logarithmic scale (logarithm of FFT coefficients vs frequency in GHz). Fig.2.5(a) shows the time series and power spectra correspond to the small scale modulation ($m = 0.002$). The optical pulse is regular and very much similar to a sinusoidal pulse. The power spectrum

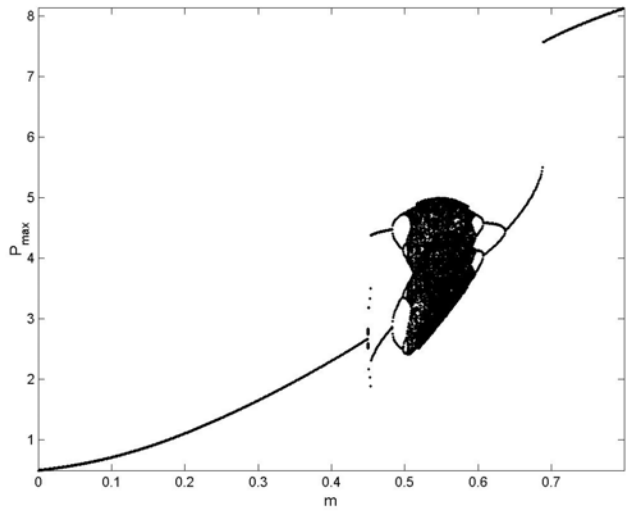

Figure 2.6: Bifurcation diagram showing Period doubling and reverse period doubling: Maxima of normalized photon density versus modulation depth.

is peaked at the frequency of modulation ($f_m = 0.8GHz$) and at a few integer multiples of these value. The output of the laser with a relatively high modulation depth (this quantity can be defined as $m = I_m/I_{th}$) is given in Fig.2.5(b). On increasing the modulation depth up to the order of 0.2, a double peak is observed. i.e., the main peak of the pulse is accompanied by a smaller maximum. Both of these maxima occur in the same modulation cycle and hence the pulse is still of period 1 which is evident from the power spectrum also.

2.7 Period doubling and chaos in directly modulated InGaAsP laser diodes

Consider the strong sinusoidal modulation applied to InGaAsP semiconductor lasers. Fig.2.6 show the bifurcation diagram showing the change of the dynamic behavior of the laser as the modulation amplitude is varied. The maximum value of the photon density (P_{max}) is plotted against the modulation depth m. The advantage of taking the maxima is that in addition to showing period of the pulse, the bifurcation diagram shows the variation of peak power of the output also.

The fundamental period of the optical pulse generated by the modulated laser is simply the inverse of the frequency of modulation ($T = 1/f_m$). The system is said to be in period

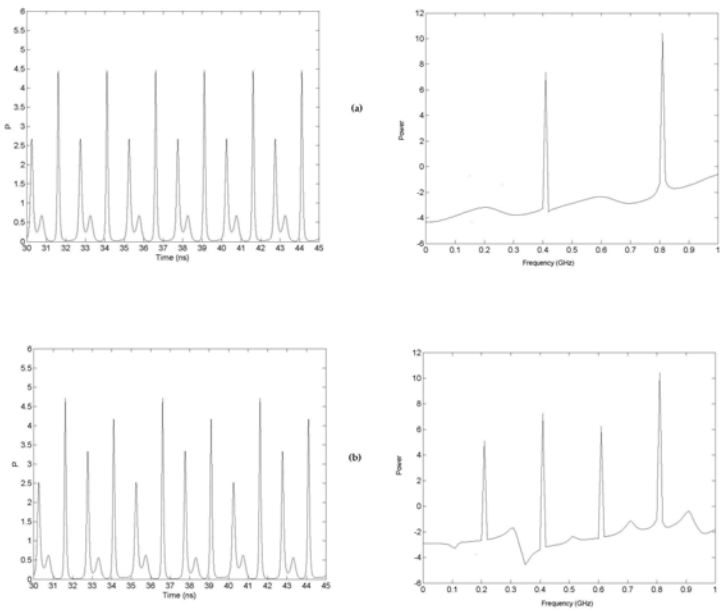

Figure 2.7: Time series plots of normalized photon density (left column) and power spectra (right column) of subharmonic pulses: (a) period 2 output (b) period 4 output.

1 state and the corresponding phase space trajectory is called a period 1 orbit. It is clear from the bifurcation diagram that the laser is in the period 1 state for all the modulation depths from 0 to 0.449. The time series plot and power spectrum of period 1 pulse is given in Fig.2.5(b). If the modulation depth is increased above 0.449, the system pass through a non-smooth transition to period 2 state. The period 2 orbit bifurcates into a period 4 orbit at m=0.482. The time series plots (left column) and power spectra (right column) of these subharmonic states are given in the Fig.2.7. There are peaks at every integer multiples of the fundamental frequency. However for convenience, only the frequency regime from 0 to 1 is shown in the power spectra. In addition to the main peak in the spectra, a peak at $f_m/2$ can also be seen in the power spectrum of period 2 orbit given in (Fig.2.7(a)). Similarly for the period 4 output ((Fig.2.7(b)), there are four peaks at the values $f_m/4$, $f_m/2$, $3f_m/4$ and f_m.

The formation of period 4 state is followed a by a sequence of period doubling bifurcations and the laser reaches chaos near the modulation depth 0.55. Fig.2.8 shows the time series and power spectrum of photon density. The power spectrum is broadband. However,

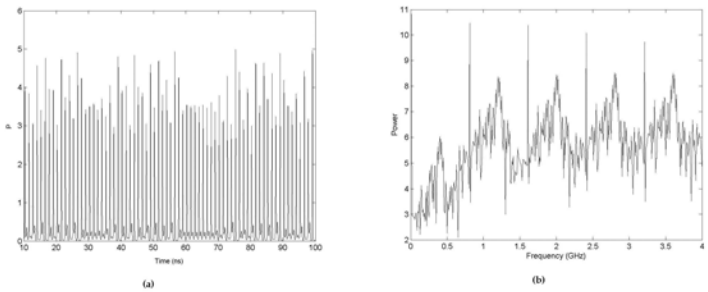

Figure 2.8: Chaotic output: (a) time series of normalized photon density (b) power spectrum.

the peaks at the fundamental and subharmonic frequencies are still present in the spectra. On further increasing the modulation depth, the system undergoes a reverse period doubling. After a number of reverse bifurcations, the system comes to a state of period 1. In addition to the period doubling and the reverse period doubling bifurcations, the directly modulated InGaAsP laser shows bistabily, i.e. the coexistence of two different stable states. Sudden jumps seen in the bifurcation diagram (Fig.2.6) corresponding to the values 0.449 and 0.663 of modulation depth are associated with the pulse position bistability and hysteresis [19] shown by the laser. A detailed description of this phenomena and its control is presented in chapter 5.

Even though these bifurcations are similar to those observed in logistic map, there are two important differences. The bifuractions are not smooth throughout the parameter space. Secondly, the bifurcation sequence show a severe truncation of Feigenbaum sequence [21]. Lamela *et. al.* have done a detailed study of these phenomena [22] . They have also investigated the significance of coexistence of low period orbits along with the chaotic orbits of directly modulated lasers [23]. The quantitative study on chaotic phenomena using Lyapunov Exponents is also given in ref.[23]. The analytical studies on the modulation response have been reported by Lee [14] and Mayol *et. al.* [19].

The time series plots give the idea about the time evolution of photon density. However, for understanding the geometrical structure of the periodic and chaotic attractors in the phase space, the phase portraits also should be considered. The phase portrait of the laser is the graphical representation of the system trajectories in the phase space constituted by the system variables (here it is normalized carrier density (N) and normalized photon density (P)). The phase portraits of different dynamical states are given in Fig.2.9. The

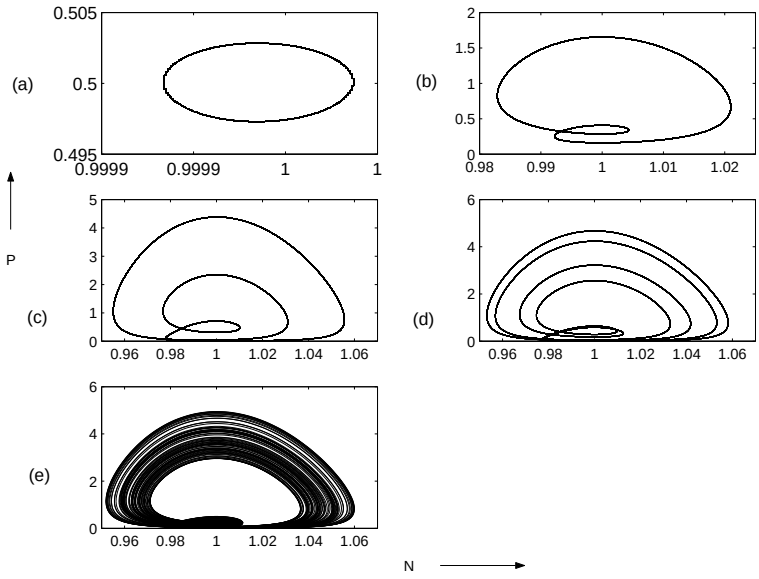

Figure 2.9: Phase portraits (normalized carrier density vs normalized photon density) of directly modulated laser diode: (a) regular periodic orbit obtained by small scale modulation (m=0.002), (b) period 1 orbit with double peak (c) period 2 orbit (d) period 4 orbit, (e) chaotic attractor.

phase portrait of the laser with small scale modulation ($m = 0.002$) (Fig.2.9(a)) is a simple closed curve. The period 1 orbit in Fig.7(b) has a double cusp since the output is a double peaked pulse. However the system completes one cycle within a time that is equal to the fundamental period of the pulse. For period 2 (Fig.2.9(c)) and period 4 (Fig.2.9(d)) orbits, the corresponding periods are $2T$ and $4T$ respectively . The chaotic orbit (Fig.2.9(e)) is considered to be a non repeating cycle and it is not a closed curve.

2.8 Dynamics of a directly modulated self pulsating semiconductor laser: Quasiperiodicity route to chaos

Output of the self pulsating laser diode is a sequence of short optical pulses with the repetition rates of a few GHz, as shown in Fig 2.4(a). If the laser diode is modulated, it will show many interesting features such as frequency locking, quasiperiodicity and chaos [22]. These phenomena have already been investigated quantitatively using Lyapunov Exponents [7]. Hence we have not done detailed investigations on these effects. However we are interested to demonstrate the quasiperiodicity route to chaos numerically with particular emphasis to the phase space dynamics and spectral properties.

The results of the numerical simulation of a directly modulated GaAs self pulsating laser diode is presented in this section. Similar to the modulation of InGaAsP semiconductor laser, modulation of self pulsating laser can also be represented by Eqn.2.6.1. The value of bias current is $30mA$ for which the laser shows self pulsating behavior without modulation. The frequency of modulation is chosen as 1.25GHz. For relatively small values of modulation amplitude, laser shows quasiperiodic behavior.

Time series plot of the laser is shown in Fig.2.10(a). The power spectrum (Fig.2.10(b)) of the output is spiked at certain frequencies. A careful calculation reveals that the spectrum is peaked at all linear combinations of two fundamental frequencies f_1 and f_2. where f_1 and f_2 are approximately equal to 1.26GHz and 2.07GHz respectively. f_1 is very near to the modulation frequency (1.25 GHz) and f_2 is in close proximity to the frequency of self pulsations (2.06GHz). The phase space trajectories forms a biperiodic torus [24]. The three dimensional (n_1, n_2, p) phase portrait of this torus is shown in Fig.2.10(c). The Poincaré section of this attractor given in Fig.2.10(d). It is obtained by recording the phase points through which the phase space trajectories cross the two dimensional hyper plane $p = 0.5$ in the forward direction normal to this hyper plane. A two dimensional (n_1, n_2) discrete map of the system is obtained by this process. The section of the biperiodic torus appears as a closed curve in the map. The attractor points in the curve uniformly fill the curve. This is because the frequency components f_1 and f_2 are incommensurate, i.e., their ratio is an

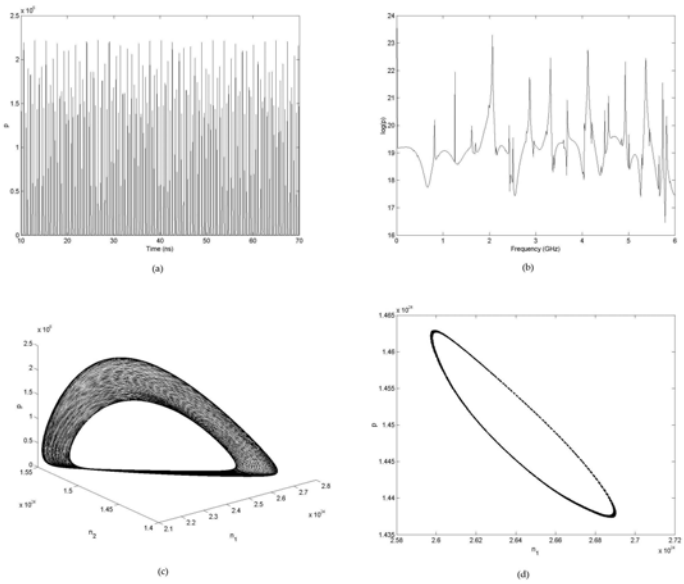

Figure 2.10: Quasiperiodic state of modulated self pulsating laser: (a) time series of photon density (b) power spectrum (c) phase portraits (d)Poincaeé section. $I_m = 2mA$

irrational number. Hence it is well evident that the laser is in two - frequency quasiperiodic state [25].

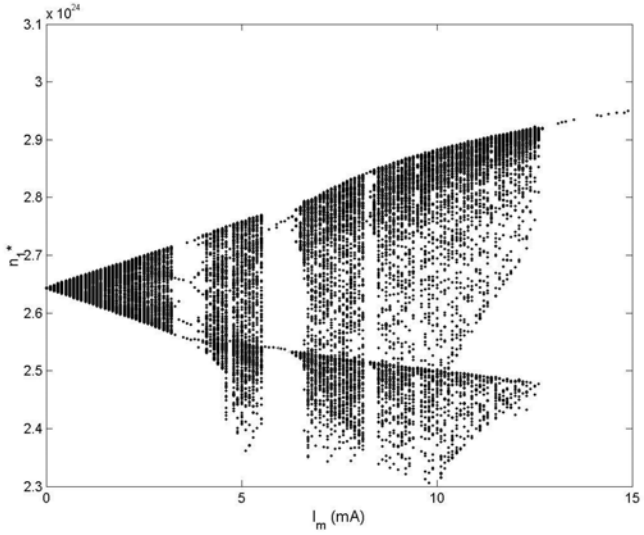

Figure 2.11: Bifurcation diagram showing quasiperiodicity route to chaos in a modulated self pulsating laser: The attractor points (photon density) in the Poincaré section is plotted against the amplitude of modulation I_m.

A bifurcation diagram (Fig.2.11) is plotted by using the Poincaré section obtained by the above process. The values of carrier density in region 1 correspond to the discrete points (n_1*) in the section is plotted versus the amplitude I_m of modulating current signal in mA. The laser shows quasiperiodic behavior for the range of amplitudes from 0 to 3.2mA. A period 3 window is formed at 3.2mA. Chaotic attractors have been created through different types of bifurcations. The chaotic state of the laser for the amplitude of modulation $I_m = 7mA$ is shown in Fig.2.12. The time time series plot showing the chaotic evolution of photon density (Fig.2.12(a), the broadband power spectrum with peaks in the continuous region (Fig.2.12(b)) and the three dimensional phase portrait (Fig.2.12(c)) and the Poincaré section (Fig.2.12(d)) of the strange attractor are given in the figure.

2.9 Conclusion

The period doubling and quasiperiodicity routes to chaos followed by semiconductor lasers have been discussed in this chapter. Most of the laser systems follow these routes to chaos.

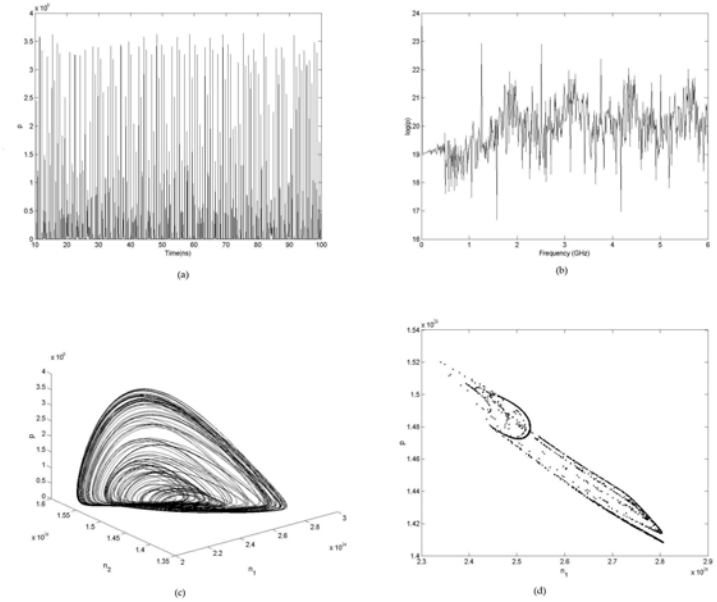

Figure 2.12: Chaotic state of a modulated self pulsating laser: (a) time series of photon density (b) power spectrum (c) phase portraits (d)Poincare*é* section. $I_m = 7mA$

The hysterisis jumps associated with the bifurcations and double peaked pulses are the distinct features of period doubling route to chaos observed in directly modulated InGaAsP lasers. The phase space approach used here for demonstrating the dynamics of modulated self pulsating laser is helpful for getting a clear understanding of the structure of the attractors. In general chaos is very common in semiconductor lasers. For most of the practical applications, chaos is unwanted and should be eliminated. However, generation of chaos is important in applications like secure communication. The knowledge of the possible regions of chaotic behavior would help us in controlling and synchronizing laser diodes.

Bibliography

[1] G. P. Agrawal, *Fiber-optic communication systems*, John Wiley and Sons, New York (1992)

[2] G. P. Agrawal and N. K. Dutta, *Long - wavelength semiconductor lasers*, Van Nostrand Reinhold, New York (1986)

[3] N. Hayashi, M. B. Panish and P. W. Foy. IEEE J. Quant. Electron. **5** (1969) 211

[4] M. Ettenberg, Appl. Phys. Lett. **27** (1975) 652

[5] R. L. Moon, G. A. Antypas and L. W. James, J. Electron. Materials. **3** (1974) 635

[6] L. G. Cohen, C. Lin and W. G. French . Electron. Lett. **15** (1979) 729

[7] G. P. Agrawal, Appl. Phys. Lett., **49** (1986) 1013

[8] T. Ikegami and Y. Suematsu, Electron. Commun. Jpn. **51B** (1968) 51

[9] T. L. Paoli and J. E. Ripper, Proc. of IEEE **55** (1970) 1457

[10] G. Arnold, P. Russer, and K. Peterman. *Semiconductor Lasers and Heterojunction LEDs.* Springer - Verlag: Berlin (1982)

[11] J. Mørk and A. Mecozzi, J. Opt. Soc. Am. B. **13** (1996) 1803

[12] S. Bauer,*et. al.* , Electron. Lett. **38** (2002)7

[13] C. Mayol, R. Toral, C. R. Mirasso, S. I. Turovets, and L. Pesquera, IEEE J. Quantum Electron. **38** (2002) 260

[14] T. H. Yoon, C. H. Lee, and S. Y. Shing, IEEE J. Quantum Electron. **25** (1989) 1993

[15] H. F. Liu, and W. F. Ngai, IEEE J. Quantum. Electron. **29** (1993) 1668

[16] C.H. Lee, T.H. Yoon, S.Y. Shin, Appl. Phys. Lett. **49** (1985) 95

[17] H. Kawaguchi, *Bistability and Nonlinearities in Laser Diodes*, Artech House, Norwood (1994)

[18] M. Yamada, IEEE J. Quantum Electron. **29** (1993) 1330

[19] H.G. Winful, Y.C. Chen, J.M, Liu, Appl. Phys. Lett. **48** (1986) 161

[20] C. Juang, T. M. Huang, J. Juang and W. W .Lin, IEEE J.Quant.Electron. **36** (2000) 300

[21] M. J. Feigenbaum, J. Stat. Physics **19**(1979) 25

[22] H. Lamela, G. Carpintero, and P. Acebo, IEEE J. Quantum Electron. **34** (1998) 491

[23] H. Lamela, G. Carpintero, and F. Mancebo, IEEE J. Quantum Electron., **34**(1998) 1797

[24] G. L. Baker, J. P. Gollub, *Chaotic Dynamics*, Cambridge Univ. Press (1990)

[25] P. W. Miloni. ,M. L. Shih and J. R, Ackerhalt, *Chaos in Laser- Matter Interactions.* World Scientific, Singapore (1987)

[26] V. I. Arnold, Trans. Amer. Math. Soc. 2nd series **46** (1965) 213

Chapter 3

Control of chaos in directly modulated InGaAsP semiconductor lasers

In chapter 2, we have demonstrated two different routes through which the directly modulated semiconductor lasers arrive at chaotic behavior. In this chapter, we present the results of our numerical studies on two different delay feedback schemes for controlling chaos and other instabilities in such lasers. The former method is based on the chaos-control algorithm known as Time Delay Auto Synchronization (TDAS) introduced by K. Pyragas [26, 27]. The latter is a simple direct delay feedback that considered for the chaotic semiconductor laser [28]. The motivation behind this attempt is the necessity of suppressing the possible double peak structure of the pulses obtained from the directly modulated InGaAsP laser diode. We show numerically that the unstable periodic orbits of the chaotic laser also contain the second maxima and the proposed direct delay feedback scheme can be used to suppress it. The performance of these two methods are compared using different computational tools such as times series plots, phase portraits, power spectra etc.

Since high-speed modulation of semiconductor lasers has vast applications in photonics technology, the study of nonlinear dynamics of laser diodes is relevant in the research in photonics and related areas. A clear understanding of the operating conditions where these lasers show chaos and other nonlinear phenomena would be useful in designing high quality optical and optoelectronic systems using laser diodes for the purposes such as optical communications [4] and optical signal processing [5]. However, it is not necessary to avoid the chaotic regimes completely for practical applications. Various techniques have been developed for controlling and suppressing chaos in different kinds of nonlinear systems [6, 7, 8, 9, 10, 11]. The basic idea behind most of these control schemes is that the

unstable periodic orbits embedded in the chaotic attractors can be stabilized using small perturbations. Besides eliminating chaos, chaos-control techniques are useful in the tracking of unstable periodic orbits [14]. Practically, it is a difficult task to visualize the unstable periodic orbits existing in a chaotic attractor without stabilize them.

3.1 Controlling chaos using a self adjusting delayed optoelectronic feedback

We first consider a delayed optoelectronic feedback based on the well known Pyragas method for controlling chaos in directly modulated lasers. There are certain reasons for choosing this particular control scheme. The method of Ott, Grebogi and Yorke (OGY scheme) [6] is the earliest and well discussed chaos-control method based on stabilization of the unstable periodic orbits(UPOs). Even though it has been successfully applied for control of many chaotic systems in various disciplines [7, 15], it has two important disadvantages. In this method, a real time computer assistance (computer interface) is needed for applying the perturbations to the chaotic system. Hence, ultra fast computation is required if the OGY method is chosen for controlling a high-speed modulated laser system. The second disadvantage is that the OGY method is already known to be highly sensitive to noise, i.e, the presence of noise in the original system causes intermittent bursts in the output of the controlled system. On the other hand, targeting and periodic perturbation require additional external signals and this make the problem more difficult. Pyragas method is based on a self adjusting delay feedback and the perturbation applied to the system does not contain any external signals and no computer interface is required for the implementation of the scheme. It has been shown that TDAS is successful in the presence of considerable amount of noise in the system. This method has successfully been applied for a variety of chaotic systems such as electronic circuits [27, 21, 22, 23], glow discharge [24], magneto-elastic ribbon [25], and periodically driven yttrium iron garnet film [26]. Recently this technique has also been employed for stabilizing high period orbits in a CO2 laser [27].

3.1.1 Model of the control scheme

Output of the considered chaotic system is optical and an easily accessible input variable of the system is the injection current. Thus we consider a delayed optoelectronic feedback scheme based on Pyragas method for controlling chaos in directly modulated semiconductor lasers and investigate the performance of such a scheme using numerical simulation. The schematic diagram of the laser system with the proposed control set up is given in the

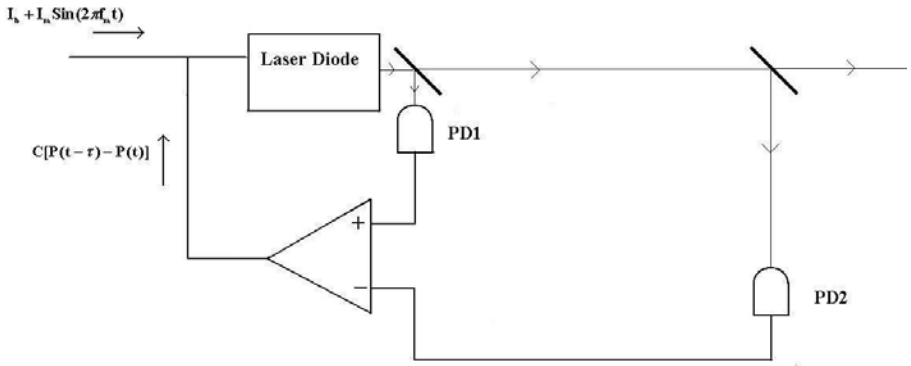

Figure 3.1: Schematic diagram of laser with self adjusting delayed optoelectronic feedback

Fig.3.1. There are two photo diodes (PD1 and PD2) as shown in the figure. These photodiodes must have high bandwidths which are sufficient for using them in GHz frequency domain. The optical signal from the laser reaches the photodiodes through different paths. A delay exists between the laser pulses incident on PD1 and PD2 and it is determined by the difference in the optical path lengths of the laser beams incident on the photodiodes. According to Pyragas, this delay must be equal to the period of the specific UPO that is to be stabilized. It would be a few nanoseconds and can be provided by the external transit of light through a predetermined distance of the order of centimeters. The desired value of delay can be obtained by adjusting the distance between the mirrors shown in the figure. PD1 and PD2 can convert the optical signals incident on them into current signals. These current signals should be given as the inputs of a differential amplifier. Let the photon density of the laser at the instant t is $P(t)$. PD1 gives a current signal proportional to $P(t)$ and the signal from PD2 would be proportional to $P(t-\tau)$, where τ is the time delay produced by the external transit of light. Thus, the output of the differential amplifier can be expressed as $C\big[P(t-\tau) - P(t)\big]$, where C is the feedback strength that is determined by the gain of the amplifier. This feedback signal can be applied as a time-continuous perturbation along with the injection current.

The dynamical equations of the above laser system can be given by

$$\frac{dN}{dt} = \frac{1}{\tau_e}\left(\frac{I}{I_{th}} - N - \frac{N-\delta}{1-\delta}P\right) \tag{3.1.1}$$

$$\frac{dP}{dt} = \frac{1}{\tau_p}\left(\frac{N-\delta}{1-\delta}(1-\epsilon P)P - P - \beta N\right), \tag{3.1.2}$$

with an injection current,

$$I = I_b + I_m sin(2\pi f_{mt}) + C\big[P(t-\tau) - P(t)\big], \tag{3.1.3}$$

Eqns. 3.1.1 and 3.1.2 are the rate equations of the laser given in Chapter 2. The definitions of the parameters and their numerical values (Table 2.1) are given in the same chapter. The expression of injection current is obtained by modifying Eq.2.6.1 by including the feedback signal $C\big[P(t-\tau) - P(t)\big]$. Here, I_b is the bias current, I_m is the amplitude of modulation and f_m is the frequency of modulation.

3.1.2 Results and discussion

We have numerically simulated the model equations 3.1.1, 3.1.2 and 3.1.3 of the control scheme using fourth order Runge-Kutta alogirthm [21]. The bias current I_b is chosen as $26mA$. The amplitude and the frequency of modulation are taken as I_m=$0.55I_{th}$ and f_m= 0.8GHz respectively, where I_{th} is the threshold current. The uncontrolled laser with these parameters behaves chaotically. There are two parameters associated with the delayed feedback. The first one is the feedback delay time. In the TDAS algorithm, the value of delay is equal to the period of the unstable periodic orbit (UPO). As described in Chapter 2, the period of the fundamental or period 1 cycle of the modulated laser is equal to the inverse of the frequency of modulation . Actually it is true for all driven chaotic systems following period doubling route to chaos. As the modulation depth is increased, the period 1 cycle and each of its subharmonic states will become unstable at certain points and new stable orbits are created. The unstable orbits exists in the attractor corresponding to each state. Chaotic orbits are created after an infinite number of period doubling bifurcations and hence an infinite number of unstable orbits are embedded in the attractor. Out of these orbits, we are interested only in the period 1 unstable cycle because the stabilization of this orbit yields the simple short optical pulses for practical applications. Considering the facts discussed here, we can definitely say that the period 1 UPO has a period $T = 1/f_m$. Thus the value of delay that is to be used for controlling chaos in a laser diode modulated by a current signal of frequency $f_m = 0.8GHz$ is $\tau = 1.25ns$. The remaining parameter is the feedback strength C. This is usually selected by trial and error method. The feedback is applied in such a manner that the perturbation term would vanish if the UPO is stabilized. Hence the deviation of the trajectories of the system from the desired UPO can be characterized by the strength of the perturbation. The instantaneous value of the deviation from the

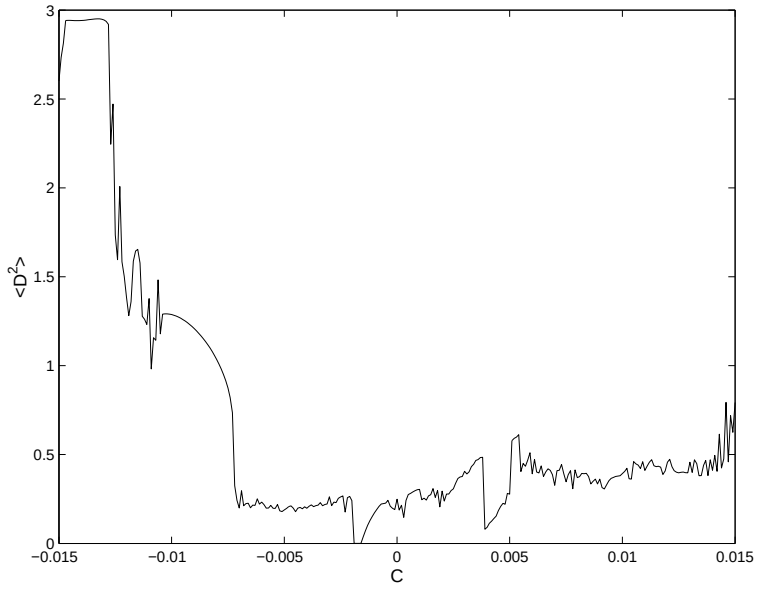

Figure 3.2: Variation of the mean squared deviation from the period 1 orbit versus feedback strength.

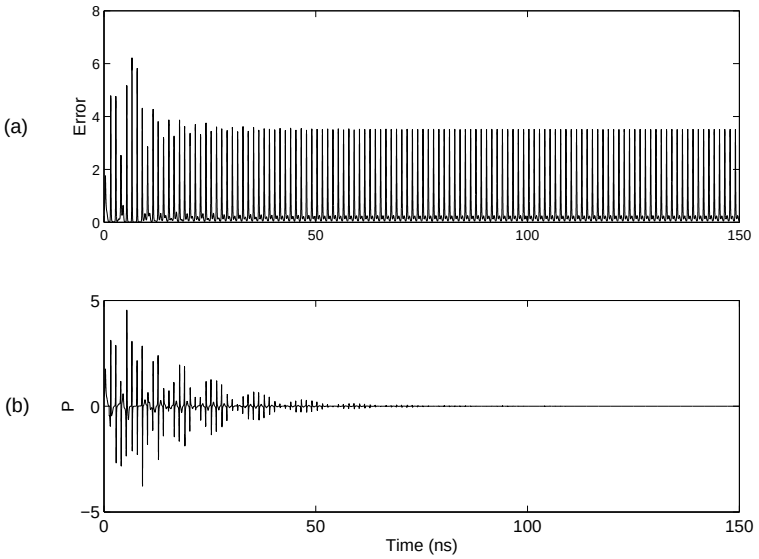

Figure 3.3: Stabilization of period 1 orbit: Time series of (a) photon density (b) $D = P(t-\tau) - P(t)$, the difference of outputs of current state and delayed state of the laser , $\tau = 1.25ns$, $C = -0.0018$.

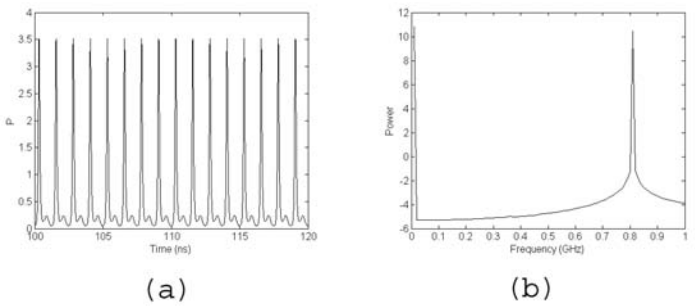

Figure 3.4: The stabilized output of the laser with self adjusting delay feedback (a) time series , (b) power spectrum. $C = -0.0018$.

periodic orbit is given by

$$D(t) = P(t - \tau) - P(t) \tag{3.1.4}$$

As described in ref.[26], we have calculated the dispersion or the mean squared average of D for a range of feedback strengths. Fig.3.2 shows the variation of this quantity with feedback strength. It is found that the perturbation will completely vanish for all the values of feedback strengths that lies between the limits -0.0019 and -0.0017.

The time series of the laser output corresponding to a feedback of strength $C = -0.0018$ is given in the Fig.3.3(a). The transient state before reaching the periodic state can also be seen in the figure. Fig.3.3(b) show the deviation D of the trajectory from period 1 state. The perturbation is C times this quantity and it vanishes within a few nanoseconds. The time series of photon density after vanishing of the transients is shown in Fig.3.4(a) and its power spectra is given in Fig.3.4(b). From these plots, we can deduce that the period 1 orbit is stabilized. Further, it is obvious from the time series that the output of the controlled laser has a double peaked structure. Phase portrait (P vs N) of the controlled laser (Fig.3.5) also show that the controlled orbit has two maxima.

We use a method based on return maps to verify whether the stabilized orbit is the original UPO itself. It is possible to construct a deterministic discrete map from a continuous dynamical system by several ways such as Poincare sections, maxima or minima of a single variable etc. However we use another approach called stroboscopic section which is commonly used for low dimensional driven chaotic systems [7]. In this method, the system variables in the phase space is periodically sampled with an interval that is equal to the period of the driving signal. Here the state variables P and N are sampled when the phase of the modulating signal is equal to $2(n + 1)\pi$, where $n = 0, 1, 2, 3....$

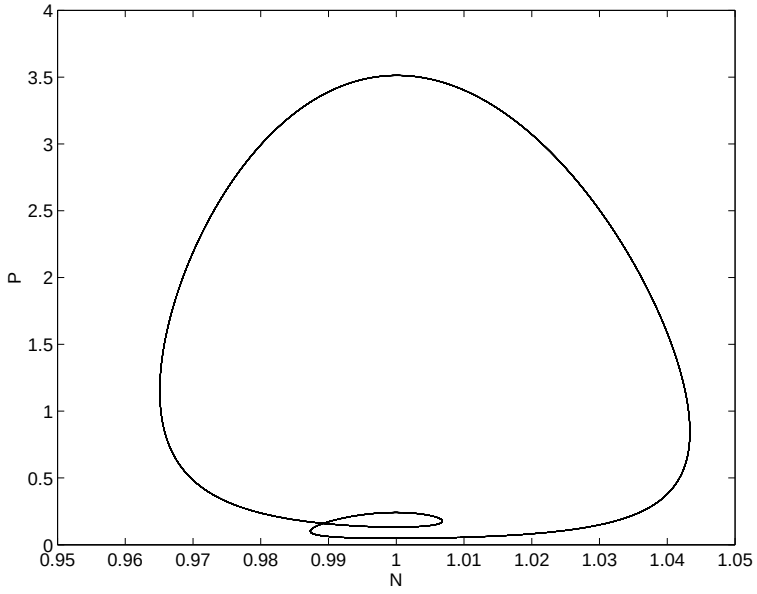

Figure 3.5: Phase portrait of the stabilized period 1 orbit. $C = -0.0018$.

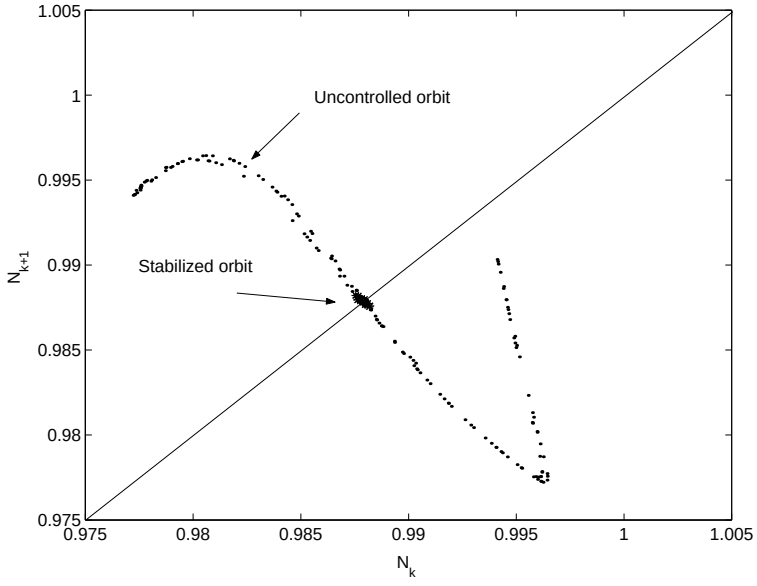

Figure 3.6: First return map of the laser: The position of the controlled orbit is shown with the arrow. $C = -0.0018$.

The first return map($N_{k+1}\, vs\, N_k$, $k = 1, 2...$) of the consecutive values of carrier densities obtained by the stroboscopic section of chaotic laser output is shown in Fig.3.6. There is an unstable fixed point in the map $N_{k+1} = N_k = 0.9882$ that corresponds to the unstable period 1 orbit. It is found that the return map obtained from the stroboscopic section of controlled orbit consists of a single point which exactly coincides with the the original unstable fixed point. This is a clear evidence to confirm that the original UPO is stabilized and the controlled orbit is not a new orbit formed as a result of feedback.

3.2 Suppression of chaos and double peak structure of pulses using a direct delayed optoelectronic feedback

It has been shown in the previous section that a self adjusting delayed optoelectronic feedback is sufficient to bring the system to period 1 state from chaos and if the control is achieved, the perturbation applied to the system would have vanished. If the period 1 output does not contain a double peaked structure this method is practically successful. Since double peaks are common in practical situations [17], we should look for an alternate feedback method which is capable for changing the structure of the stabilized orbit. From the point of view [14] of chaos-control, the control scheme must have two main distinctions. 1)The perturbation must vanish or be negligibly small 2) The structure of the original UPO should be retained. However, for technical applications using the semiconductor laser, there is no practical difficulty due to the existence of a non vanishing perturbation signal that acts upon the system provided that the system has a stable and regular operation. On the other hand, change in the structure of the period 1 orbit is desirable since a well-shaped pulse can be produced by this process. A perturbation signal applied in the Pyragas method vanishes after the control is achieved because it is self adjusting or adaptive. A better choice for a non vanishing feedback signal is a direct optoelectronic feedback. That is, a current directly proportional to the photon density (and hence the output power) is fedback to the laser. A delay is also incorporated with the feedback and that can be provided by the external transit of light signal. Effect of delay in the feedback is also studied numerically and we show that the delay enhances the suppression and it can reduce the value of minimum feedback strength required for the suppression of chaos.

A direct delayed optoelectronic feedback has been already shown to be successful in the generation of chaotic optical signals which are useful in chaotic secure communication [19]. However, we show that the same technique can be used in suppression of chaos also.

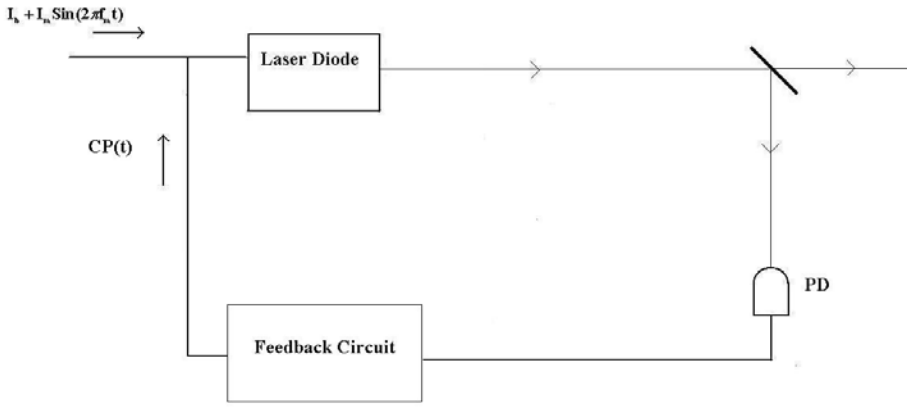

Figure 3.7: Schematic diagram of laser with a direct delay feedback

3.3 Model of the control scheme

The schematic diagram of the laser with direct delayed optoelectronic feedback is shown in Fig.3.7. The control set up differs from the self adjusting feedback in two ways. There is only one photo diode (PD). Secondly, the differential amplification is not required and the feedback signal proportional to the photon density corresponding to the delayed state ($P(t-\tau)$) is applied as the perturbation. The instantaneous value of this signal can be expressed as $CP(t-\tau)$ where C is the feedback strength determined by the gain of the amplifier and τ is the delay. Thus the expression for the injection current is given by

$$I(t) = I_b + I_m sin(2\pi f_m t) + CP(t-\tau) \tag{3.3.1}$$

3.4 Results and discussions

There was only a single parameter in TDAS control scheme for diectly modulated semiconductor laser- the feedback strength C. It was already known that the value of the other parameter, delay $\tau = 1.25ns$ must be equal to the period of the modulating current signal. However, in the direct delay feedback, our aim is not to stabilize any UPO present in the chaotic attractor, but to create a new period 1 orbit with out double peaked structure using the feedback. Therefore, our attempt is to study the behavior of laser for a considerable

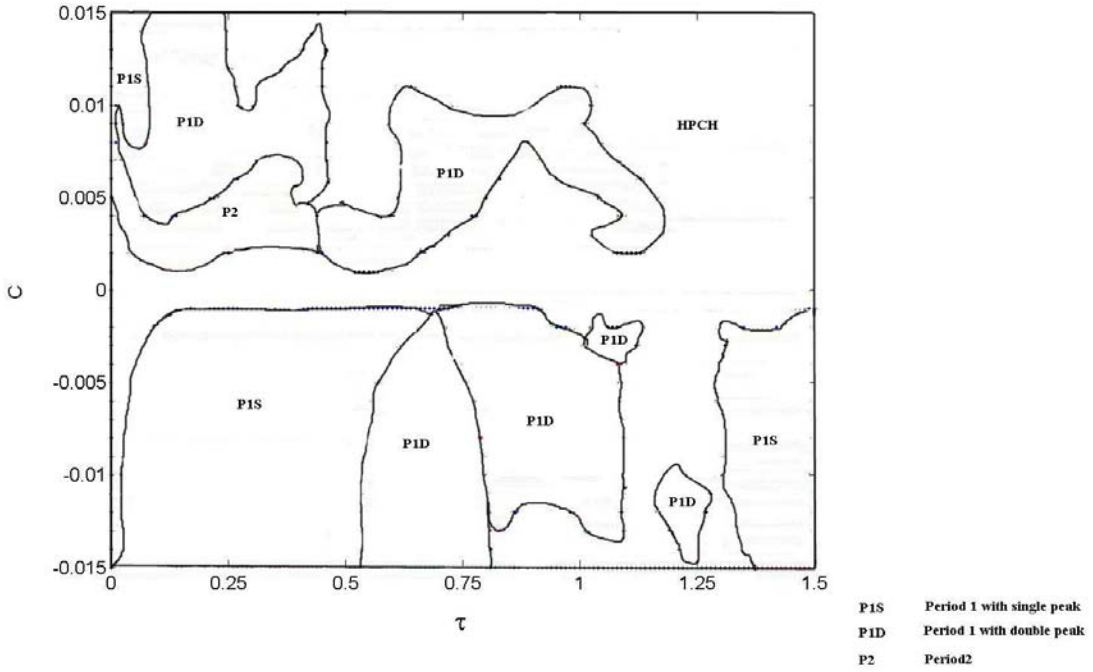

Figure 3.8: Global bifurcation diagram of the laser with direct delayed optoelectronic feedback.

range of parameters C and τ. Then an optimal combination of delay and feedback strength yielding the desired performance can be selected from the information obtained in this way. The delay is varied from 0 to an upper limit of 1.5ns. Both positive and negative feedback is considered and therefore the feedback strength C is varied from -0.015 to 0.015 and the behavior of the laser is studied. The parameter space defined by τ and C is classified into different regimes such as chaotic, higher subharmonic, lower subharmonic(period 2, period 4 etc.), period 1 with double peak and period 1 without double peak. The global bifurcation diagram showing these regimes is shown in Fig.3.8.

Different kinds of bifurcation phenomena can be observed when the parameters of the delay feedback is varied. Delay feedback systems are well known examples of infinite dimensional dynamical systems which show very complex bifurcations [9]. Reverse bifurcations are very common in delay feedback systems. In the context of suppression of chaos in lasers, such bifurcations deserve particular attention. The bifurcation diagram shown in Fig.3.8. gives a general understanding of the regions in parameter space where the laser shows chaotic and periodic behavior. As mentioned earlier, period 1 state has been given the highest importance considering its application in short pulse generation. Period 2 regions are also shown in the figure. However, they are relatively narrow compared to the period 1 regions. The regions corresponding to Period 4 and higher periodic states are too narrow to be described separately in the global bifurcation diagram. Thus they are combined with the chaotic region and shown in the diagram as a single region. Very small areas corresponding to the period 2 states are also omitted from the diagram. In addition to the periodic portions shown in Fig.3.8, there are certain regimes in chaotic region where the sudden formation of low periodic states are taking place. The single parameter bifurcation diagrams given in the next two sections provide a detailed view of such transitions.

3.5 Reverse bifurcations: The routes through which the laser acquires periodicity from chaos

If we look at the global bifurcation diagram carefully, we can see that as the feedback strength is increased (keeping delay as a constant) the dynamical state of the laser is changed from chaos to period 1. Here we present the variation of dynamical behavior of the system with the change of a single parameter (the feedback strength C), which is changed from 0 to an upper limit 0.015. We first consider the positive feedback case. Since our aim is to obtain the period 1 state without double peak, we select the delay that gives such output ($\tau = 0.05ns$). The bifurcation diagram is given in Fig.3.9. This diagram is drawn by calculating the maxima of the photon densities in every modulating cycles. (There may be

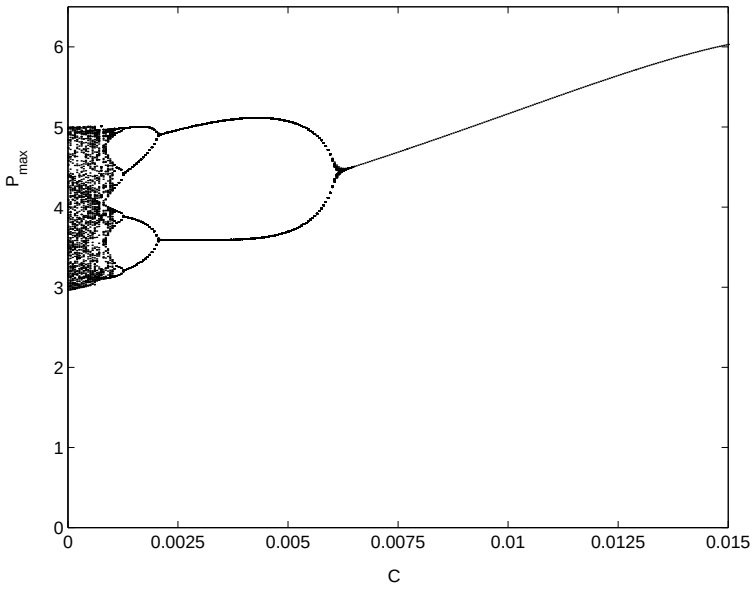

Figure 3.9: Bifurcation diagram: maxima of photon density vs feedback strength. $\tau = 0.05ns$

two maxima in every cycle and the maxima corresponding to the main peaks only are taken). This is is done for a range of feedback strength and the set of peak values of photon densities is plotted against feedback strength. It can be seen that an infinite number of reverse period doubling takes place and finally the system arrives at period 1 state. The elimination of the double peak structure is demonstrated by a different bifurcation diagram (Fig.3.10) that includes the second maxima also. It is possible by taking the values of photon densities corresponding to all the maxima of the pulse instead of taking the maxima in each modulation cycle. There are two distinct portions in the bifurcation diagram. The upper portion is already present in the bifurcation diagram shown in Fig.3.9 and the lower portion is expected to represent the second peaks. The peaks corresponds to the second maxima are always shorter compared to the main peaks. The attractor points corresponding to the second peaks can easily be distinguished from the main peaks. It is clear from Fig.3.9 that there is no attractor point corresponds to the main peak below the value 3. All the attractor points in the lower portions have the values less than 1. Hence we can confirm that the lower portion of the bifurcation diagram shown in Fig.3.10 is the contribution of the second maxima only.

Fig.3.10 shows that there is only a single attractor point corresponds to each value

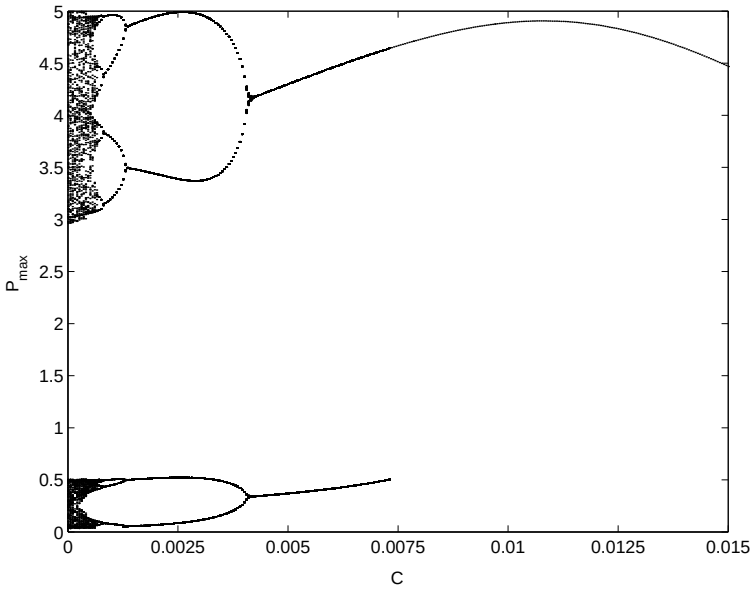

Figure 3.10: Bifurcation diagram: maxima of the photon densities (second maxima in the modulating cycles are also included) vs feedback strength, $\tau = 0.05ns$

of feedback strength greater than 0.0075 and it implies that the second maxima of the laser-pulse is absent for these set of parameters.

The suppression of chaos with the feedback of delay $\tau = 0.05ns$ is further demonstrated by time series and power spectra. For the feedback strength $C = 0.001$ the laser has become period 4 (Fig.3.11). The laser yields the period 2 output (Fig.3.12) and period 1 output (Fig.3.13) for feedback strengths 0.002 and 0.0045 respectively . However, the double peak is still there in the period 1 pulses. As obtained from the bifurcation diagram (Fig.3.10) period 1 optical pulses without double peaks are obtained for a feedback strength (C=0.008) and it is given in Fig. 3.15. The reverse period doubling is illustrated using phase portraits (carrier density vs photon density) also. Fig.3.15 shows the phase portraits of different states which are given in Figs. 3.12-3.14. For $C = 0.0045$ (Fig.3.15(d)), the period 1 orbit has a double cusp that corresponds to the second maxima. Even though the second maxima is absent in the orbit shown in Fig.3.15(d), there are some distortions present in the orbit.

Besides the suppression of chaotic behavior in the laser, a delayed optoelectronic feedback with proper feedback strength can completely eliminate the subharmonic generation that is produced due to the modulation. The bifurcation diagrams of the laser with and without the delay feedback is given in Fig.3.16. Fig. 3.16 (a) shows the bifurcation diagram

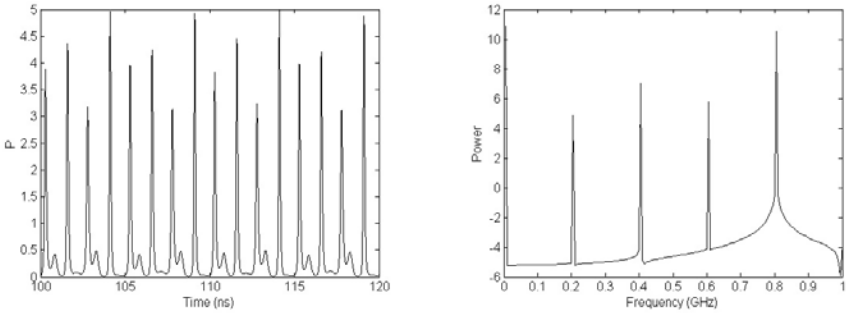

Figure 3.11: Period 4 output: (a) time series (b) power spectrum, $\tau = 0.05ns$, $C = 0.001$

,

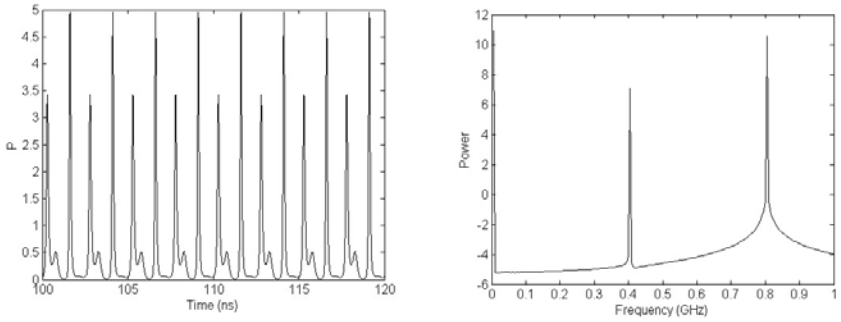

Figure 3.12: Period 2 output: (a) time series (b) power spectrum, $\tau = 0.05ns$, $C = 0.002$

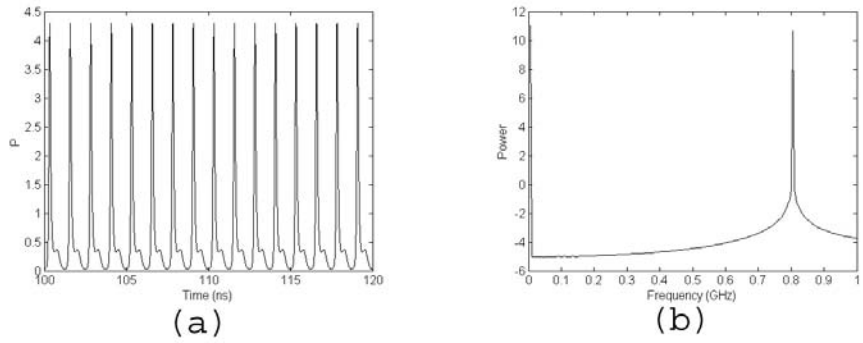

Figure 3.13: Period 1 output: (a) time series (b) power spectrum, $\tau = 0.05ns$, $C = 0.0045$

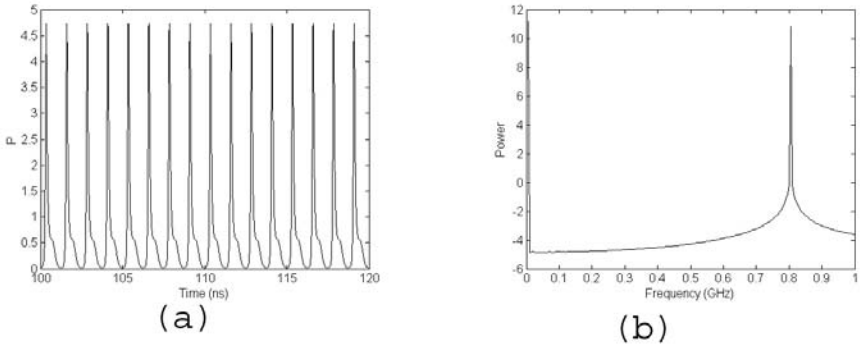

Figure 3.14: Period 1 output without double peak: (a) time series (b) power spectrum, $\tau = 0.05ns$, $C = 0.008$

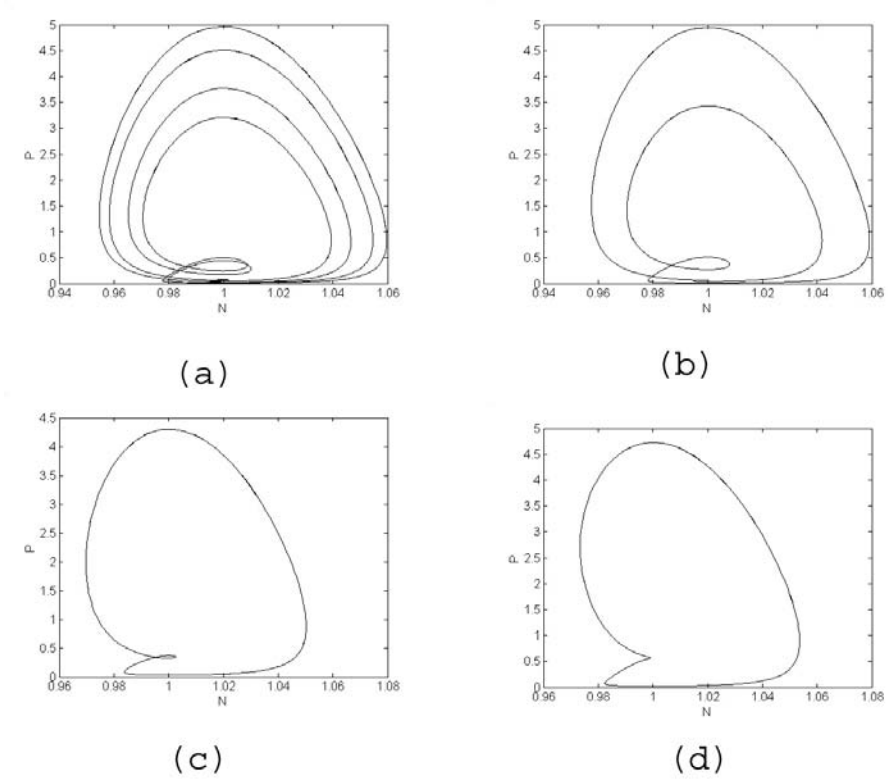

Figure 3.15: Phase portraits (photon density vs carrier density): (a)period 4 cycle($C = 0.001$), (c) period 2 cycle ($C = 0.002$), (d) period 1 cycle ($C = 0.004$), (e) period 1 cycle without double peak. ($C = 0.008$).$\tau = 0.05ns$.

(maxima of photon density P_{max} vs modulation depth m) of the laser without feedback. The period doubling and reverse period doubling sequences are present in the diagram. Fig.3.16 (b) shows a similar bifurcation diagram of the laser with a feedback of delay $\tau = 0.05ns$ and feedback strength $C = 0.008$. This diagram shows only a smooth increase in output power with the increase of modulation depth.

Negative feedback can also be considered for the purpose of suppression of chaos. Fig.3.17 show the bifurcation diagram showing the transition of laser from chaos to periodicity due to the effect of a delayed negative feedback. The transition is not through reverse period doubling bifurcations and the structure of the attractor has changed abruptly from chaos to period 1. The output of the controlled laser does not have a double peaked structure. The time series, power spectra and phase portrait of this output is given in the Fig.3.18. The pulse is very sharp and its peak-power is greater than that of the UPO of the laser which is stabilized by TDAS algorithm. The phase portrait of the laser shows that the structure of the period 1 orbit formed due to the negative feedback is much symmetric and well-shaped when compared to the orbit obtained by positive feedback. The feedback strength required for obtaining single-peaked pulse is relatively lower than the positive feedback case.

3.6 The Significance of delay in suppression of chaos

There are certain regions in the diagrams showing that the suppression of chaos is possible without delay. However, the feedback strength corresponding to this regions is relatively high. It is clear from the global diagram that delay can enhance suppression of chaos. A considerable increase of delay can reduce the necessary value required for getting the period 1 output. We can confirm this result by a single parameter bifurcation diagram where delay is varied and feedback strength is kept constant. Fig.3.19 shows such a diagram. Feedback strength is taken as -0.002. In this case, the laser show sudden transformation from chaos to periodic state as delay is increased. If delay is increased to very high values, the laser becomes unstable again and certain subharmonic states are generated for these values of delay and disappeared shortly. Thus it is better to choose small delays for achieving suppression of chaos.

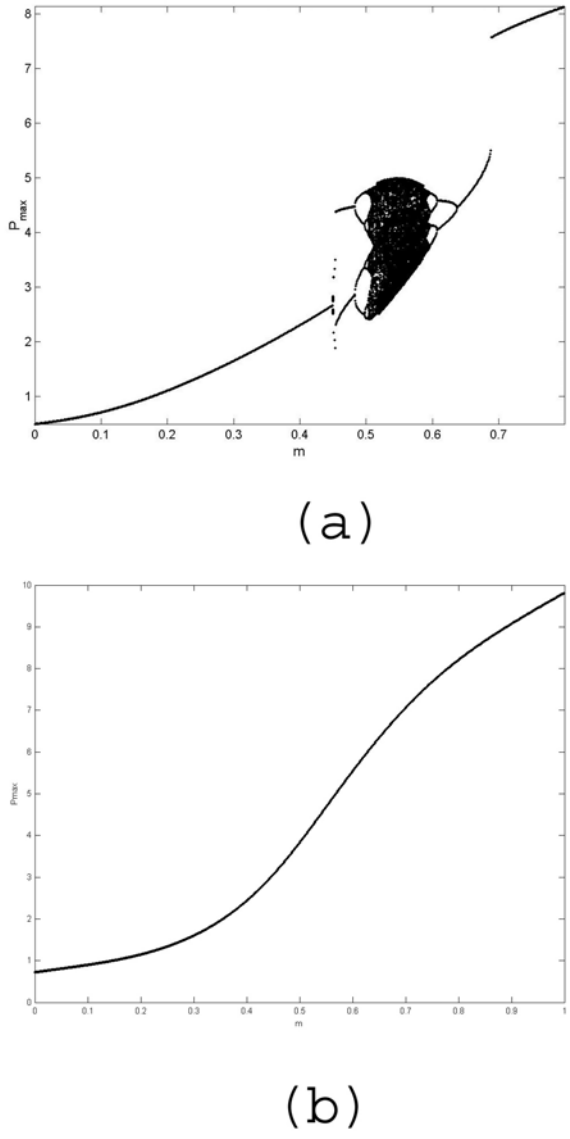

Figure 3.16: Bifurcation diagrams: maxima of the photon density vs modulation depth, $\tau = 0.05ns$, (a) $C = 0$.(b)$\tau = 0.05ns, C = 0.008$

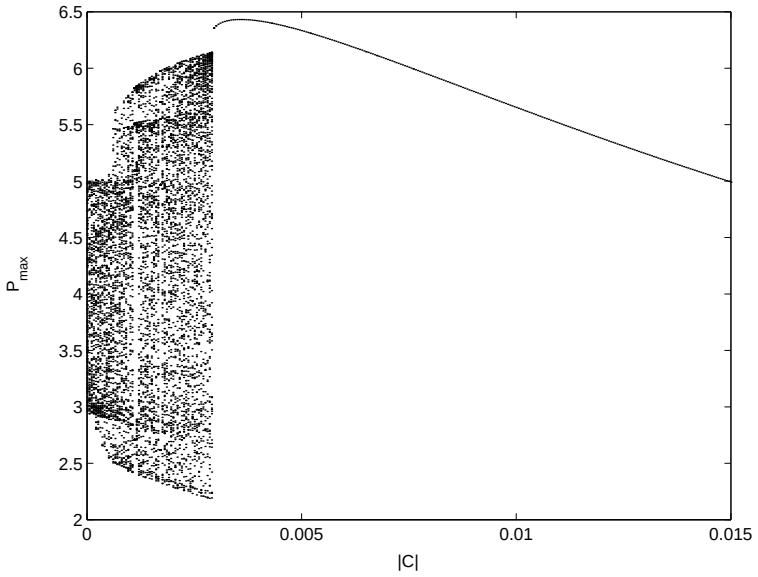

Figure 3.17: Bifurcation diagram: Maxima of the photon density vs magnitude of feedback strength.$\tau = 0.09ns$

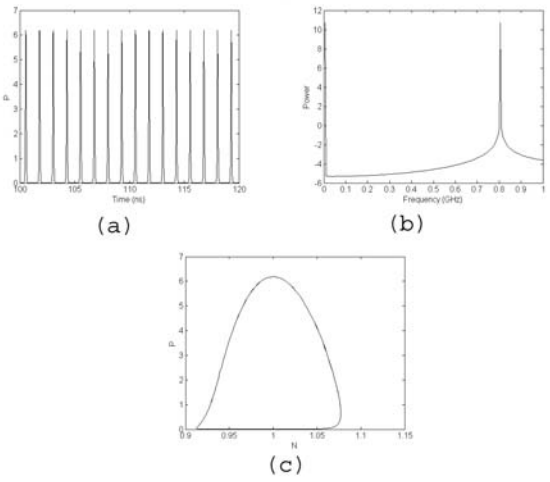

Figure 3.18: Period 1 pulse without double peak: negative feedback case- (a) time series (b) power spectrum (c)phase portrait. $\tau = 0.09ns$, $C = -0.0045$

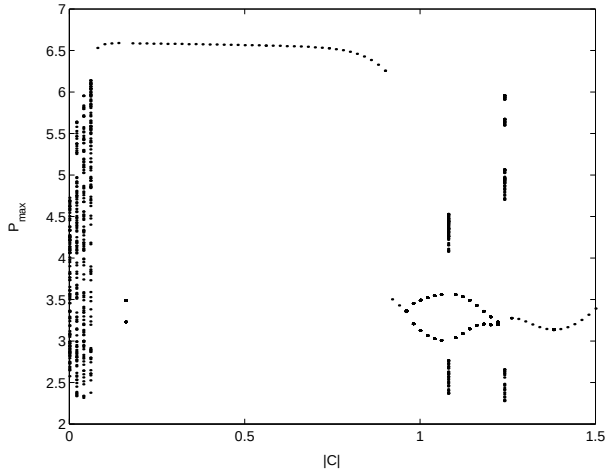

Figure 3.19: Bifurcation diagram: Maxima of the photon density vs delay in nano seconds.$C = -0.002ns$

3.7 Conclusion

Two different feedback-control schemes for directly modulated semiconductor lasers is studied. The effects of delayed optoelectronic feedback on a directly modulated InGaAsP laser diode is numerically investigated using both TDAS and direct delay feedback models. TDAS control scheme has certain advantages. The perturbation will practically vanish after the control is achieved. However it cannot be used in the practical situations where double peak is present in the laser pulse. The nonvanishing type direct delay feedback is shown to be successful in suppressiong chaos, subharmonic generation and double peak structure in pulse. The direct delay feedback is commonly used for generating chaos. However in this work we have shown similar type of feedback can efficiently be used for controling chaos. It is found that both negative and positive feedback can be used for the control. Negative feedback gives sharp periodic outputs of greter power for relatively low feedback levels. From the results presented in this chapter, we can conclude that the delayed optoelectronic feedback is an efficient method for controlling chaos, subharmonic generation and double peaked structure of pulses in directly modulated semiconductor lasers.

Bibliography

[1] K Pyragas, Phys. Lett.A **170** (1992) 421

[2] K.Pyragas, Phys. Lett. A **181** (1993) 99

[3] S. Rajesh and V. M. Nandakumaran, Phys. Lett. A **319** (2003) 340

[4] G. P. Agrawal, *Fiber-optic communication systems* (John Wiley and Sons, New York (1992)

[5] J. Mørk and A. Mecozzi, J. Opt. Soc. Am. B., **13** (1996) 1803

[6] E. Ott, C. Grebogi, and J. A. Yorke, Phys. Rev. Lett. **64** (1990) 1196

[7] W. L. Ditto, S. N. Rouso and M. L. Spano, Phys. Lev. Lett. **65** (1990) 3211

[8] B. Huberman and H.L. Lumer, IEEE Trans. Circuits Syst. **37**, (1990) 547

[9] S. Sinha, R. Ramaswamy and J. Subba Rao, Physica D **43** (1990) 118

[10] R. Lima. and M. Pettini, Phys. Rev. A **41** (1990) 726

[11] P.Colet, Y.Braiman, Phys.Rev.E **53** (1996) 200

[12] T. Kuruvilla and V. M. Nandakumaran, Phys. Lett. A **254** (1999) 39

[13] V. Bindu and V. M. Nandakumaran, Phys. Lett. A **227** (2000) 345

[14] M. Ding, E. J. Ding, W. L. Ditto B. Gluckman, V. In, J. H. Peng M. L. Spano and W. Yang, Chaos **7** (1997) 644

[15] R. Roy, T. W. Murphy Jr., T. D.Maier, Z. Gills, E. R. Hunt, Phys. Rev. Lett.**68** (1992) 259

[16] T. S. Parker and L. O. Chua, Practical numerical algorithms for chaotic systems, Springer-Verlag, New York (1989)

[17] M. Tang and S. Wang, Appl. Phys. Lett. **47** (1985) 208

[18] S. Tang and J.M. Liu, IEEE J. Quantum Electron. **37** (2001) 329.

[19] K. Ikeda and K. Matsumoto Physica D **29** (1987) 223

[20] K.Pyragas, Phys. Lett. A **181** (1993) 99

[21] C.Batlle, E. Fossas, G.Olivar, Int. J. Circuit Theory and Applications **27** (1999) 617

[22] D. J. Gauthier, D. W. Sukow, H. M. Concannon, J. E. S. Socolar, Phys. Rev. E **50** (1994) 2343

[23] A. Namajunas, K Pyragas, A. Tamasevicius, Phys. Lett. A **204** (1995) 255

[24] Th. Pierre, G. Bonhomme, A. Atipo, Phys. Rev. Lett. **76** (1996) 2290

[25] T. Hikihara and T. Kawagoshi, Phys. Lett. A **211** (1996) 29

[26] M. Ye, D. W. Peterman, P. E. Wigen, Phys. Lett. A **203** (1995) 23

[27] F.T.Arecchi, R.Meucci, E.Allaria, A.DiGarbo , L.S.Tsimring, Phys.Rev.E **65** (2002) 046237 g572

[28] K. Ikeda and K. Matsumoto, Physica D **29** (1987) 223

Chapter 4

Control of chaos in directly modulated self pulsating semiconductor lasers

Quasiperiodicity is a familiar phenomenon in nonlinear dynamical systems like any other effects such as period doubling, chaos and multistability. A forced van der Poll oscillator is a well known example for quasiperiodic systems [18]. Many physical systems like fluid flows [3, 4, 5] mechanical oscillators [27], electronic circuits [6, 7] and lasers [8, 9, 10, 11, 12, 22] show quasiperiodic behavior and quasiperiodicity route to chaos. Most of these systems have practical applications and they are generally operated in static or periodic mode. Hence, quasiperiodic behavior is generally unwanted and it must be eliminated from these systems. The efforts towards this direction deserve considerable attention. However, very few attempts have been reported on the control of quasiperiodicity [16, 17, 18] when compared to the works on the control of chaos in nonlinear systems . This is because of the fact that the methods for controlling chaos are mainly based on the stabilization of unstable periodic orbits and there are no such orbits on the attractors (tori) associated with quasiperiodicity.

Many types of laser systems show quasiperiodicity and quasiperiodic route to chaos [8, 9]. Semiconductor lasers also show such phenomena under various circumstances such as external optical feedback [10, 11] and optical injunction [12] and direct modulation [22]. Self pulsating laser diodes follow quasiperiodicity route when they are modulated directly. The numerical and experimental investigations done by Winful *et. al.* have revealed many interesting features of quasiperiodicity route to chaos [22]. The quasiperiodic and chaotic behavior shown by the directly modulated self pulsating lasers are numerically illustrated in Chapter 2. Since high speed modulation of semiconductor lasers has practical

applications, we consider the possible methods for controlling quasiperiodicity and and chaos in such lasers. Considering the practical issues of controlling a high frequency laser system, the delay feedback can be chosen for these purposes. The performance of two different delay feedback schemes (TDAS) and direct delay feedback) are compared using numerical simulations [14, 15].

4.1 Failure of TDAS method in stabilizing the period 1 orbit

Delayed optolectronic feedback based on the Time Delay Auto Synchronization (TDAS) algorithm can be considered for controlling chaos in the self-pulsating laser diode as in the case of modulated InGaAsP lasers. The results of the numerical investigations on the effect of a self adjusting delayed optoelectronic feedback on a modulated self pulsating laser operating in the chaotic regime is presented in this section. The proposed setup of the control scheme is the same that is given in Fig.3.1 of chapter 3.

The laser system with the control can be modelled by the set of equations given by

$$\frac{dp}{dt} = \Big[a_1\xi_1(n_1 - n_{g1}) + a_2\xi_2(n_2 - n_{g2}) - G_{th}\Big]p + b\frac{n_1 V_1}{\tau_s} \tag{4.1.1}$$

$$\frac{dn_1}{dt} = -\frac{a_1\xi_1}{V_1}(n_1 - n_{g1})p - \frac{n_1}{\tau_s} - \frac{n_1 - n_2}{T_{12}} + \frac{I}{qV_1} \tag{4.1.2}$$

$$\frac{dn_2}{dt} = -\frac{a_2\xi_2}{V_2}(n_2 - n_{g2})p - \frac{n_2}{\tau_s} - \frac{n_2 - n_1}{T_{21}} \tag{4.1.3}$$

where

$$I = I_b + I_m sin(2\pi f_m t) + C \times 10^{-6}\big[p(t) - p(t-\tau)\big], \tag{4.1.4}$$

is the injection current, C is the feedback strength and τ is the feedback delay time.
The Eq. 4.1.1, 4.1.2 and 4.1.3 are the rate equations of the self pulsating laser diode described in chapter 2. There are three variables in the equations , i.e. , the carrier density n_1 in the gain region, the carrier density n_2 in the saturable absorbtion region and the photon density p. Definitions and numerical values of the parameters of the laser are given in the same chapter. The bias current I_b and the frequency of modulation f_m is chosen as 30mA and 1.25GHz respectively. The laser without feedback show quasiperiodicity and chaos for these values of parameters The feedback signal is almost similar to that given in the case of InGasAsP laser. However, a constant (10^{-6}) is included in the expression of the feedback signal. This is because the photon density is not normalized and it is in the order of $10^6 m^{-3}$.

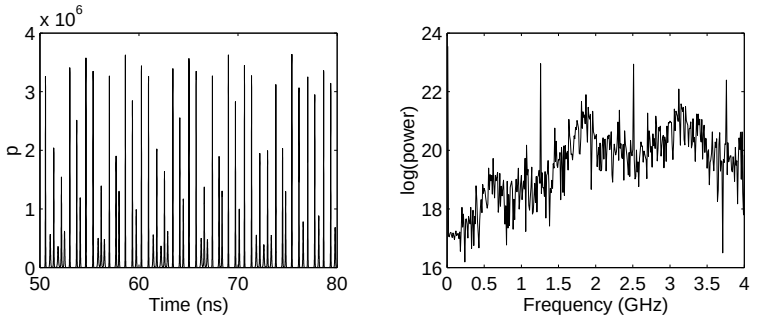

Figure 4.1: Chaotic output of the laser without feedback: (a) time series (b) power spectra. I_m=7mA.

4.2 Results and discussions

We have simulated the dynamical behavior of the laser system represented by Eqns. 4.1.1, 4.1.2, 4.1.3 and 4.1.4. As obtained in the earlier observations, the laser shows chaos for relatively high values of modulation amplitudes. The chaotic output of the laser with a modulation of amplitude 7mA is given in Fig.4.1(a). Fig.4.1(b) show the broadband power spectra of this output. Since period 1 pulses have many practical applications, our attempt is to stabilize the period 1 orbit of the chaotic laser. The perturbation applied to the laser is proportional to the quantity that is given by

$$D(t) = p(t-\tau) - p(t) \tag{4.2.1}$$

To determine the possible regimes of control, the mean squared average of D is calculated for a range of feedback strengths from -0.02 to 0.02. The delay is taken as $\tau = 0.8ns$ which is the inverse of the modulating frequency ($f_m = 1.25GHz$). The dispersion $< D^2 >$ is plotted in Fig.4.2 as a function of feedback strength. There is no region in the plot where the dispersion vanishes completely. Hence it can be deduced that a self adjusting delayed optoelectronic feedback based on the TDAS algorithm is unable to stabilize a period 1 orbit of the modulated self pulsating laser. Let us discuss why the TDAS based control method fails in controlling the chaos in self pulsating laser. It is already known that the the TDAS scheme does not guarantee the stabilization of all kind of periodic orbits. It will not work in the case where the specific periodic orbit is highly unstable or having a high torsion [19]. Socolar and Gauthier [20] have been shown that the domain of control of TDAS method is

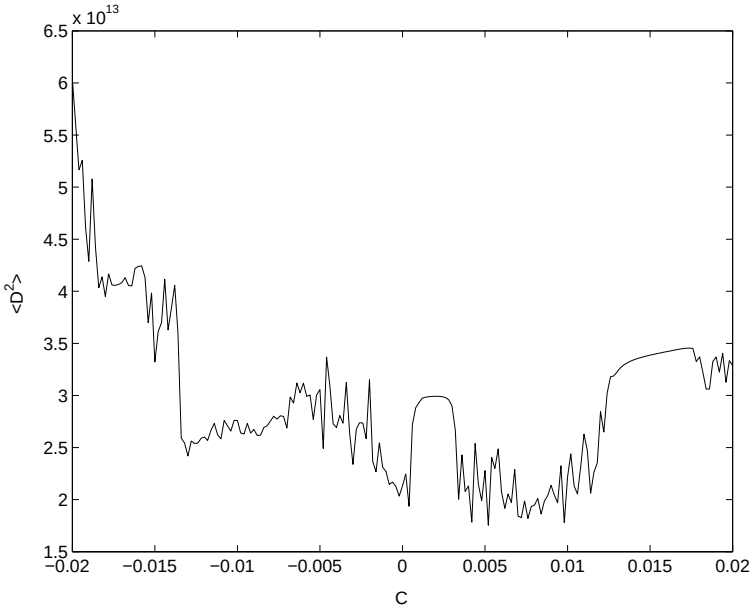

Figure 4.2: Variation of the mean squared deviation from the period 1 state versus feedback strength.

limited to certain regions in parameter space.

4.3 Effect of a direct delayed optoelectronic feedback

It is found that a self adjusting delayed optoelectronic feedback would not work in controlling chaos in self pulsating lasers. The next possibility is to study the effect of a direct delayed optoelectronic feedback on the chaotic laser. The control set up for this feedback is the same as the set up given in Fig. 3.1 in chapter 3.

The modified expression for the injection current signal is given by

$$I = I_b + I_m sin(2\pi f_m t) + C \times 10^{-6} \times p(t - \tau) \tag{4.3.1}$$

The equation is similar to Eq.3.3.1 except in the presence of the constant 10^{-6} which is included since the photon density unnormalized.

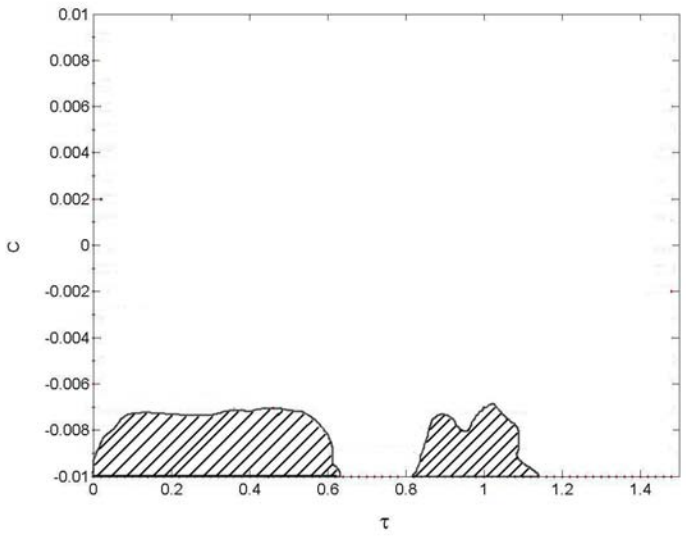

Figure 4.3: Global classification of period 1 in the parameter space of delay and feedback strength: shaded areas show the possible regimes of stable frequency-locking in the ratio 1:1.

4.3.1 Results and discussions

Behavior of the laser with feedback for a range of values of delay and feedback strength is investigated numerically and the possible regions of period 1 state of the laser is plotted. Fig.4.3 shows such regimes in the parameter space defined by τ and C. The laser shows 1:1 frequency locking (period 1 state) for the values of delay and feedback strength corresponding to the shaded regions in the figure. The other regions are corresponding to chaos, quasiperiodicity or frequency locked state with the ratios other than 1:1. The laser yields 1:1 locked state only for negative feedback with relatively high feedback strengths.

The reverse bifurcation associated with the suppression of chaos can be illustrated by single parameter bifurcation diagrams. Fig.4.4 shows the variation of the dynamical behavior of the laser when the feedback strength is increased. Delay of the feedback is kept as a constant value (0.1ns). It is shown in the global classification diagram that suppression of chaos is possible with the delays of this order. The bifurcation diagram is drawn by taking the maxima of the photon density (p_{max}) and plotting it against the absolute value $|C|$ of feedback strength. In addition to showing the periodicity of the cycles, this bifurcation diagram shows the variation of peak power of the laser-output (Similar diagrams have been

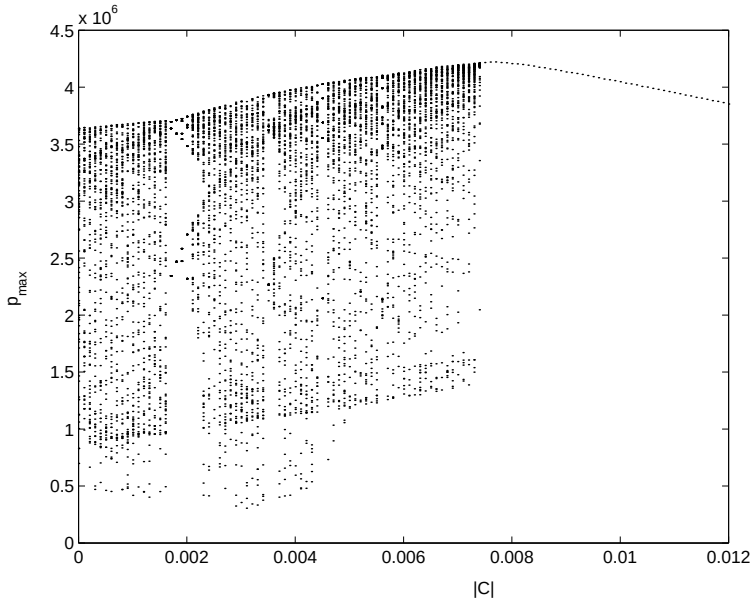

Figure 4.4: Bifurcation diagram (maxima of photon densities vs absolute value feedback strength) showing suppression of chaos in the laser with direct delayed optoelectronic feedback. The applied feedback is negative here. ($\tau = 0.1ns$)

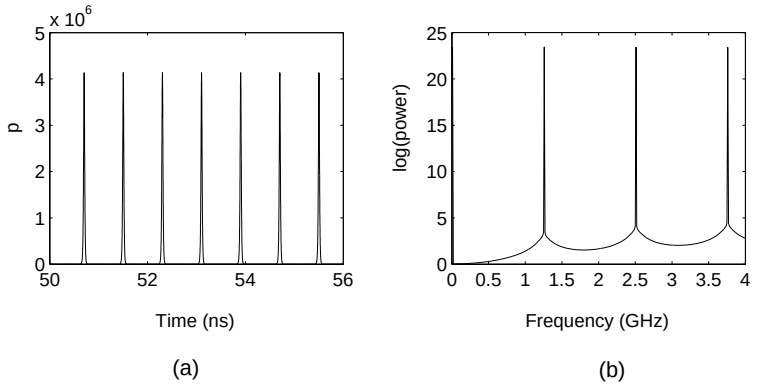

Figure 4.5: Period 1 orbit obtained by the suppression of chaos using a direct delay feedback ($C = -0.008$, $\tau = 0.1ns$)

used for studying the suppression of chaos in InGaAsP laser diodes). The negative feedback is preferred here since the period 1 state can be obtained by a feedback with a minimum feedback strength of a magnitude around 0.008 in this way. On the other hand, no period 1 state is possible if a positive feedback with a strength of the same order is applied. It is evident from the global diagram itself. On increasing the feedback strength gradually, many types of complex bifurcation structures appears and the attractors formed in this way disappear when the low periodic windows appear. However, we cannot distinguish a considerably long periodic window or a regular reverse bifurcation like reverse period doubling. The laser shows chaotic behavior up to a value of feedback strength $C = -0.0075$ and acquires period 1 state through a sharp change in the dynamical behavior. The bifurcations shown by the laser is essentially different from the reverse period doubling observed when a direct delay feedback is applied to a directly modulated InGaAsP laser diode. If the feedback strength is further increased, the peak value of photon density decreases gradually. The period 1 orbit corresponds to a feedback strength $C = -0.008$ is given in Fig.4.5. Time series plot (Fig.4.5(a)) of the laser output shows that the laser with feedback yields sharp optical pulses with a repetition rate that is equal to the frequency of modulation and it is obvious from the power spectrum (Fig.4.5(b)).

The variation of laser dynamics with the increase of time delay has also been investigated. Fig.4.6. is the bifurcation diagram drawn by taking the maxima of photon densities and plotting them against the delay in nanoseconds. The feedback strength is kept to be a constant value $C = -0.008$. The effect of delay is very much significant in the suppression of chaos in self pulsating lasers also. Lower values of delay enhance the suppression and

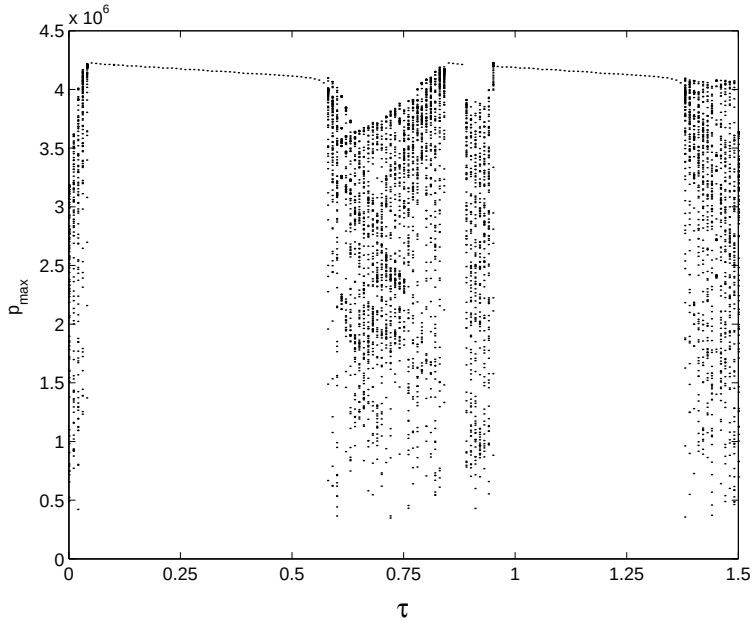

Figure 4.6: Bifurcation diagram (maxima of photon density vs delay in nanoseconds) of laser with direct delay feedback. ($C = 0.002$)

higher delays makes the laser chaotic again. The formation of high dimensional chaotic attractors in have been reported in nonlinear delay feedback systems with large delays.

It is evident from the diagram that two long period 1 windows are present among the complex dynamical states of the laser. The first one starts at 0.05ns and ends at 0.57ns. The second window lies between the values 0.96ns and 1.37ns. The period 1 orbits mainly belongs to these regimes. On further increasing the delay, the laser loses periodic behavior and it becomes chaotic [21]. The suppression of chaos on increasing delay is usually observed in delay feedback systems [9]. The delay induced instabilities are also familiar in the delay feedback systems such as external cavity laser diodes [11]. It is well known that the effect of delayed optical feedback usually causes loss of periodic behavior.

4.4 Suppression of quasiperiodicity using a direct delayed optoelectronic feedback

We have shown that a direct delay feedback can suppress chaos in the modulated self pulsating laser and the regular short pulses can be obtained from the laser by applying a feedback with proper delay and strength. Therefore we consider the possibility of suppressing quasiperiodic behavior in the laser. As has been done in the case of chaotic laser, we simulate the behavior of a laser operating in quasiperiodic regime ($I_m = 2mA$) [15]. Time series and power spectra of quasiperiodic pulses generated by the laser are given in Fig.4.7 . Power spectra given in Fig.4.7(b) contains all the linear combination of two incommenssurate (having a ratio, which is equal to an irrational number) frequencies ($f_1 \cong 1.26$GHz, $f_2 \cong 2.07$GHz). The parameters, i.e., the feedback strength and delay are varied within a considerable range of values. The possible regimes of period 1 or 1:1 locked state in the parameter space are shown in Fig.4.8 as shaded areas. The parameter space contain only a few regions corresponding to the period 1 state. There is a wide area representing the 1:1 frequency locking in the positive feedback regime. However the isolated region around the point ($\tau = 0.54ns, C = 0.002$) is corresponding to the formation of period 1 orbits with very low values of feedback strength.

The variation of dynamical state of laser with respect to the increase of feedback strength is also studied using bifurcation diagrams. Fig.4.9 is the bifurcation diagram (maxima of photon density versus feedback strength). The delay is taken as 0.54ns. It is clear from the diagram that there is a range of feedback strength (from 0.002 to 0.004) yielding the period 1 pulses. The peak power of the output is maximum at $C = 0.0038$. Time series plot and power spectra of the corresponding output is given in Fig.4.10. The out of the laser is sharp and resembles the pulses obtained as a result of self pulsation. However there

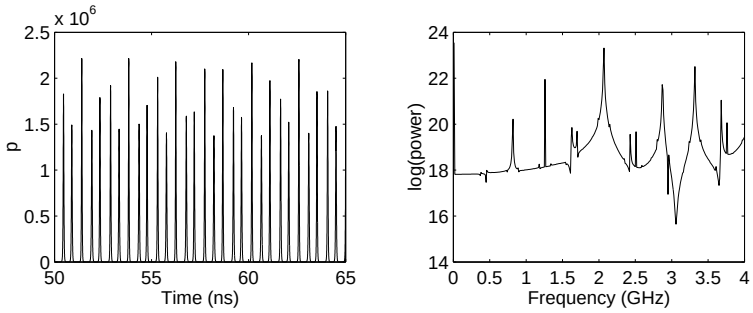

Figure 4.7: Chaotic output of the laser without feedback: (a) time series (b) power spectra.I_m=2mA.

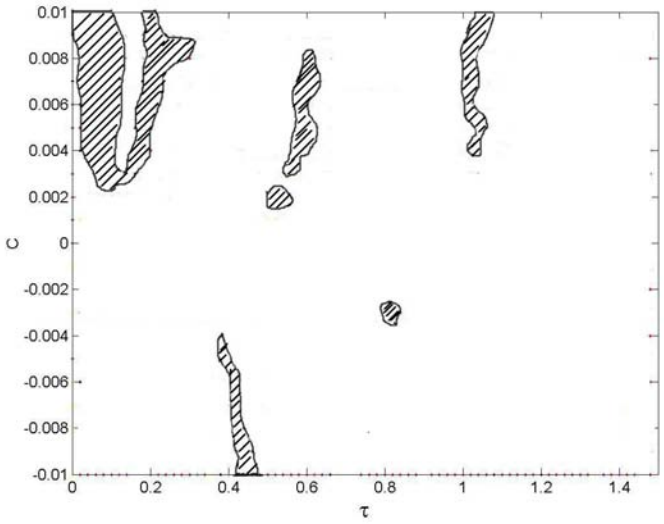

Figure 4.8: Possible regimes of period 1 output (shaded portions) in the parameter space of delay and feedback strength from an originally quasiperiodic laser with direct delay feedback.

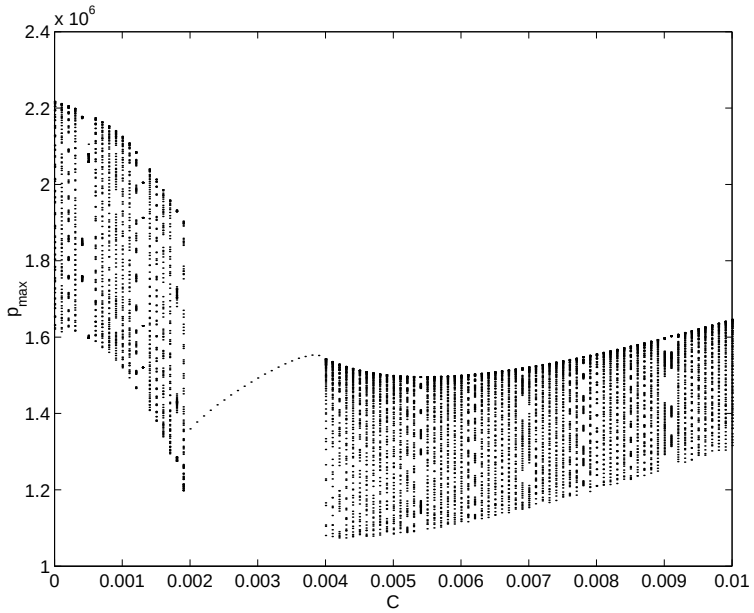

Figure 4.9: Bifurcation diagram showing the suppression of quasiperiodicity using direct delay feedback; maxima of photon density is plotted against feedback strength. ($\tau = 0.4ns$)

is an important difference between these pulses; the repetition rate of the pulse shown in Fig.4.10 is equal to the frequency of the driving signal and the frequency of self pulsation is determined by the intrinsic parameters of the laser. The bifurcation given in Fig.4.11 shows the effect of the increase in delay on laser dynamics. The feedback strength is kept as a constant value 0.002. The period 1 states can be found only in very short region (from 0.5ns to 0.55ns) in the diagram. This implies that a careful adjustment of delay is required for achieving the control.

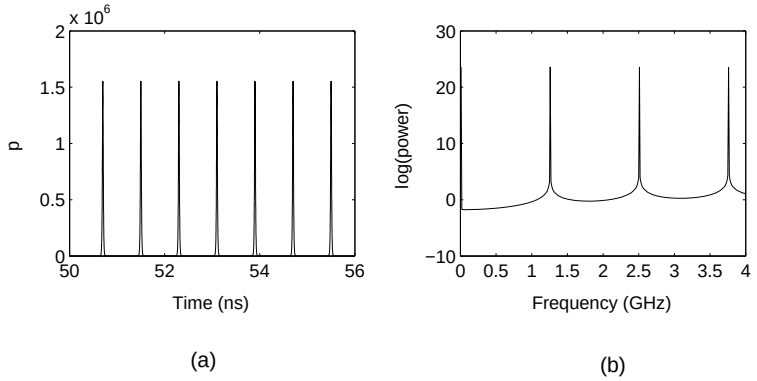

Figure 4.10: Period 1 orbit obtained by the suppression of quasiperiodicity using a direct delay feedback ($C = 0.002$, $\tau = 0.54ns$)

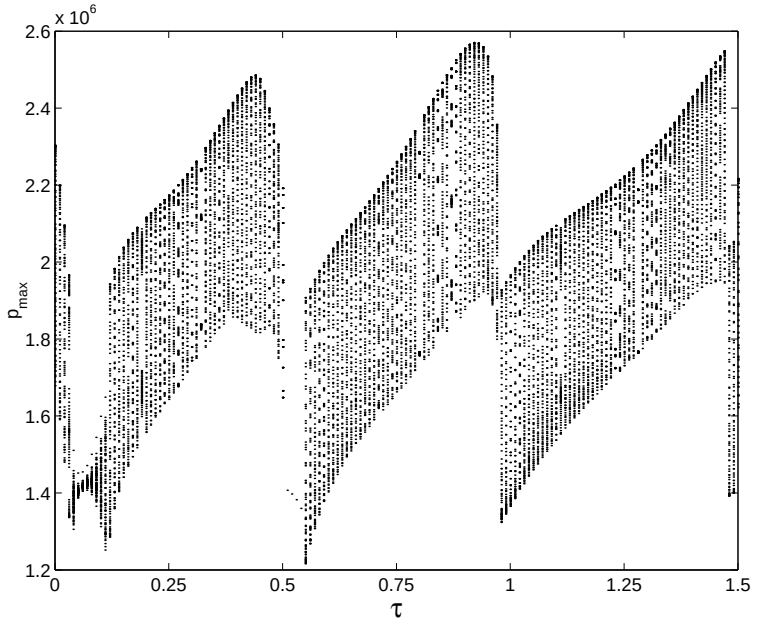

Figure 4.11: The bifurcation diagram (maxima of photon density versus delay in nanosecond): dependence of the suppression of quasiperiodicity on feedback delay time. $C = 0.002$)

4.5 Conclusion

In this chapter, we have shown that a direct delayed feedback efficiently suppresses chaos and the quasiperiodic behavior in a directly modulated self pulsating semiconductor laser. It is also evident from the numerical results that a delayed optoelectronic feedback based on TDAS algorithm is unable to eliminate chaos from such lasers. The direct delay feedback scheme has been found to be successful in suppressing the quasiperiodicity also. The results regarding the suppression of quasiperiodicity have special significance since the control of quasiperiodicity is not a well developed area of research.

Bibliography

[1] U. Parlitz and W.Lauterborn, Phys. Rev. A **36** (1987) 1428

[2] J. Guckenheimer and P. Holmes, *Nonlinear Oscillations, Dynamical System, and Bifurcations of Vector Fields,* Springer - Verlag, New York (1983)

[3] A. Brandstater and H. L. Swinney, Phys. Rev. A **35** (1987) 2207

[4] J. P. Gollub and H. L. Swinney, Phys. Rev. Lett. **35** (1975) 927

[5] C. Simmendinger and O. Hess, Phys. Lett. A **216** (1996) 97

[6] M. Lakshmanan and K. Murali *Chaos in Nonlinear Oscillators: Controlling and Synchronization* World Scientific, Singapore (1996)

[7] L. O. Chua ,*IECE Trans. on Fundamentals Electron. Commun. Sci.* E. **76A** (1993) 704

[8] S. R. Bolton and M. R. Acton Phys. Rev. A **62** (2000) 063803

[9] D. J. Biswas and R. G. Harrison Phys. Rev. A **32** (1985) 3835

[10] J. Mork, B. Tromborg, and J. Mark, IEEE J. Quantum Electron. **28** (1992) 9

[11] A. T. Ryan, G. P. Agrawal, G. R. Gray. IEEE J. Quantum Electron. **30** (1994) 668

[12] S. Wieczorek,1, B. Krauskopf,and D. Lenstra Phys. Rev. E. **64** (2001) 056204

[13] H.G. Winful, Y.C. Chen, J.M, Liu, Appl. Phys. Lett. **48** (1986) 161

[14] S Rajesh and V M Nandakumaran *Control of chaos in directly modulated semiconductor lasers*, Proc.of Photonics-2002, International Conference on Fiber optics and Photonics, Tata Institute of Fundamental Reasearch, Bombay, December 2002

[15] S Rajesh and V M Nandakumaran , *Stabilization of Quasiperiodic and Chaotic Pulses from a Directly Modulated Self Pulsating Semiconductor Laser* , Proc. of Photonics-2004, International Conference on Fiber optics and Photonics, Cochin, December 2004

[16] A. Labate, M. Ciofini, and R. Meucci, Phys. Rev. E. **57** (1998) 5230

[17] C. M. Kim, S. Rima, W. H. Kyea, J. M. Kimb and K. S. Leeb, Phys. Lett. A **329** (2004) 28

[18] A. Maccari and G. Cardano, Physica Scripta Online **70** (2004) 79

[19] W. Just, T. Bernard, M. Ostheimer, E. Reibold, and H. Benner Phys. Rev. Lett. **78** (1997) 203

[20] J.E.S. Socolar and D.J. Gauthier Phys. Rev. E, **57** (1998) 6589.

[21] S Rajesh and V M Nandakumaran, *Quasiperiodicity and chaos in directly modulated semiconductor lasers*, Proc.of National Laser Symposium (NLS 2002), Sree Chitra Thirunal Institute of Medical Science, December 2002

Chapter 5

Control of bistability in directly modulated semiconductor laser

Phase space trajectories of nonlinear systems often converge asymptotically to a single attractor. However, certain nonlinear systems possess multiple attractors in their phase spaces. The dynamical behavior of such systems are critically determined by the initial conditions. This phenomenon is generally referred to as multistability [1, 2]. Various nonlinear systems such as chemical oscillators [3, 4, 5], nonlinear electronic circuits [6, 7, 8], passive optical resonators [9, 10, 11] and lasers [12, 13, 14, 15, 16] show multistability. Bistability is a special case of multistability where two distinct states corresponding to the same set of parameters of a system are stable. Bistability in driven nonlinear oscillators are usually observed in association with the hysteresis effect. A well known example is the hysteresis observed in the driven double well Duffing oscillator [17, 18]. A detailed study of hysteresis and bistability in Duffing oscillator is given in ref.[18]. A similar effect has been reported in directly modulated semiconductor lasers [19]. In this chapter we numerically demonstrate the hysteresis and bistability shown by directly modulated InGaAsP semiconductor lasers. Further, we show that a direct delayed optoelectronic feedback with proper delay and feedback strength can eliminate this bistable behavior.

5.1 Bistability in directly modulated InGaAsP laser

A semiconductor laser with a sinusoidal current modulation can be modelled by the set of equations [20]

$$\frac{dN}{dt} = \frac{1}{\tau_e}\left(\frac{I}{I_{th}} - N - \frac{N-\delta}{1-\delta}P\right) \tag{5.1.1}$$

$$\frac{dP}{dt} = \frac{1}{\tau_p}\left(\frac{N-\delta}{1-\delta}(1-\epsilon P)P - P - \beta N\right), \tag{5.1.2}$$

where the injection current,

$$I = I_b + I_m sin(2\pi f_m t), \tag{5.1.3}$$

The variables involved in the above equations are the normalized photon density P and the normalized carrier density N of the laser. The definitions of the parameters appearing in the above equations are given in Chapter 2. Their numerical values are also given (Table 2.1). I_b is the bias current which is assumed to be a constant (26mA) throughout our simulations. I_m and f_m are the amplitude and the frequency of modulation respectively. Frequency is taken as 0.8GHz which falls in the range of frequencies where the modulation for the communication purposes are usually done. Hysteresis and bistability appear when the modulation amplitude is continuously varied while the laser is in operation.

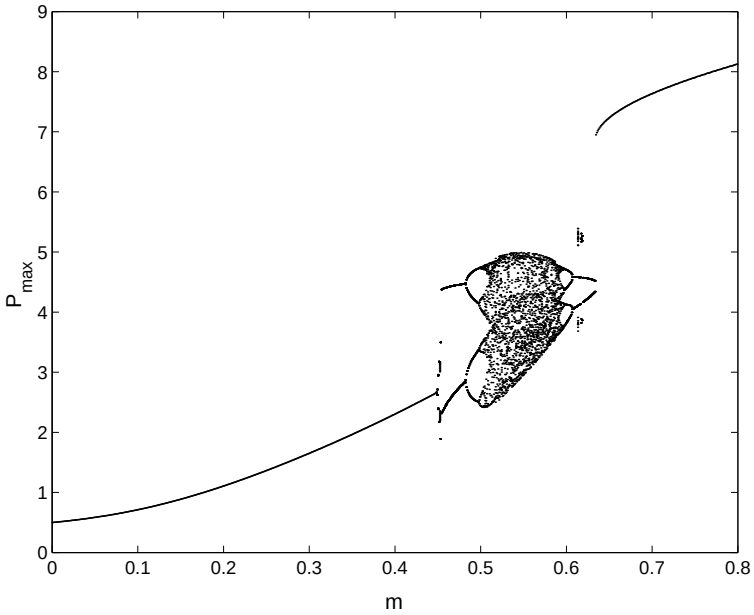

Figure 5.1: Bifurcation diagram of the modulated laser showing the stable attracting sets of peak photon densities. Maxima of photon densities are plotted against the modulation depth. The jumps observed at certain points are due to the hysteresis.

The subharmonic route to chaos has already been demonstrated in Chapter 2 using bifurcation diagrams (maxima of the photon density versus modulation depth) obtained from the numerical integration of the above set of equations. Such a bifurcation diagram (Fig.5.1) is used here for illustrating the hysteresis effect observed when the amplitude of the modulating signal is varied around certain values. The diagram is obtained by the

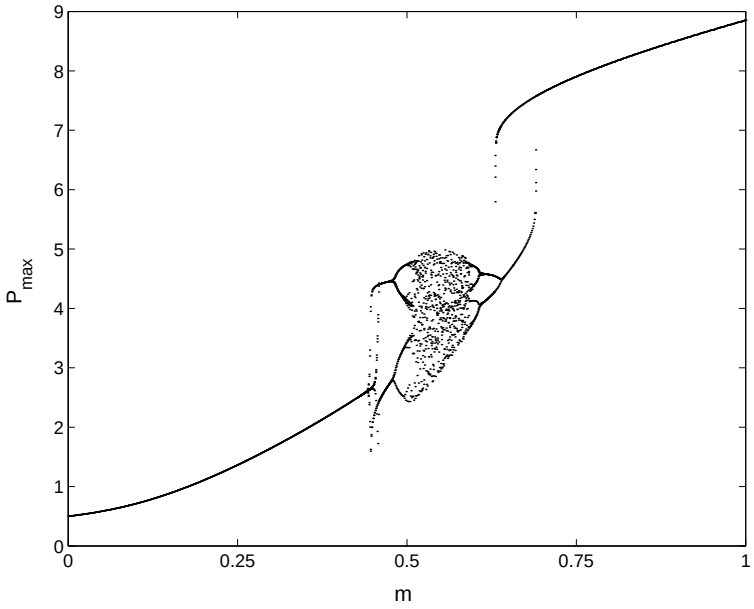

Figure 5.2: Bifurcation diagram of the modulated laser obtained by continuous-time simulation. The modulation depth is varied from 0 to 0.8 and viceversa. Hysteresis loops are present in the place of 'jumps' here.

following method. The simulation is started with arbitrarily chosen initial conditions and a minimum value of the parameter (here it is the modulation depth $m = I_m/I_{th}$). It is found that the phase space trajectory of the system starting from a typical initial condition converges to the attractor (it can be periodic or chaotic) within a finite time. The maxima of the photon density after vanishing the transients are recorded and they are used for constructing the bifurcation diagram. For obtaining the attractor points corresponding to another parameter value, the parameter is increased slightly and the maxima of photon densities belonging to the stable state are recorded again. This process is repeated for a the complete range of parameter. This method is called brute force approach [21] and it has an advantage. The bifurcation diagram plotted using this method (Fig.5.1) contains only the stable attracting sets of the phase points. However, it does not show the hysteresis effect in a proper way. Certain non smooth transitions (jumps) are present in the bifurcation diagram and they are the results of hysteresis. This is because, the attractor usually goes through a sudden change in the structure at the hysteresis region. For showing the hysteresis properly, a different numerical approach can be used [21]. In this method, the simulation is done in such a way that the modulation depth of the laser is continually varied during

its operation. The modulation depth is supposed to be increased from a minimum value to a maximum and it is decreased again to the minimum limit. The bifurcation diagram of the directly modulated InGaAsP laser diode obtained by this method (continuous-time approach) is shown in Fig.5.2. The modulation depth has varied from 0 to 0.8 and viceversa . This bifurcation diagram reveals the complete structure of the period doubling, reverse period doubling, chaos and hysteresis observed in the early investigations. In the places of the sudden 'jumps' present in Fig.5.1, we can see the hysteresis loops. A detailed view of

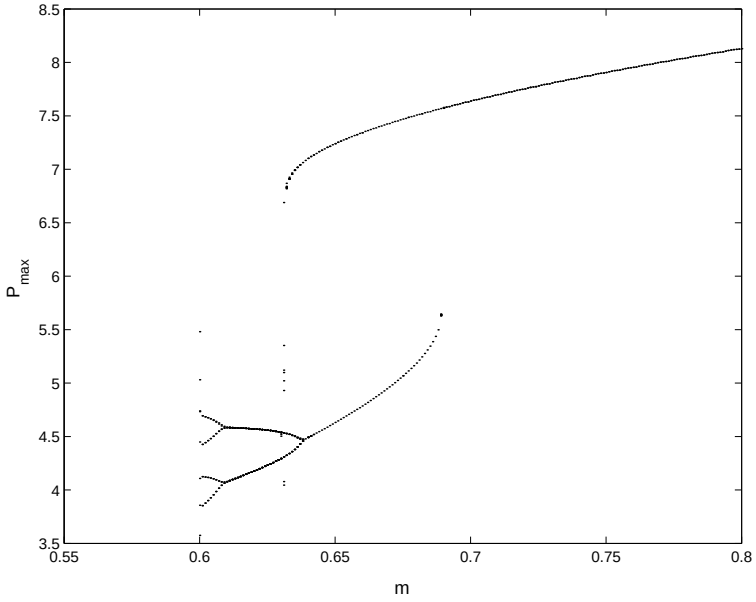

Figure 5.3: Bifurcation diagram plotted using continuous-time method. Two separate paths of hysteresis is clearly shown.

the hysteresis loop formed in one of the periodic region of the laser is given in Fig. 5.3. This region corresponds to the formation of period 1 orbits after chaos and reverse period doubling. (We prefer this domain for illustrating the bistability and its control since the bistability is usually a problem for the lasers operating in periodic state.) It shows that on increasing the modulation depth from 0.6 to 0.8, the variation of the peak photon densities takes place through the lower path in the figure. The peak of the pulses follows a sudden transition to a higher value 7.57 at $m = 0.689$ and then varies almost linearly up to $m = 0.8$. The modulation depth is assumed to be decreasing after reaching the value 0.8. The return path of the peak values is almost straight until the modulation depth reaches the value 0.631. This path deviates from the path followed when the modulation depth is increased.

The deviation takes place at the point m=0.689. A sudden reduction in the peak values takes place at m=0.631 and then the return path meets the line representing the forward transition at $m = 0.631$. The loop ends at this value of modulation depth where period 2 solution exists. The loop formed in this bifurcation diagram is the hysteresis loop associated with the well known pulse-position bistability shown by directly modulated semiconductor lasers. It is clear from Fig.5.3 that for any values of modulation depth lying between 0.631 and 0.689, there will be two stable solutions for laser diode and two types of optical pulses can be obtained. The time series plots of the pulses for a modulation depth 0.65 corresponds to the lower and upper values are given in Fig.5.4 and Fig.5.5 respectively. The pulse associated with the upper branch has a relatively higher amplitude. Since both the two solutions are stable, sudden transitions are possible between these states as a result of noise. Thus the bistable behavior is definitely harmful for the regular operation of semiconductor lasers. Thus bistable behavior of modulated laser diode is harmful to their regular operation when they are used for communications or any other engineering purposes. Hence, the bistability and hysteresis should definitely be eliminated from directly modulated semiconductor lasers.

In short, we have numerically demonstrated the early reported hysteresis and bistability

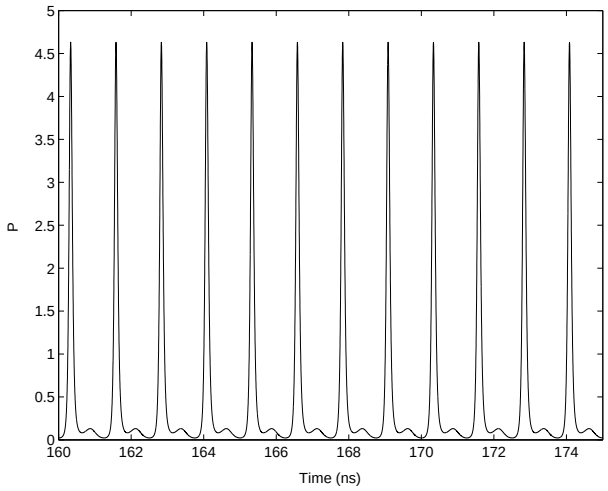

Figure 5.4: Time series of the optical pulse corresponds to the lower branch. $m = 0.65$

in directly modulated semiconductor lasers. Even though the bistable behavior has certain applications like photonic switching devises [22], bistability should be suppressed in most of the practical devises using semiconductor lasers. In this situation, we consider the

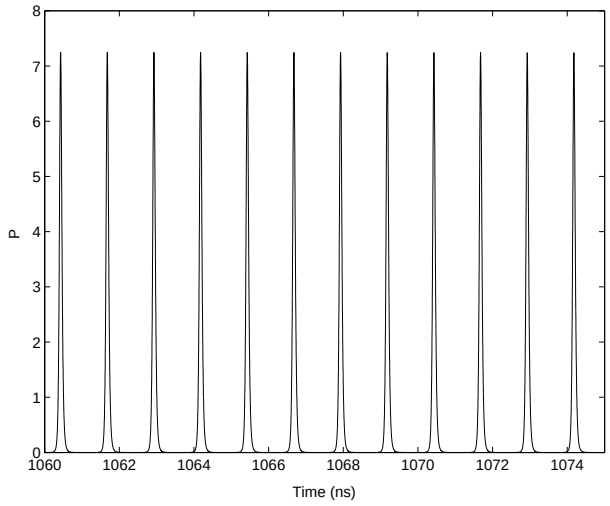

Figure 5.5: Time series of the optical pulse corresponds to the upper branch, $m = 0.65$

possible methods for controlling bistability in modulated laser diodes. Several methods for controlling bistability in lasers have been reported earlier [23, 24]. However, most of these schemes are not aimed at eliminating the bistability completely but to allow the system to switch from one of the stable states to the other. Pisarchik and Kuntsevich has proposed a control a scheme which was based on periodic perturbation to the selected state [25]. They have numerically shown that such a scheme would suppress the bistability completely. It is important to mention that the perturbation is external in nature. However we consider the direct delay feedback for suppressing the bistability. This method has been shown to be efficient in a completely eliminating subharmonic generation and chaos in directly modulated laser diodes. The main advantage of this scheme is that no external signal is used as the perturbations. The numerical results regarding the suppression of chaos using this method is given in the following section.

5.2 Control of bistability using a direct delayed optoelectronic feedback

It is found that a direct delay feedback is able to suppress chaos and subharmonic phenomena in directly modulated semiconductor lasers. The self adjusting delay feedback can efficiently stabilize the period 1 orbit in an InGaAsP semiconductor laser (despite there is a double maxima in the pulse). However we are not considering TDAS scheme [26, 27] for

controlling bistability because of a simple reason. For a bistable laser, there is no unstable period 1 orbit to stabilize, but two stable states are present and the feedback should destabilize one of the state and retain the other. If a self adjusting feedback is applied to the laser, there will be no feedback signal to perturb the system when the laser is operating in any one of the stable state, since the initial strength of this signal would be zero and hence the effect of such feedback is trivial. On the other hand, a direct delay feedback with a proper delay and strength makes a non-vanishing perturbation to the system and it may cause the destabilization of one of the stable state and help the system to confine to a single state. We study the effect of such a feedback which has been applied to InGaAsP laser diodes for controlling chaos.

5.2.1 Model of the control scheme

In the direct delayed optoelectronic feedback, a current signal proportional to the photon density of the laser delayed by a time τ is added to the injection current. The schematic diagram of such a feedback is given in Fig.3.1 in chapter 3. The conversion of optical signal into the electronic signal can be done by a photodiode and the necessary delay can be produced by the external transit of the light signal. The current signal obtained from the photodiode can be amplified to the required strength by using an operational amplifier and added to the input injection current of the laser. The feedback signal would be proportional to the intensity of the optical signal delayed by a time τ and hence it can be represented by $CP(t-\tau)$, where C is the feedback strength that is determined by the gain of the amplifier. Thus the expression for the injection current becomes.

$$I_(t) = I_b + I_m sin(2\pi f_m t) + CP(t-\tau), \tag{5.2.1}$$

5.2.2 Results and discussions

The simulation of Eqns. 5.1.1, 5.1.2 and 5.2.1 are done using the fourth order Runge-Kutta algorithm. For studying the effect of delayed optoelectronic feedback, the effect of the feedback on the structure of the hysteresis loop is investigated. Thus the area of the hysteresis loop can be taken as a quantitative measure of the hysteresis effect. Hence, this area is calculated numerically for a wide range of two parameters of feedback, i.e., the delay and the feedback strength. It is found that the area of the loop vanishes completely when a delay feedback of certain combinations of delay and feedback strength is applied to the system. Fig.5.6. gives a global understanding of the possible combination of delay and feedback strengths for which the hysteresis and bistability will be eliminated. The regimes where the area of the loop completely vanishes are classified as the regions, which are

shaded by lines. There are three regions in the diagram showing the complete suppression of bistability. Some of their neighboring regions corresponds to the delay and feedback strength for which the area of the loop becomes almost negligible (the areas shaded with dots show the regions where area is less than 10^{-4} units). It is obvious from the figure that isolated regions in the negative feedback domain represents the suppression of chaos with relatively lower feedback strengths.

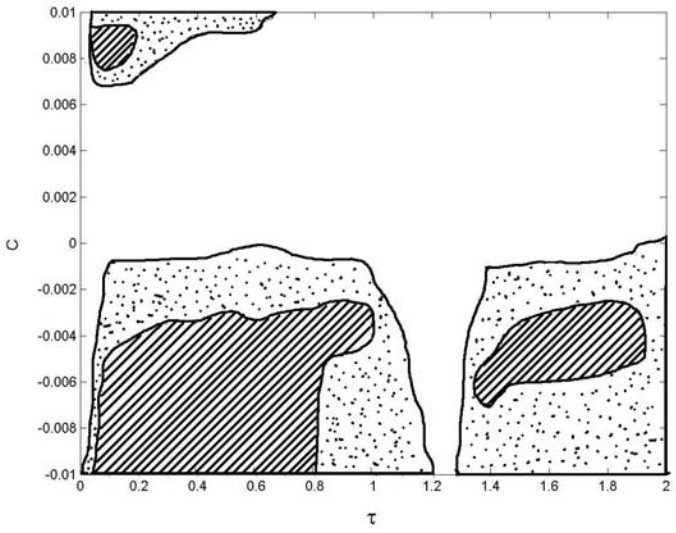

Figure 5.6: Regimes of delay and feedback strength where the bistability has suppressed: The portions shaded with lines correspond to the complete disappearance of hysteresis loop. The dotted portions shows the regions where the area of the loop becomes less than 10^{-4} units.

The area of the hysteresis loop is plotted as a function of feedback strength in Fig.5.7. Here, the delay is taken to be the constant value 0.4ns. From Fig.5.6, it is evident that the suppression of hysteresis is possible by the feedback of delays of this order. The area becomes almost negligible with the feedback of very small values (around -0.6×10^{-3}). It vanishes completely for all the values of feedback strength greater than 4×10^{-3} (absolute value) for this value of delay. The bifurcation diagram of the laser with a feedback of delay 0.4ns and feedback strength -5×10^{-3} drawn by continuous time method is given in Fig.5.8. The upper and lower branches coincide with each other and the variation of peaks in forward and reverse direction takes place through the same path and there is only one stable attracting state corresponding to each value of modulation depth. Thus,

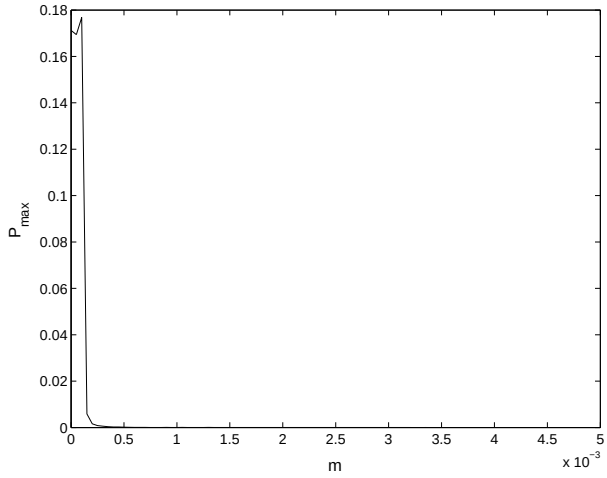

Figure 5.7: Variation of the area of hysteresis loop versus the absolute value of feedback strength. Feedback is negative with a delay $\tau = 0.4ns$. Notice that the area of the loop becomes almost negligible for very low values of feedback strength.

if a negative feedback with very small feedback strength can be used for the controlling bistability in directly modulated laser diode.

The feedback delay time plays a crucial role in the elimination of bistability. It is clear from the global classification diagram that the area of hysteresis loop is vanishing only for the feedback with a non-zero delay. The variation of the area of the loop with the increase of delay is shown in Fig.5.9. The feedback is taken to be a constant -0.002 since it is evident from the global classification diagram that the feedback of this much strength is sufficient to eliminate bistability. The area becomes negligible for a value of delay 0.02ns. On further increasing the delay, it vanishes completely at 0.235ns. A considerably large hysteresis loop is formed for the feedback with delay times that occurs between the values 1.1ns and 1.3ns. This implies that the value of the delay must be between some limits for achieving the suppression of bistability.

The results presented here show that the suppression of hysteresis is possible if the delay and feedback strength are chosen properly. It is not a difficult task because of two reasons, the feedback strength and delay can be easily adjusted by varying the gain of the perturbational amplifier and the distance between the laser and the photodiode respectively. Further, the domains of the elimination is considerably large and hence the required accuracy of the adjustment not too high.

The suppression of chaos is possible with positive feedback also. However, the required

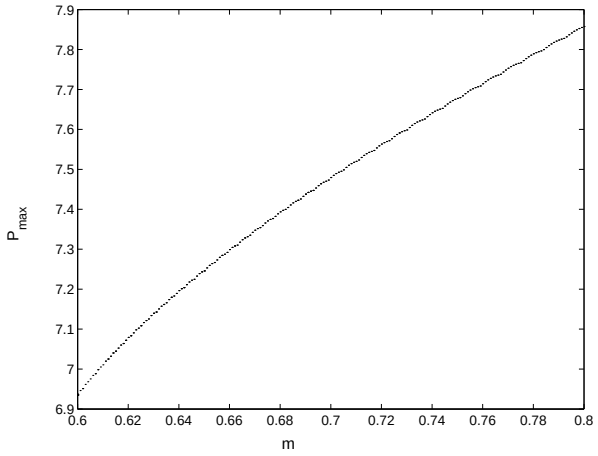

Figure 5.8: Variation of the peaks of photon density of the laser with delay feedback. The upper and lower branches of the hysteresis coincides with each other showing that the bistability has disappeared. $\tau = 0.4ns$ and $C = 0.005$

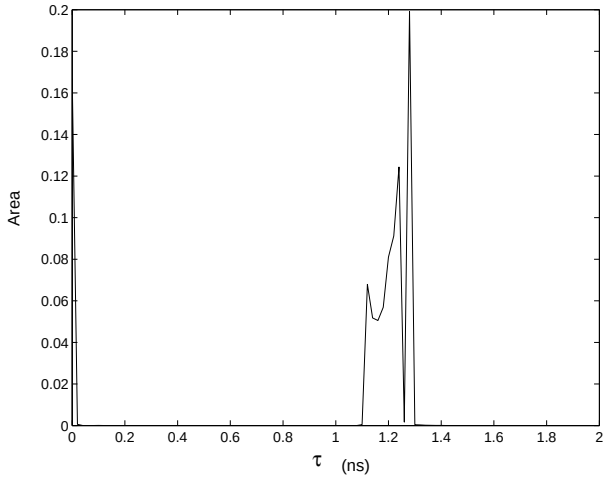

Figure 5.9: Variation of the area of hysteresis loop versus the delay. $C = -0.004$

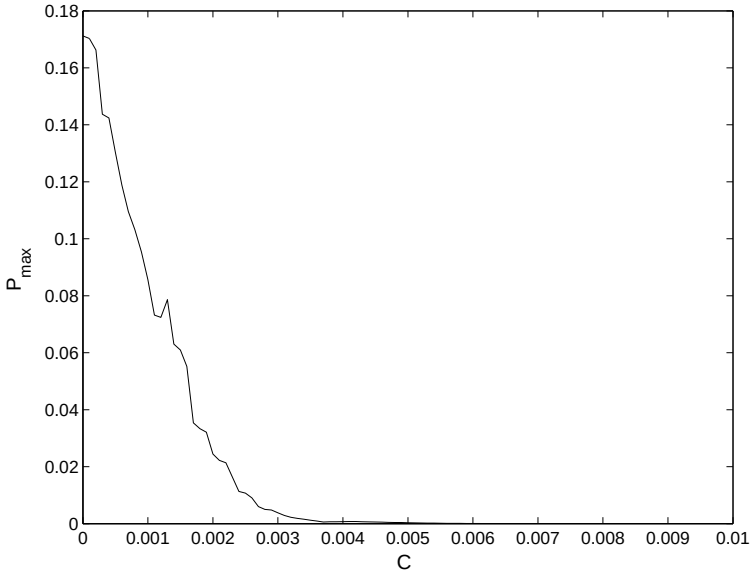

Figure 5.10: Variation of the area of the hysteresis loop of the laser with a delayed positive feedback with the increase of feedback strength. $\tau = 0.05ns$

feedback strength is relatively high in this case. Fig. 5.10 gives the variation of the area of the hysteresis with the increase of feedback strength. The delay is chosen to be equal to 0.05ns. The small isolated region in Fig.5.6 corresponds to the delays of this order. The area becomes negligibly small around the value 0.0056 and the complete disappearance of the loop takes place at $C = 0.0074$. There will be no hysteresis for the laser if a feedback of strengths greater than or equal to this value is applied. Fig.5.11 shows the hysteresis loops corresponding to different values of feedback strengths (τ=0.05ns). For C=0.0003, the area of the hysteresis loop (Fig. 5.11(a) is equal to 0.1437 units. (The area of the loop in the absence of feedback is found to be equal to 0.1712units). The shape of the loop has changed and the area has reduced to 0.06 units when a feedback of strength 0.0015 is applied (Fig.5.11(b)). The size of the loop has again decreased and the area has become 0.012 when C is increased to 0.0024 (Fig.5.11(c)). Fig.5.11(d) shows that the hysteresis has almost disappeared for C=0.005. The area of the loop corresponding to this value of feedback strength is 3.35×10^{-4}. The upper and lower branches of this loop with extremely small area cannot be distinguished in the figure. Fig.5.12 shows the complete bifurcation diagram of the laser with a feedback of delay 0.05ns and strength 0.008 feedback obtained by continuous time approach. The variation of the peak photon densities is smooth and the

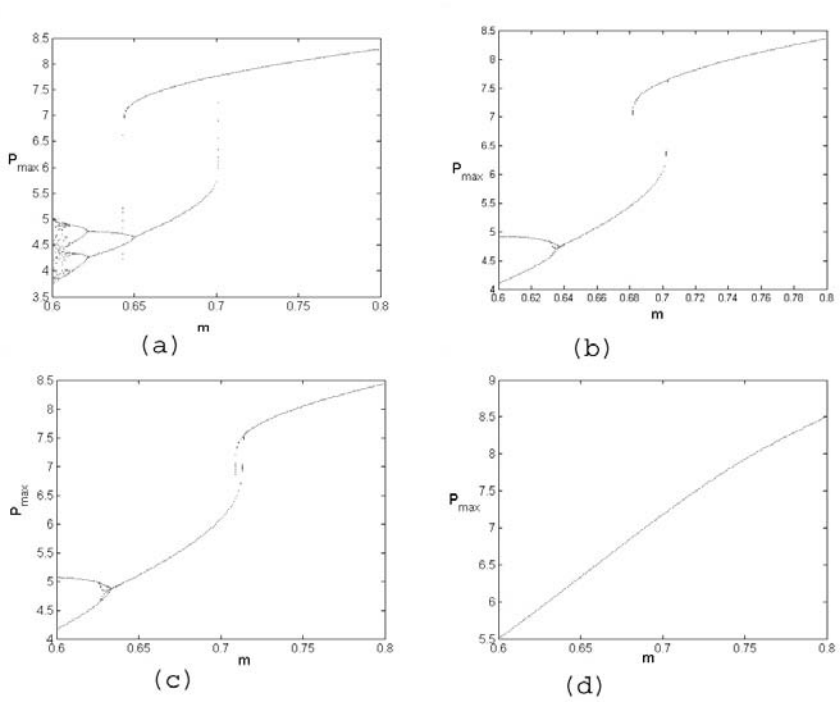

Figure 5.11: Variation in the structure of the hysteresis loops with the increase of feedback strength. Positive feedback with a delay 0.05ns is applied here. (a)$C = 0.0003$, (b)$C = 0.0015$, (c)$C = 0.0024$, $C = 0.005$

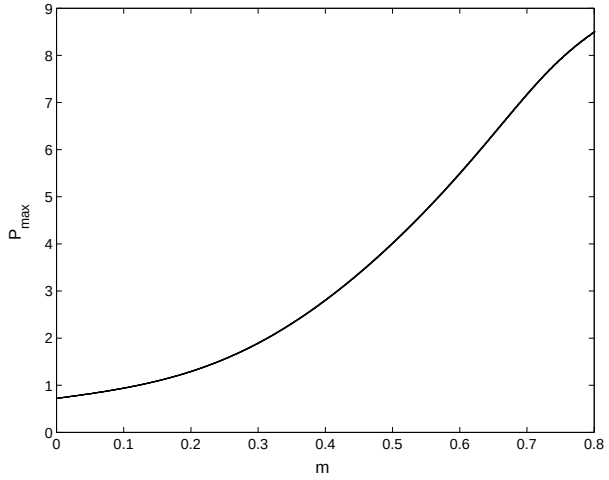

Figure 5.12: Bifurcation diagram showing the peaks of photon densities of the laser with a delayed positive feedback as a function of modulation depth. It is plotted using continuous-time approach. The coincidence of forward and reverse paths shows that the bistability is completely eliminated. $C = 0.008$ and $\tau = 0.05ns$

hysteresis loop has disappeared. All type of bifurcations shown in Fig.5.1. and Fig.5.2. are absent here. We have already shown that this combination of feedback strength and delay gives a complete elimination of period doubling and chaos in the laser [28]. It is interesting to notice that the hysteresis can also be eliminated by applying the same feedback to the laser diode.

5.3 Conclusion

We have shown that a direct delay feedback of very low feedback strength can suppress the hysteresis and bistability in directly modulated semiconductor lasers. The results presented here are very much interesting since the suppression of bistability is achieved by a process which is exactly opposite to control of chaos. In TDAS method, the unstable periodic orbits are stabilized. However, one of the stable states becomes unstable as a result of the direct feedback applied here. Further, the delay plays a significant role in suppressing bistability. The mechanism behind the elimination of hysteresis can be studied in detail and such studied may reveal many of the interesting features of nonlinear systems with delay feedback

Bibliography

[1] U. Feudel and C. Grebogi, CHAOS **7**(1997) 597

[2] U. Feudel,C. Grebogi, B. R. Hunt and J. A. Yorke, Phys. Rev. E **54** (1996) 71

[3] M. Brambilla, F. Battipede, L. A. Lugiato, V. Penna, F. Prati, C. Tamm, and C. O. Weiss, Phys. Rev. A **43** (1991) 5090

[4] F. Prengel, A. Wacker, and E. Scholl, Phys. Rev. B **50** (1994) 1705

[5] P. Marmillot, M. Kaufmann, and J.-F. Hervagault, J. Chem. Phys. **95** (1991) 1206

[6] F. Prengel, A. Wacker, and E. Scholl, Phys. Rev. B **50** (1994) 1705

[7] J. Kastrup, H. T. Grahn, and E. Scholl, Appl. Phys. Lett. **65** (1994) 1808

[8] J. Foss, F. Moss, and J. Milton, Phys. Rev. E **55** (1997) 4536

[9] K. Ikeda, K. Matsumoto, Physica D **29** (1987) 223

[10] K. Ikeda Opt. Commun. **30** (1979) 257

[11] K. Ikeda, H. Daido and O. Akimoto Phys. Rev. Lett. **45** (1980) 709

[12] M. Brambilla, F. Battipede, L. A. Lugiato, V. Penna, F. Prati, C. Tamm, and C. O. Weiss, Phys. Rev. A **43** (1991) 5090

[13] M. Brambilla, L. A. Lugiato, V. Penna, F. Prati, C. Tamm, and C. O. Weiss, Phys. Rev. A **43** (1991) 5114

[14] Z. Wang, W. Guo, and S. Zheng, Phys. Rev. A **46** (1992) 7235

[15] F. T. Arecchi, R. Meucci, G. Puccioni, and J. Tredicce, Phys. Rev. Lett. **49** (1982) 1217

[16] F. T. Arecchi, R. Badii, and A. Politi, Phys. Rev. A **32** (1985) 402

[17] C. L. Olson and M. G. Olsson American. J. Phys. **59**, (1991) 907

[18] M. Lakshmanan and K. Murali *Chaos in Nonlinear Oscillators:Controlling and Synchronization* World Scientific, Singapore (1996)

[19] C. Mayol, R. Toral, C. R. Mirasso, S. I. Turovets, and L. Pesquera, IEEE J. Quantum Electron., **38** (2002) 260

[20] G. P. Agrawal, Appl. Phys. Lett., **49** (1986) 1013

[21] T.S. Parker and L.O.Chua, Practical numerical algorithms for chaotic systems, Springer-Verlag, New York,(1989)

[22] H. Kawaguchi, *Bistability and Nonlinearities in Laser Diodes*, Artech House, Norwood (1994)

[23] V. N. Chizhevsky and S. I. Turovets , Phys. Rev. A. **50** (1994) 1840

[24] V. N. Chizhevsky and R. Corbalain and A.N. Pisarchik , Phys. Rev. E **56** (1997) 1580

[25] A. N. Pisarchik and B. F. Kuntsevich IEEE J. OF Quant. Electron. , **38** (2002) 1594

[26] K Pyragas, Phys. Lett.A **170** (1992) 421

[27] K.Pyragas, Phys. Lett. A **181** (1993) 99

[28] S. Rajesh and V. M. Nandakumaran, Phys. Lett. A **319** (2003) 340

Chapter 6

Effects of phase mismatch, delay and frequency detuning on the synchronization of chaos in directly modulated self pulsating laser diodes and nonlinear oscillators.

Synchronization of chaos is one of the well-studied areas of research in nonlinear dynamics for the last two decades. Yamada and Fujisaka has shown that, when two identical chaotic systems are coupled together by sending the information to each other, they get synchronized [1]. Later Afraimovich *et. al.* analyzed many features of synchronized chaos [2]. However, the widespread study of chaos-synchronization was started only after the important work of Pecrora and Caroll in 1990 [3]. They introduced a new criteria of synchronization, i.e., the drive-response scenario based on complete replacement of the variables of one system by another. They have also introduced a commonly accepted stability-criteria for synchronized chaotic systems- the Transverse Lyapunov Exponents. Even though Pecora and Caroll method is very efficient in synchronizing different kinds of analogue electronic circuits [4, 5], coupling is the commonly accepted synchronization scheme for the chaotic systems other than the electronic circuits. For example, various types of chaotic laser systems have been synchronized using coupling [7, 9, 10]. Coupling can be bidirectional [9, 10] or unidirectional [7] according to the specific situations.

One of the most important applications of chaotic synchronization is in the field of secure communications. The concept of synchronization-based secure communication is relatively simple and highly promising. Several attempts have been made for sending messages using

synchronized chaos [6, 11, 12, 13, 14, 15]. Consider two nearly identical chaotic systems that are synchronized by coupling them together. The coupling can be be achieved by sending the output of a system (transmitter) to the other system. A message is added to the output of the drive system. The amplitude of this signal must be very small so that it should not affect the synchronized state. The added message can be simply decoded by taking the difference of outputs of these two systems [16]. It is practically impossible for an external observer to decode the message unless he has an exact replica of the drive system. It should be noted that complete synchronization of systems is required for sending signals by direct addition of the signal. Another important scheme is chaos-shift keying (CSK) [12]. In this method, one of the parameters of the drive system is changed according to the variation of the encrypting digital signal. The encoded signal can be decoded from the response system in terms of the synchronization error. This method has an advantage over the former method that is, it does not require complete synchronization of the chaotic systems. However the bit rate of the encryption is less compared to the direct addition method.

The chaotic encryption has been demonstrated using various chaotic systems such as electronic circuits and laser systems. Secure communication schemes based on synchronization of lasers are of high importance since they provide a simple and efficient way of high speed optical transmission of encrypted data. Thus, synchronization of chaotic lasers has become a very interesting area of current research. Many kinds of lasers have been synchronized using coupling and secure communication schemes utilizing synchronization has been demonstrated using such lasers [7, 17, 18, 19, 20, 21]. Some of these schemes uses modulated laser systems which belong to the non-autonomous category [7, 19]. The phase of modulation provides the extra degree of freedom for generating chaos in these systems. A common modulating source is used in most of the communication schemes using modulated laser systems. The real physical situation is very much different from this case. Since drive and response systems are situated at different places, definitely there exist a channel delay and the effect of this delay must also be considered while considering synchronization. The phases of the modulated signals will be independent of each other and a frequency detuning is also possible. We consider these effects and perform a theoretical study on the possible problems arising in this situation. We show that synchronization is lost as a result of the phase mismatch or channel delay. Synchronization can be retained by exactly compensating the effect of delay by the effect of phase difference and viceversa. However,the effect of detuning is rather serious and it make the synchronization of modulated lasers practically impossible. The issues that we are considering here may be applied to any types of non-autonamous chaotic systems. Hence, we analyze the problem using a general model of

coupled oscillators. The results show that the same problems exist for any driven chaotic systems coupled by the conventional techniques.

6.1 Effects of delay and detuning on synchronization of modulated self pulsating Lasers

Modulated self pulsating lasers are well known sources of chaotic optical signals [22]. It was proposed by Juang *et. al.* that these lasers can be synchronized using an optoelectronic coupling method [7]. They have shown that a complete synchronization is possible by a unidirectional coupling scheme. However they have assumed that a common modulating source is used for the generation of chaos. In contrast to this approach, we consider a possible channel delay associated with the coupling (since the optical signal must travel through an optical fiber before reaching the response laser) [8]. Since the lasers are situated at two remote places and the modulating sources are independent to each other, it is reasonable to assume that there exists at least a small detuning between the signal sources of the drive and response lasers.

6.1.1 Model of the coupled laser system

A single directly modulated self pulsating semiconductor laser can be modelled by the following equations [23]

$$\frac{dp}{dt} = \left[a_1\xi_1(n_1 - n_{g1}) + a_2\xi_2(n_2 - n_{g2}) - G_{th}\right]p + b\frac{n_1 V_1}{\tau_s} \tag{6.1.1}$$

$$\frac{dn_1}{dt} = -\frac{a_1\xi_1}{V_1}(n_1 - n_{g1})p - \frac{n_1}{\tau_s} - \frac{n_1 - n_2}{T_{12}} + \frac{I}{qV_1} \tag{6.1.2}$$

$$\frac{dn_2}{dt} = -\frac{a_2\xi_2}{V_2}(n_2 - n_{g2})p - \frac{n_2}{\tau_s} - \frac{n_2 - n_1}{T_{21}} \tag{6.1.3}$$

with an injection current,

$$I = I_b + I_m sin(\omega t + \phi) \tag{6.1.4}$$

where $\omega = 2\pi f_m$, is the angular frequency of modulation and ϕ is the initial phase of the modulating signal. I_b is the bias current and I_m is the amplitude of modulation. The variables in the rate equations (Eqns. 6.1.1 , 6.1.2, and 6.1.3) of the laser are the carrier densities in the gain region and the saturable absorbtion region and the photon density. The terminology and the numerical values of the parameters appearing in the equations are given in Chapter 2. It is well known that the modulated laser described by the above set

of equations show chaotic behavior for appropriate values of modulation depth. The time series and power spectra of the chaotic output obtained by a current signal of modulation of amplitude 7mA is given in Fig.6.1.

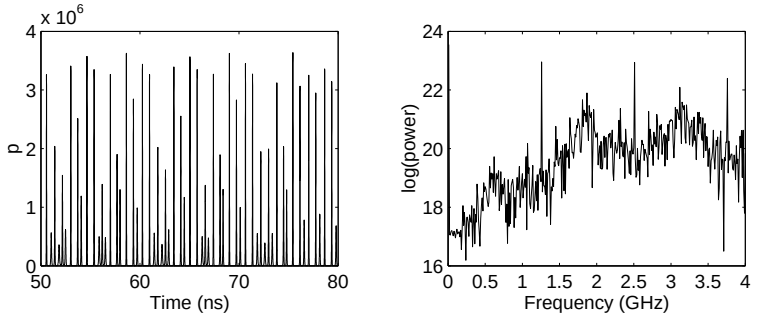

Figure 6.1: Chaotic output of the directly modulated self pulsating laser diode: (a) time series (b) power spectra. I_m=7mA.

Now, we address the question of the synchronization of two unidirectionally coupled semiconductor lasers separated by a considerable distance (of the order of a few kilometers and thus producing the delay of the order of nanoseconds). The schematic diagram of the proposed controlled scheme is given in the Fig.6.2. It is an optoelectronic coupling scheme. The output optical pulses of the first laser (drive system) have to travel a certain distance through an optical fiber channel before reaching the second laser (response) system. The photodiode PD1 converts this optical signal into an electronic signal. The second photodiode PD2 converts the output of the response laser into the corresponding current signals. The signals from PD1 and PD2 can be given to the inverting and non-inverting inputs of a differential amplifier respectively. A current signal proportional to the difference between the the photon density of the drive laser corresponding to a past state and the present photon density of the response laser can be obtained from the differential amplifier by adjusting its gain. This signal can be represented by the expression $C[p(t-\tau)-p(t)]$, where τ is the delay and C is the feedback strength. It is applied as a feedback to the response laser through its injection current. Our aim is to synchronize the response system to the earlier state of the drive system and the feedback is designed in such a manner that the feedback signal vanishes when the synchronization is achieved. This is a common method of coupling that has been used in many synchronization schemes. Such a method has been used for synchronization of chaos in lasers with delayed optoelectronic feedback

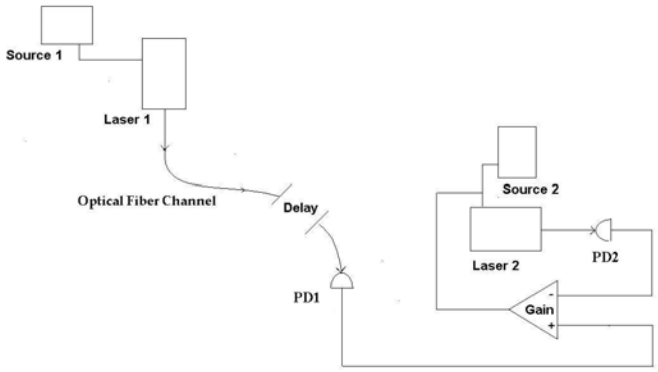

Figure 6.2: Schematic diagram of the coupled laser system.

and in directly modulated semiconductor lasers[24]. Juang *et. al.* have also considered an optoelectronic coupling scheme for synchronizing directly modulated self pulsating laser diodes [7]. However they gave no importance to the channel delay or the independence of the modulating sources. In the present work, these effects are also considered.

When the delay, independence of phases and detuning are incorporated in the model, the corresponding model equations of the coupled laser system can be written as

$$\begin{aligned}\frac{dp_d(t-\tau)}{dt} &= \Big\{\big[a_1\xi_1(n_{1d}(t-\tau)-n_{g1})+a_2\xi_2(n_{2d}(t-\tau)-n_{g2})-G_{th}\big] \\ &\qquad p_d(t-\tau)(t-\tau)\Big\}+b\frac{n_{1d}(t-\tau)V_1}{\tau_s} \qquad (6.1.5)\end{aligned}$$

$$\begin{aligned}\frac{dn_{1d}(t-\tau)}{dt} &= -\frac{a_1\xi_1}{V_1}(n_{1d}(t-\tau)-n_{g1})p_d(t-\tau)-\frac{n_{1d}(t-\tau)}{\tau_s} \\ &\quad -\frac{n_{1d}(t-\tau)-n_{2d}(t-\tau)}{T_{12}}+\frac{Ib+I_mSin(\omega(t-\tau)+\phi_d)}{qV_1} \qquad (6.1.6)\end{aligned}$$

$$\frac{dn_{2d}(t-\tau)}{dt} = -\frac{a_2\xi_2}{V_2}(n_{2d}(t-\tau)-n_{g2})p_d(t-\tau)$$

$$-\frac{n_{2d}(t-\tau)}{\tau_s} - \frac{n_{2d}(t-\tau) - n_{1d}(t-\tau)}{T_{21}} \tag{6.1.7}$$

$$\frac{dp_r(t)}{dt} = \Big[a_1\xi_1(n_{1r}(t) - n_{g1}) + a_2\xi_2(n_{2r}(t) - n_{g2}) - G_{th}\Big]p_r(t)$$

$$+b\frac{n_{1r}(t)V_1}{\tau_s} \tag{6.1.8}$$

$$\frac{dn_{1r}(t)}{dt} = -\frac{a_1\xi_1}{V_1}(n_{1r}(t) - n_{g1})p_r(t) - \frac{n_{1r}(t)}{\tau_s}$$

$$-\frac{n_{1r}(t) - n_{2r}(t)}{T_{12}} + \frac{I_b + I_m Sin[(\omega + \Delta\omega t + \phi_r)] + C[(p_d(t-\tau) - p_r(t)]}{qV_1} \tag{6.1.9}$$

$$\frac{dn_{2r}(t)}{dt} = -\frac{a_2\xi_2}{V_2}(n_{2r}(t) - n_{g2})p_r(t) - \frac{n_{2r}(t)}{\tau_s}$$

$$-\frac{n_{2r}(t) - n_{1r}(t)}{T_{21}}, \tag{6.1.10}$$

where the indices d and r represent the drive and response systems respectively, τ is the delay, $\delta\omega$ is the frequency detuning and C is the coupling strength.

Three important factors are considered while simulating the coupled laser system, the initial phase difference of the modulating signals, channel delay and frequency detuning. The phase effect is addressed first assuming that there is no delay, then the effect of delay alone is considered and will be shown the equivalence or complementary nature of these effects. Finally the effect of detuning is studied separately.

6.1.2 Complete synchronization in the absence of delay and detuning

It has already been shown numerically that two directly modulated self pulsating laser diodes would be completely synchronized when a unidirectional coupling of proper feedback strength is applied [7]. It is also assumed that there exist no phase mismatch, delay or detuning . ($\phi_1 = \phi_2$; $\tau = 0.$, $\Delta\omega = 0.$). Here, it is found that a feedback strength of -0.0058 is sufficient for complete synchronization of the laser. Fig.6.3 (a) and Fig. 6.3 (b) show the time series plots of the photon densities of drive and resopnse lasers respectively. The time series in Fig.6.3(c) shows the evolution of the synchronization error (Here it is the difference between the photon densities of the lasers) of the two directly modulated lasers which are

started with nearly the same initial conditions. The error vanishes after a few nanoseconds. Fig.6.3(d) gives the plot of the trajectories in the two dimensional space constituted by the photon densities of the drive and response lasers after vanishing the transients. (We shall refer to such diagrams as synchronization plots since they can be used to check whether the coupled systems have synchronized or not). The trajectories of the coupled system converges to the line p_d=p_r showing the complete synchronization. Even though this result has already been proved numerically [7], it has been done in a highly idealized way. That is, the same sinusoidal function has been used as the modulating signals for both the drive and response lasers. To the best of our knowledge, there is no theoretical or experimental evidence for the synchronization of modulated lasers with separate modulating sources. Therefore, it will be interesting to study such a situation in detail.

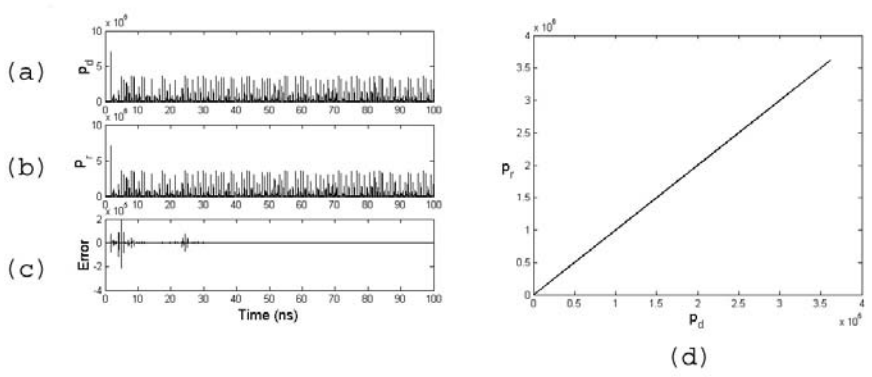

Figure 6.3: Perfect synchronization of coupled lasers when there is no delay or phase mismatches: time series plots of of (a) drive, (b)response and (c) synchronization error. (d) synchronization plot $C = -0.0058$.

6.1.3 Quantitative study of synchronization: similarity function

For a quantitative understanding of the extent of synchronization of lasers, we can use the well known similarity function of the photon densities of the two individual lasers. Actually we are calculating the similarity function of photon density of the drive laser corresponding to a past state and the present photon density of the drive laser since our target is to synchronize the response to the past of the drive. The similarity function of these variables

is defined as

$$S(\tau) = \frac{< (p_d(t-\tau) - p_r(t))^2 >}{[< (p_d(t-\tau))^2 >< (p_r(t))^2 >]^{1/2}} \tag{6.1.11}$$

where τ is the delay and the brackets show the time averaging of the variables. Thus, the similarity function is the mean squared deviation of the variables normalized by the product of their averages. Rosenblum *et.al* have used this function for characterizing the lag synchronization observed in the nonidentical chaotic oscillators coupled bidirectionally [33]. It is important to notice that the problem considered here is very much different. Here the coupling is unidirectional and the delay is arising due to the transit of the output signal. The delay associated with the lag synchronization is a result of symmetry breaking in bidirectional coupling of the chaotic oscillators and its value depends the coupling parameters and the asymmetry of the coupled systems . However, the similarity function can conveniently be used to evaluate the extent of synchronization of these two lasers in the presence of phase mismatch and delay. The function becomes zero if the coupled systems synchronize perfectly. The small values of the function correspond to different types of partial synchronization and relatively high values are obtained for asynchronous states.

6.1.4 Effect of phase mismatch

Since the driving sources are assumed to be independent, their initial phases will also be different. Let us assume now that the frequencies of the signal sources are the same. Then the phase difference of the sources will be constant in time. For simplicity, suppose that no delay is existing between the lasers. The time series plots of the coupled laser system with a very small phase mismatch ($\pi/1000$) is given in Fig.6.4. Fig.6.4(a) and Fig6.4(b) shows the output time series of the drive and response lasers respectively. Fig.6.4(c) gives the synchronization error $E = p_d - p_r$. It is clear from these figures that the coupled system shows only partial synchronization and strong bursts of errors takes places intermittently. These bursts correspond to the intermittent loss of synchronization. Fig6.4(d) shows the synchronization plot of coupled system. Photon density of the drive laser is plotted against the photon density of the response laser. The trajectories in this plot spend most of the time near the line $p_d = p_r$ showing the partial synchronization and they get out from these region and come back after wandering outside the region. These evolutions correspond to the intermittent bursts.

A quantitative understanding of the effect of phase mismatch on synchronization can be obtained by calculating the similarity function for a range of phase differences. Fig.6.5 shows the variation of similarity function with respect to the phase difference. It can be seen that the function vanishes only at zero and at the points which are even integer multiples of π.

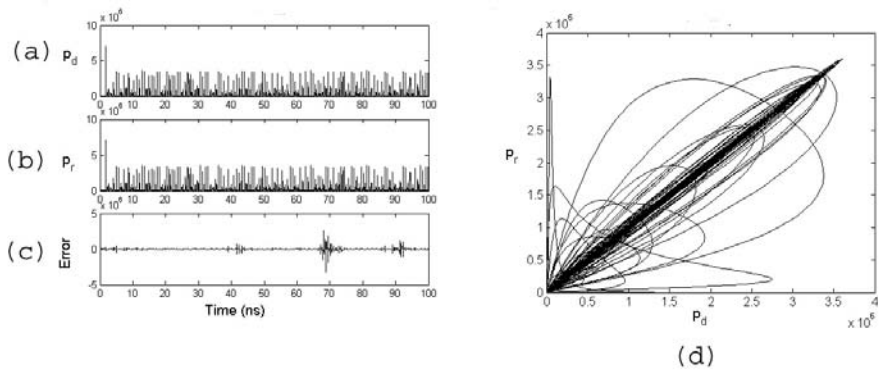

Figure 6.4: Partial synchronization with intermittent bursts : time series plots of (a) drive, (b)response and (c) synchronization error. (d) synchronization plot; $\phi_1 - \phi_2 = \pi/1000$, $\tau = 0.0$, $C = -0.0058$.

Further, the variation of the function around these points is very sharp indicating that the synchronization is highly sensitive to the phase mismatches. The maxima of the similarity function occurs at the odd integer multiples of π. Thus, the maximum asynchronous states possibly belong to these values. The time series plots of the photon densities the drive and response systems are given in Fig.6.6(a) and Fig.6.6(b). Fig.6.6(c) show the time series of the synchronization error. Fig.6.6(d) show the evolution of trajectories in the subspace defined by the variables p_d and p_r. These figures are the clear evidence of highly asynchronous state of the coupled lasers.

6.1.5 Effect of delay

In the previous section, we have shown that the synchronization is destroyed as result of the phase mismatch. Now, we can consider the effect of delay on synchronization. In our model of the coupled system, the delay does not give any extra degree of freedom (as in the delay feedback case). It makes the time scale of the response system shifted by a few nanoseconds. Thus, according to the response system the effective phase of the modulating signal has shifted backwards by $\omega\tau$. Hence, even if there is no phase difference between the modulating sources, the delay causes a virtual phase difference and it can destroy synchronization. In short, the effect of delay is not trivial. But, it is complementary to the effect of initial phase difference. i.e, delay produces the same effect that is produced by

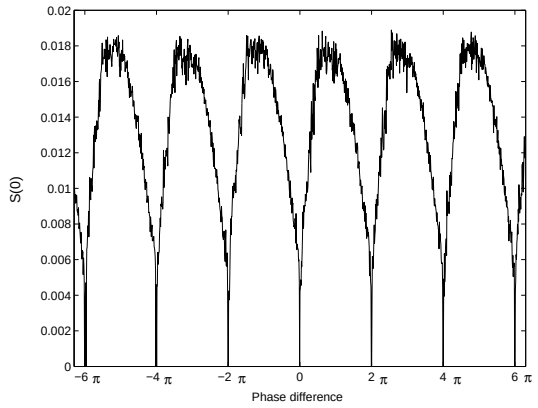

Figure 6.5: Variation of similarity function with respect to the phase difference. $\tau = 0.$, $C = -0.0058$

the phase mismatches in the coupled system and hence the effect of delay can be balanced by the effect of phase difference and viceversa. We have numerically verified the loss of synchronization due to the effect of delay. It is assumed that the initial phase mismatch is zero. Fig.6.7 shows the time series error plot and synchronization plot of the coupled lasers when a delay 0.005ns is present. The partial synchronization with intermittent bursts is obtained in this case also. Thus the coupled laser system shows a high sensitivity to delay. Fig.6.8 show the variation of similarity function $S(\tau)$ with the increase of delay τ. It can be seen in the figure that the complete synchronization is possible only for the values of delay which are equal to the integer multiple of the period of the modulating signal. It is simply because such a delay corresponds to the time required to complete modulation- cycles and hence produces the phase differences which are equal to the even integer multiple of π.

Similarly, the maximum value of similarity function occurs for value of delays which are equal to the odd integer multiples of $T/2$, where $T = 0.8ns$ is the period of modulating sinusoidal signal.

The time series of synchronization error and the synchronization plot of the lasers corresponding to a delay $\tau = 0.4ns$ $(T/2)$ is given in Fig.6.9. The system has a completely asynchronous evolution in this case.

Thus, the effect of the delay on synchronization is not different from the effect of phase mismatches. The modulating phase of the response laser can be carefully adjusted so that the effective phase difference can be made an even multiple of 2π. We will make this idea more clear while dealing with a general model of coupled non-autonomous chaotic systems.

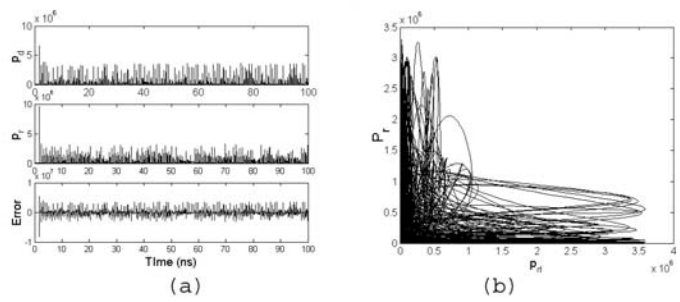

Figure 6.6: Totally asynchronous state of the lasers in the presence of large phase mismatch : time series plots of (a) drive, (b)response and (c) synchronization error. (d) synchronization plot; $\phi_1 - \phi_2 = \pi$, $\tau = 0.0$, $C = -0.0058$.

6.1.6 Effect of frequency detuning

It was assumed while studying the effect of phase mismatches and delay that the frequencies of the modulating signals of the two signals are the same. This assumption was made in almost all the earlier investigation on the synchronization of coupled driven chaotic systems. However, it is impossible to design two exactly identical signal sources. Hence, their frequencies will also be different at least by a small extent. Many theoretical investigations have been done on different practical issues of synchronization such as effect of noise and parameter mismatches. The parameters considered in these works do not include the frequency of the modulating source. Detuning or the mismatch in frequency deserves a special consideration compared to the other parameters. It is shown in the previous section that the synchronization of modulated semiconductor lasers is highly sensitive to the phase difference of the modulating signals. In the presence of frequency detuning, this phase difference will no longer be a constant and it may seriously affect the synchronization. Hence it is necessary to check whether the synchronization is robust to the frequency detuning of the modulating signal sources. The results of numerical simulations show that the synchronization of two remote directly modulated self pulsating lasers is no longer possible with the conventional coupling method.

It is found that the synchronization completely disappears for any non zero detuning. The loss of synchronization is totally independent of the initial phase difference or delay. Fig.6.10 (b)gives the time series-error plot illustrating the effect of a very small detuning ($\Delta\omega = 0.1\%$ of ω). The initial phase difference and delay is supposed to be zero. However

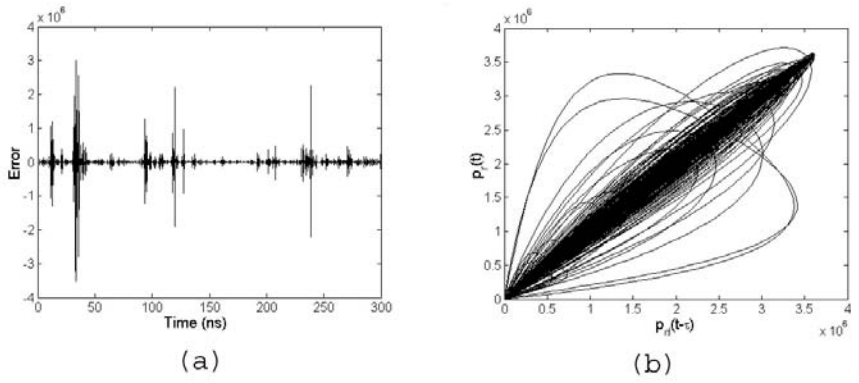

Figure 6.7: Partial synchronization synchronization of coupled lasers with very small channel delay: (a) Time series plot of the synchronization error (b) synchronization plot. $\phi_d = \phi_r$, $\tau = 0.005ns$

the synchronization is lost within a few nanoseconds. If the detuning is too small, synchronization is retained for relatively long time. However synchrony will completely disappear later. There will be short regimes of synchrony which repeats in the equal intervals of time $4\pi/\Delta\omega$. The difference of the modulating signals also is shown in the figure (Fig.6.10(a)). It is interesting to note that the temporal synchrony has been observed where the amplitude of this function vanishes. This can be easily understood since, the phase difference of modulating signals becomes equal to the integer multiples of 2π at these moments.(A detailed analytical explanation will be given in Section 6.2 using a generalized model of coupled no-autonomous systems.) The laser system is completely asynchronous in every other instant. This is obvious from the synchronization plot also. The system is said to be robust to a parameter, only if we get at least an almost synchronized state for very small mismatches of that parameter. However here the system does not give even the partial synchronization in presence of small detuning. This implies that the synchronization of the unidirectionally coupled driven laser systems reported by the earlier numerical investigations is not a physical reality, but it might be a numerical artifact. In the simulation, the frequencies have been assumed to be equal within only a finite precision . Hence, physically there will be a non-zero detuning in the frequencies of the independent signal sources. We can conclude that the synchronization is impossible without a proper phase matching of the signal sources.

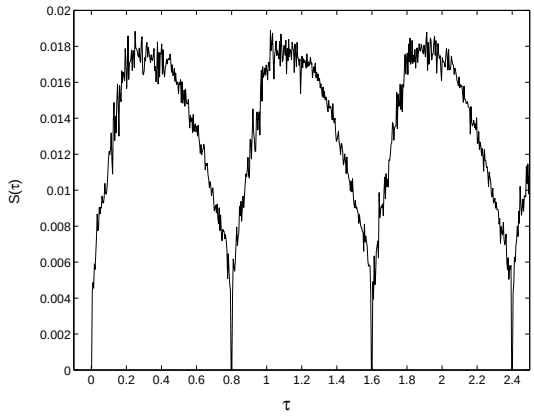

Figure 6.8: Variation of similarity function with respect to the delay. $\phi_d = \phi_r$, $C = -0.0058$

6.2 Analytical study of a general model of unidirectionally coupled remote non-autonomous system

The loss of synchronization shown by the simulation of coupled lasers is due to the independent nature of modulating signals and hence it does not depend on the details of the laser system. We can expect similar effects in all types of driven chaotic systems. Therefore we investigate the mechanism of the loss of synchronization in unidirectionally coupled non autonomous chaotic oscillators [34]. A general model of unidirectionally coupled oscillators is formulated and the necessary conditions for synchronizing due to delay, phase mismatches and frequency detuning are obtained. Such a study gives a clear understanding of the mechanism behind the divergence of trajectories from the synchronized state. Further, the results obtained by this approach is valid for all driven chaotic systems coupled in an adaptive unidirectional way. These results confirm the requirement of a proper phase matching scheme for synchronizing non-autonomous systems.

6.2.1 A general model of driven chaotic oscillators

Chaos in driven nonlinear oscillators is a widely studied topic in non-linear dynamics. Such oscillator belong to the non-autonomous category, i.e., the time appears explicitly in their dynamical equations. Chaos is produced in them as a result of external driving. Sinusoidal modulation is commonly used for this purpose. The phase of the modulating signal provides the extra degree of freedom necessary for generating chaos in most of the driven nonlinear oscillators. Many dissipative nonlinear oscillators show chaotic behavior when modulated

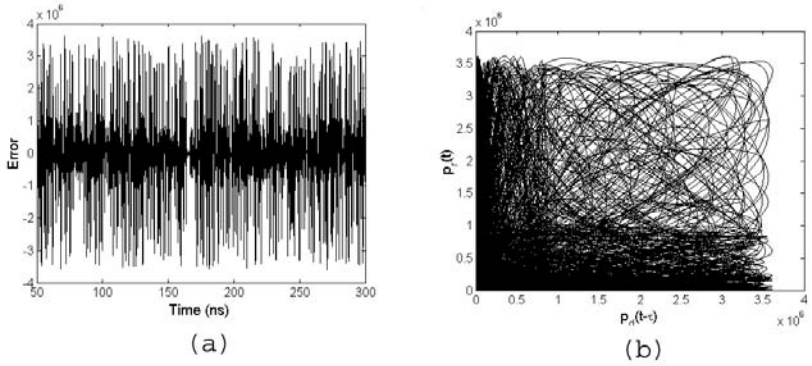

Figure 6.9: Totally asynchronous state of the coupled laser system for large delay: (a) time series plot of the synchronization error (b) synchronization plot. $\phi_d = \phi_r$, $\tau = 0.4ns$

with a sinusoidal signal with appropriate frequency and amplitude. Driven pendulum, Duffing oscillator, diode resonator, Murali- Lakshmanan -Chua (MLC) circuit etc. are the examples of them. Their dynamical equations are relatively simple and have a common structure. Hence, we can study the issues of their synchronization with a general model.

The dynamics of a single dissipative driven nonlinear oscillator can be described by a second order differential equation of the general form,

$$\frac{d^2x}{dt} + \alpha\frac{dx}{dt} + g(x) = Asin(\omega t + \phi), \tag{6.2.1}$$

where x is a state variable of the oscillator, α is the damping coefficient, A is the amplitude of modulation, ω is the angular frequency of modulation and $g(x)$ is a nonlinear function of x. (For example, the nonlinear function of a Duffing oscillator is a cubic function given by $\omega_0^2 x + \beta x^3$, where ω_0 and β are two constants [26]).

For convenience of analytical and numerical studies, the above equations can be written as a set of three first order autonomous differential equations. Two new variables should be defined now. The first one is y, the time derivative of x. The other variable is the phase of the modulating signal given by

$$z = \omega t + \phi, \tag{6.2.2}$$

where ϕ is the initial phase.

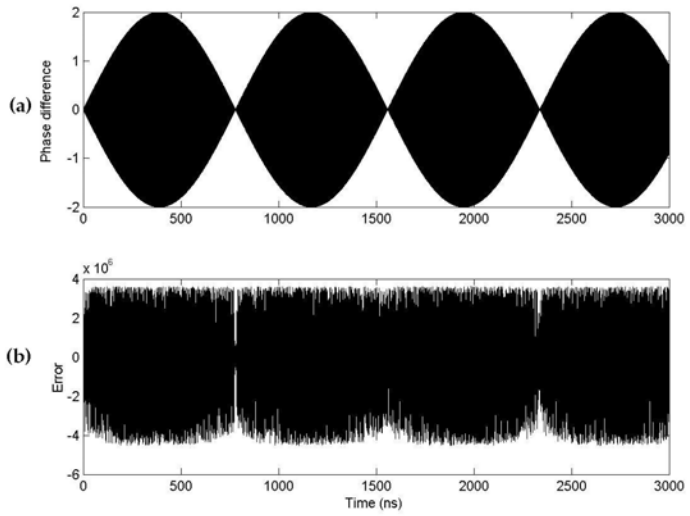

Figure 6.10: Totally asynchronous state of the lasers due to a very small detuning time series plot of (a) difference of modulating signals and (b) synchronization error: $\phi_1 = \phi_2$, $\tau = 0\, C = -0.0058.$, $\Delta\omega = 0.1\%$ of ω

The corresponding first order equations are,

$$\begin{aligned} \frac{dx}{dt} &= y \\ \frac{dy}{dt} &= -\alpha y - g(x) + A\sin(z) \\ \frac{dz}{dt} &= \omega \end{aligned} \tag{6.2.3}$$

The chaotic systems like driven Duffing oscillator [27], diode resonator [28], driven pendulum [29] etc. can be expressed in the general form given by Eq.6.2.1 and the other systems such as Murali-Lakshmanan-Chua (MLC) circuit [30], modulated CO_2 laser [31], directly modulated laser diode [22] are modelled by systems of first order differential equations those are very much similar to Eq.6.2.3. The details of the dynamic equations of these systems are different. However, all of them show chaos for certain ranges of parameter values. Their routes to chaos mainly belong to two universal categories, i.e., the period doubling route and the quasiperiodicity route.

6.2.2 Model of the unidirectionally coupled oscillator with delay

In this section, we consider the problem of two unidirectionally coupled identical chaotic oscillators. The coupling can be achieved by sending a signal proportional to a state variable of the drive system to the response system and applying a feedback proportional to the difference between two systems to the response system. The coupling is said to be diffusive since the feedback signal would vanish if the synchronization is achieved. It is assumed that the systems are separated by some distance and there exists a certain time delay τ which is equal to the time of transit of the signal from transmitter to receiver. A small frequency detuning $\Delta\omega$ is also considered here since it is practically difficult to maintain exactly the same frequency in two independent signal generators. The dynamical equations of the coupled system can be expressed as

Drive:

$$\begin{aligned} \frac{dx_1(t-\tau)}{dt} &= y_1(t-\tau) \\ \frac{dy_1(t-\tau)}{dt} &= -\alpha y_1(t-\tau) - g(x_1(t-\tau)) \\ &\quad + A\sin(z_1(t-\tau)) \\ \frac{dz_1(t-\tau)}{dt} &= \omega \end{aligned} \tag{6.2.4}$$

Response:

$$\begin{aligned} \frac{dx_2(t)}{dt} &= y_2(t) \\ \frac{dy_2(t)}{dt} &= -\alpha y_2(t) - g(x_2(t)) + A\sin(z_2(t)) \\ &\quad + C[x_1(t-\tau) - x_2(t)] \\ \frac{dz_2(t)}{dt} &= \omega + \Delta\omega, \end{aligned} \tag{6.2.5}$$

where C is the coupling strength.

6.2.3 Zero detuning case: The effects of delay and phase mismatches

We first consider the situation where there is no frequency detuning. The oscillators are assumed to be forced by two external modulators having the same signal frequency and amplitude. In spite of the practical difficulty of these situations, this assumption is common in most of the theoretical studies on synchronization of non-autonomous chaotic systems. It is assumed that for $\tau = 0$, there exists a stable synchronized solution of the coupled

system for a particular value of the feedback strength and for a particular set of initial conditions. This has been shown in many of the previous investigations on synchronization of different types of chaotic systems such as electronic analogue circuits [5] and lasers [7]. The existence of synchronization implies that if the two oscillators are started with slightly different initial conditions the trajectories of both systems converges to a single trajectory within a finite time. The synchronization is said to be stable if it is robust to external perturbations. Suppose that we make small perturbations in the directions perpendicular to the synchronization manifold, i.e., the hyper plane in the phase space to which the trajectories of the synchronized system are confined. If the synchronization is stable these perturbations will vanish shortly. Here the synchronization manifold is the hyper plane defined as

$$x_1(t-\tau) = x_2(t),\ y_1(t-\tau) = y_2(t),\ \ z_1(t-\tau) = z_2(t) \tag{6.2.6}$$

The stability of synchronization can be easily examined by defining new variables which correspond to the difference between similar variables of individual oscillators,

$$\begin{aligned} X(t) &= x_1(t-\tau) - x_2(t) \\ Y(t) &= y_1(t-\tau) - y_2(t) \\ Z(t) &= z_1(t-\tau) - z_2(t) \end{aligned} \tag{6.2.7}$$

On subtracting Eq.(6.2.5) from Eq.(6.2.4) we obtain the differential equations governing the dynamics of the difference system defined by Eq.(6.2.7). For zero detuning case, they are given by

$$\begin{aligned} \frac{dX(t)}{dt} &= Y(t) \\ \frac{dY(t)}{dt} &= -\alpha Y(t) - [g(x_1(t-\tau)) - g(x_2(t))] + \\ &\quad A[\sin(z_1(t-\tau)) - \sin(z_2(t))] - CX(t) \\ \frac{dZ(t)}{dt} &= 0 \end{aligned} \tag{6.2.8}$$

We can consider the variables X, Y, and Z as the small deviations from the synchronized state. As a first order approximation we can write the nonlinear term in the equation as

$$\begin{aligned} g(x_1(t-\tau)) - g(x_2(t)) &= g(x_2(t)+X) - g(x_2(t)) \\ &= \frac{\partial g(x_2(t))}{\partial x_2(t)} X(t) \\ &= \frac{\partial g(x_1(t-\tau))}{\partial x_1(t-\tau)} X(t) \\ &= \left(\frac{\partial g}{\partial x}\right)_{x=x(t)} \end{aligned} \tag{6.2.9}$$

These differential equations can be expressed in the matrix form

$$\mathbf{E}(t) = \mathbf{J}\mathbf{E}(t) + \mathbf{K}(t), \tag{6.2.10}$$

where

$$\mathbf{E}(t) = \begin{pmatrix} X(t) \\ Y(t) \\ Z(t) \end{pmatrix} \tag{6.2.11}$$

$$\mathbf{J} = \begin{pmatrix} 0 & 1 & 0 \\ -\frac{\partial g}{\partial x} - c & -\alpha & 0 \\ 0 & 0 & 0 \end{pmatrix} \tag{6.2.12}$$

$$\mathbf{K}(t) = \begin{pmatrix} 0 \\ A[\sin(z_1(t-\tau)) - \sin(z_2(t))] \\ 0 \end{pmatrix} \tag{6.2.13}$$

6.2.4 A familiar example: The coupled driven duffing oscillator

Driven Duffing oscillator is a well known chaotic system which can be represented by the generalized second order differential equation (Eq.6.2.1). The commonly used parameters for simulating Duffing oscillator are $\alpha = 0.2$, $\beta = 1$, $\omega_0^2 = -1$, $\omega = 1$[26]. The time series and power spectra of the driven Duffing oscillator with an amplitude of modulation A=0.3 is given in Fig.6.11. In this section, we study two unidirectionally coupled remote Duffing oscillators having these parameters values. Our aim is to illustrate the analytical results obtained in the previous section numerically. Murali and Lakshmananan have shown that perfect synchronization of two driven Duffing oscillators coupled in a similar way (with a common driving source) is possible [11]. We have investigated the behaviour of coupled Duffing oscillator for a range of values of the coupling strength. It is found that perfect

synchronization is possible if the coupling strength C is chosen to be a value in between the limits $C_{min} = 0.268$ and $C_{max} = 0.536$ (which are the lower and upper limits respectively). Fig.6.12 shows the perfect synchronization of the coupled system with the initial conditions slightly different from the synchronized state. The coupling strength is $C = 0.33$. The convergence to the synchronized state is shown with the time series plot of synchronization error (Fig.6.12(a)). The phase plot of the trajectories (after removing the initial transients) in the (x_1, x_2) subspace is also given in the Fig.6.12(b). The stability of synchronization is

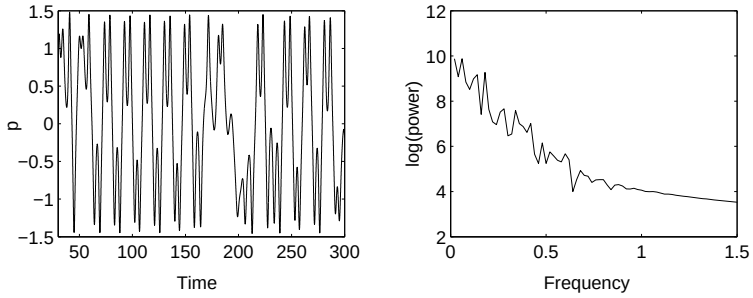

Figure 6.11: Chaotic output of the Duffing oscillator without feedback: (a) time series (b) power spectra. A=0.3.

determined by the matrices **J** and **K** given Eqns. 6.2.12 and 6.2.13. Consider a system such that the second matrix is absent in the equation. The first matrix does not contain any term that depends on the delay. Therefore if stable synchronization exists without time delay, it will be stable even if there is certain delay. This situation is always satisfied in the case of unidirectionally coupled autonomous chaotic systems because, the stability is determined by the eigenvalues of the matrix similar to **J** which is a function of the state variables defined in the synchronization manifold. It is an invariant set of the phase points to which the trajectories of the synchronized system converge, irrespective of the transmission delay. However this invariance does not hold in the case of driven systems because there is now an additional periodic term that affects the stability as given in the Eq.6.2.13. Therefore the stability criteria for the coupling without delay cannot ensure the stability of delay-coupled system

The periodic term in the matrix **K** is given by

$$\begin{aligned} P(t) &= A[\sin(z_1(t-\tau)) - \sin(z_2(t))] \\ &= A[\sin(\omega(t-\tau)+\phi_1) - \sin(\omega t + \phi_2)] \\ &= 2A\cos\left(\omega t + \frac{\phi_1+\phi_2-\omega\tau}{2}\right)\sin\left(\frac{\phi_1-\phi_2-\omega\tau}{2}\right) \end{aligned} \tag{6.2.14}$$

The above expression contains two sinusoidal functions. The first one has the frequency of the modulating sources. The later is a constant term that determines the strength of the sinusoidal perturbation around synchronization manifold. For retaining the stability of the synchronization, this function must vanish.

These condition can be written as

$$\phi_1 - \phi_2 - \omega\tau = 2n\pi, \tag{6.2.15}$$

where n is any integer or zero.

We refer the term $\phi_1 - \phi_2 - \omega\tau$ as the effective phase difference, since it plays the roll of phase difference when there is no delay to the synchronization. Perfect synchronization is possible only if this term is equal to zero or an integer multiple of 2π.

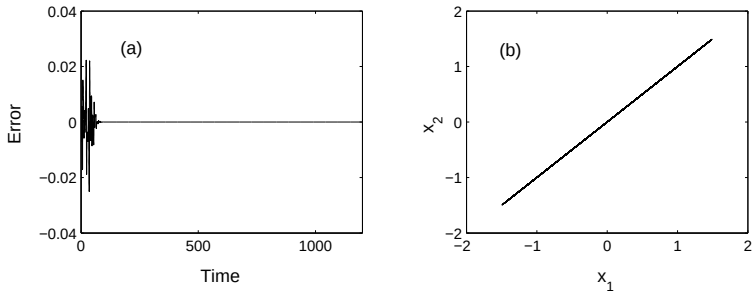

Figure 6.12: Perfect synchronization for no delay or phase mismatch. (a) time series plot of the synchronization error (b) synchronization plot. $C = 0.33$.

If the time delay is absent the above expression reduces to the actual phase difference of modulating signals and the synchronization is possible only if the actual phase difference is zero. If there is a certain amount of delay, the necessary condition for perfect synchronization is that the above expression (in the place of actual phase difference) must be zero or even multiple of π. Hence, we can refer this term as effective phase difference ϕ_{eff}.

The synchronization can be quantitatively described by the similarity function of the coupled system. It determines the strength of synchronization of the coupled system and efficiently characterizes perfectly synchronized, partially synchronized and asynchronous states. It is defined as,

$$S(\tau) = \frac{< (x_1(t-\tau) - x_2(t))^2 >}{[< (x_1(t-\tau))^2 >< (x_2(t))^2 >]^{1/2}} \tag{6.2.16}$$

The function $S(\tau)$ determines the extent of synchronization between any two variables (here x_1 and x_2) of the drive and response systems with a possible time lag τ, which is

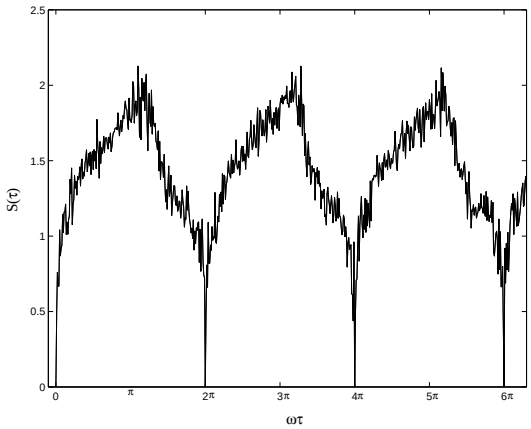

Figure 6.13: Similarity function vs $\omega\tau$; $\phi_1 = \phi_2 = 0$, $C = 0.33$.

the channel delay of the transmitted signal. If $S(\tau) = 0$, the response system is exactly synchronized to the state of the drive system at an earlier time $t - \tau$, which is our target state. For numerical calculation the values of ϕ_1 and ϕ_2 are taken to be zero. The similarity function of the coupled Duffing oscillator is calculated for a range of values of the delays and plotted as a function of $\omega\tau$ (Fig.6.13). It is clear that perfect synchronization occurrs when $\omega\tau$ has the value zero or an integer multiple of 2π as obtained in equation (6.2.15). The variation of similarity function around these points is very rapid showing that synchronization is very much sensitive to delay. Fig.6.14(a) shows the time series of the error function $X(t) = x_1(t-\tau) - x_2(t)$ and the phase space plot of the subspace $(x_1(t-\tau), x_2(t))$ is given in Fig.6.14(b). The delay is $\frac{\pi}{1000}$. There is no perfect synchronization and synchronization is lost intermittently. The synchronization is totally lost for higher delays. The maximum desynchronized state is for $\omega\tau = \pi$. This is because the sinusoidal term given in equation (6.2.14) is maximal for these values. The time series and synchronization plots are given in figure Fig.6.15.

Even though the delay can destroy synchronization, it is still possible to obtain perfect synchronization by carefully adjusting the initial phases of the individual oscillators such that the condition 6.26 is satisfied. Fig.6.16 shows that synchronization is recovered by adjusting ϕ_2 to the value π so that the effective phase difference is still zero. Fig.6.16(a) shows the phases of the modulating signals of drive (solid curve) and response (dashed curve) and Fig.6.16(b) shows the time series plot of the synchronization error. The time variable is normalized by the constant π. Here the response system is synchronized to a state of drive system before a time $\pi/\omega = \pi$ units.

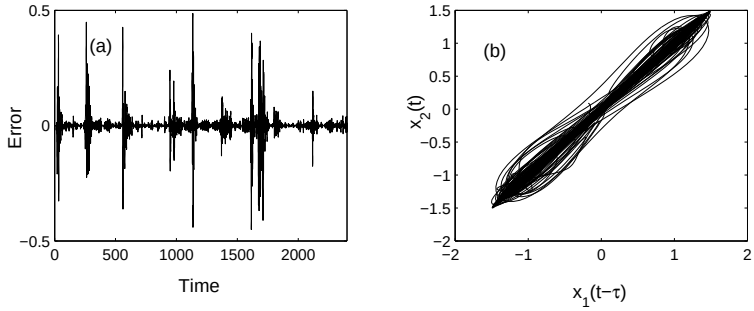

Figure 6.14: Partial synchronization with intermittent bursts: (a) time series of the synchronization error (b)synchronization plot; $\omega\tau = \pi/1000$, $\phi_1 = \phi_2 = 0$, $C = 0.33$.

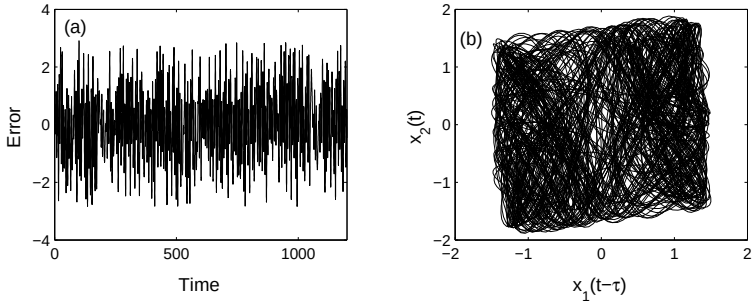

Figure 6.15: Maximum asynchronous state (a) Time series of the synchronization error (b) $x_1(t-\tau)$ vs $x_2(t)$; $\omega\tau = \pi$, $\phi_1 = \phi_2 = 0$, $C = 0.33$.

6.2.5 Effect of frequency detuning

We have shown that the synchronization can be maintained by exactly compensating for the phase difference due to the channel delay by the initial phase differences. However, even a very small phase difference can destroy the synchronization. It was assumed that the frequencies of the modulating sources were exactly the same. Physically this is an ideal case since there will always exist at least a small detuning. If the synchronization is robust to frequency detuning, synchronization must be retained even with small detuning or at least partial synchronization is obtained in the presence of detuning.

If there is a small detuning exists between the frequencies of two modulating sources, the matrix **K** in the equation becomes,

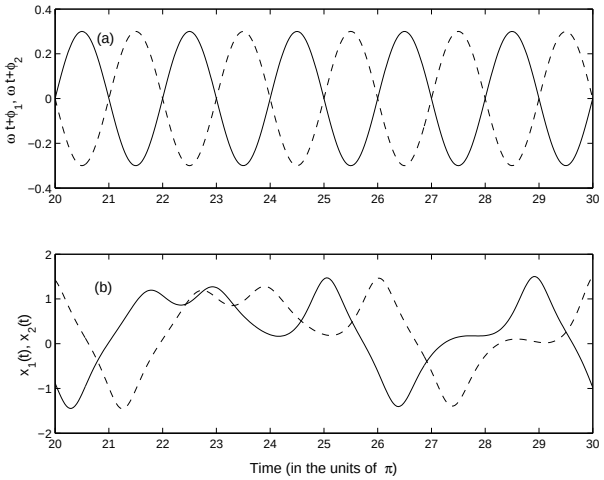

Figure 6.16: Synchronization is achieved by the adjustment of phases of the modulating sources so that the delay effect is exactly compensated by initial phase difference. (a) Time series plots of phases of drive (solid curve) and response (dashed curve) (b) Time series plot of x_1 (solid curve) and x_2 (dashed curve). The response system is lagging by π units of time. $\omega\tau = \pi$, $\phi_1 = \pi$, $\phi_2 = 0, C = 0.33$.

$$\mathbf{K} = \begin{pmatrix} 0 \\ A[\sin(z_1(t-\tau)) - \sin z_2(t)] \\ \Delta\omega \end{pmatrix} \tag{6.2.17}$$

The sinusoidal function is given by,

$$\begin{aligned} P(t) &= A[\sin(\omega(t-\tau)+\phi_1) - \sin((\omega+\Delta\omega)t+\phi_2)] \\ &= 2A\cos\left((\omega+\frac{\Delta\omega}{2})t + \frac{\phi_1+\phi_2-\omega\tau}{2}\right) \\ &\quad \times \sin\left((\frac{\Delta\omega}{2})t + \frac{\phi_1-\phi_2-\omega\tau}{2}\right) \end{aligned} \tag{6.2.18}$$

This function contains two sinusoidal functions varying with two frequencies, one is the mean frequency of two modulating signals and the other is the half of the detuning. Eq.6.2.14 is a special case of Eq.6.2.18 with $\Delta\omega = 0$. The periodic perturbation around the synchronization manifold will not vanish except in this case. Suppose we adjust the phases according to Eq. 6.2.15, the second term will be zero for $t = 0$. However, as time goes on the value of this term will increase and the synchronization will be lost. However small be

the detuning, the synchronization will be destroyed in a finite time. Only the required time depends on the magnitude of the detuning. As a consequence of the above facts practically there will be no synchronization. We confirm these by numerical simulation.

The time evolution of the coupled Duffing oscillator with a detuning of 0.1% ($\frac{1}{1000}$) of the modulation frequency) is given in Fig.6.17. The function $P(t)$ in Eq.6.2.18 is given on the top (Fig.6.17(a)) and the synchronization error at the bottom (Fig.6.17(b)). Initially the phase was adjusted and the synchronization is lost after a few units of time. The periodic function $P(t)$ vanishes at the intervals separated by a period equal to 2000π as given by Eq.6.2.18. (It should be noted that the period of the above function is equal to the duration of two 'lobes' in Fig.6.17(b) because the sine function approaches zero twice in a cycle) The synchronization error becomes smaller in those instants. However the system is perfectly asynchronous except at these points. Thus, synchronization of the unidirectionally coupled

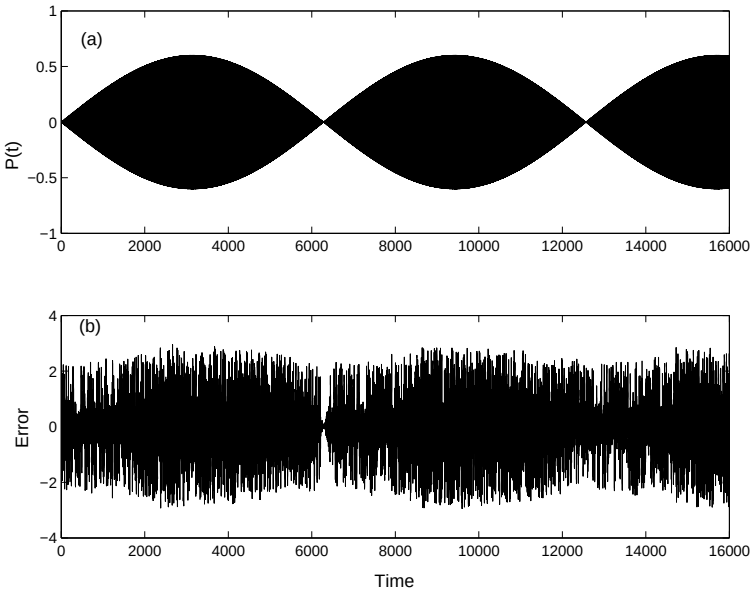

Figure 6.17: Asynchronous behaviour of the system due to small detuning: Time series plots of (a) the periodic term defined in Eq.6.2.18 (b) synchronization error; $\omega\tau = \pi$, $\phi_1 = \pi$, $\phi_2 = 0, C = 0.33$.

system represented by the general model is possible only if the frequencies of the modulating signals are exactly the same. The behavior of the system under such an ideal situation can be simulated numerically by assuming that the frequencies are equal. However, physically

there will be a nonzero detuning and the synchronization is definitely impossible by the coupling method described here. It is well evident from the analytical results that the loss of synchronization does not depend on the details of the specific chaotic system. Hence, the issues discussed here is valid for all type of unidirectionally coupled non- autonomous chaotic systems including lasers and electronic circuits.

6.3 Conclusion

In this chapter, we have shown that two remote unidirectionally coupled driven nonlinear oscillators cannot be synchronized by the conventional coupling scheme. Frequency detuning is found to be the most serious problem in synchronizing them. The results presented in the last section is valid for all types of non-autonomous systems such as electronic oscillators and driven laser systems. Therefore finite dimensional autonomous systems and delay feedback systems (infinite dimensional systems with finite dimensional attractors) are more preferable in generating chaos for secure communication purposes when compared to the driven system. However, the results presented here does not imply that the synchronization of driven chaotic systems is impossible by any means. It is possible to synchronize the coupled system if the phases of the signal sources of the drive and response systems are exactly matched by certain techniques. Hence, one of the challenges in the synchronization of driven systems is the development of an efficient phase-matching scheme which works in the high frequency domain also.

Bibliography

[1] T. Yamada and H. Fujisaka, Prog. Theor. Phys. **70** (1983) 1240

[2] V. S. Afraimovich, N. N. Verichev, and M. I. Rabinovich, Inv. VUZ Rasiofiz. RPQAEC **29** (1986) 795

[3] L. M. Pecora and T. L. Carroll, Phys. Rev. Lett. **64** (1990) 821

[4] T. L. Caroll and L. M. Pecora, IEEE Trans. Circuits. Syst. **38** (1991) 453

[5] Carroll T. L. and Pecora L. M., IEEE Trans. Circuits. Syst. II **40** (1995) 646

[6] K. Murali and M. Lakshmanan, Phys. Rev. E **49** (1994) 4882

[7] C. Juang, T. M. Huang, J. Juang and W. W. Lin, IEEE J. Quant. Electron. **36** (2000) 300

[8] S. Rajesh and V. M. Nandakumaran, *Synchronization of chaos in unidirectionally coupled modulated self pulsating semiconductor lasers: effects of delay and detuning*, Proc. of the international conference, Perspectives in Nonlinear Dynamics (PNLD 2004), IIT Madras Chennai, July 2004

[9] R. Roy and K. S. Thornburg Jr., Phys. Rev. Lett. **72** (1994) 2009

[10] V. Bindu and V. M. Nandakumaran, Phys. Lett. A **227** (2000) 345

[11] K. Murali and M. Lakshmanan Phys. Rev. E **48** (1993) 1624

[12] T. Yang, C. W. Wu, and L. O. Chua, IEEE Trans. Circuits. Syst. I **44** (1997) 469

[13] K. M. Cuomo and A. V. Oppenheim, Phys. Rev. Lett. **71** (1993) 65

[14] K. M. Cuomo, A. V. Oppenheim, and S. H. Strogatz IEEE Trans. Circuits. Syst. II **40**(1993) 626

[15] Lj. Kocarev, K. S. Halle, K. Eckert, L. O. Chua and U. Parlitz 1992 Int. J. Bifurcation Chaos **2** 709

[16] P. Chelka IEEE Trans. Circuits. Syst. I **40** (1995) 455

[17] C. R. Mirasso, P. Colet and P. Garcia-Fernandez IEEE Photon. Technol. Lett. **8** (1996) 299

[18] G. D. VanWiggeren and R. Roy Phys. Rev. Lett. **81** (1998) 3547

[19] H. F. Chen and J. M. Liu. IEEE J. Quant. Electron. **36** (2000) 27

[20] A. Uchida , M. Shinozuka , T. Ogawa , and F. Kannari Opt. Lett. **24** (1999) 890

[21] Y. Takiguchi, H. Fujino , and J. Ohtsubo, Opt. Lett. **24** (1999) 1570

[22] H.G. Winful, Y.C. Chen, J.M, Liu, Appl. Phys. Lett. **48** (1986) 161

[23] M. Yamada, IEEE J. Quantum Electron. **29** (1330) 1993

[24] H. D. I. Abarbanel, M. B. Kennel, L. Illing, S. Tang, H. F. Chen, and J. M. Liu IEEE Trans. Circuits. Syst. I **48** (2001) 1475

[25] H. W. Yin, J. H. Dai and H. J. Zhang, Phys. Rev. E **58** (1998) 5683

[26] M. Lakshmanan and K. Murali *Chaos in Nonlinear Oscillators:Controlling and Synchronization* World Scientific, Singapore (1996)

[27] J. Guckenheimer and P. Holmes *Nonlinear Oscillations, Dynamical Systems and Bifurcation of Vector Fields* Springer- Verlag, New York (1983)

[28] Z. Su, R. W. Rollins, E. R. Hunt, Phys. Rev. A **40** (1989) 2698

[29] D. D'Humieres, D. Beasley, B. A. Huberman and A. Libchaber, Phys. Rev. A **26** (1982) 3483

[30] K. Murali, M. Lakshmanan and L. O. Chua, (1994) IEEE Trans. Circuits. Syst. I **41** (1994) 462

[31] F. T. Arecchi, R. Meucci, G. Puccioni and J. Tredicce, Phys. Rev. Lett. **49** (1982) 1217

[32] H. G. Winful, Y. C. Chen, and J. M. Liu, Appl. Phys. Lett. **48** (1986) 616

[33] M. G. Rosenblum, A. S. Pikovsky and J. Kurths, Phys. Rev. Lett. **78** (1997) 4193

[34] V M Nandakumaran and S Rajesh , *Synchronization of non autonomous systems: effects of delay and detuning*, Proc. of the international conference, Perspectives in Nonlinear Dynamics (PNLD 2004), IIT Madras Chennai, July 2004

Chapter 7

Conclusions and future prospects

7.1 Summary

Nonlinear phenomena such as period doubling, chaos, quasiperiodicity, bistability, and the formation of double peaked pulses are common in directly modulated semiconductor lasers. Since semiconductor lasers have many practical applications in the fields such as high speed optical communications and data processing, the control of these effects is important in photonics and related areas.

We have numerically demonstrated two different routes to chaos followed by two types of directly modulated semiconductor lasers, i.e., the period doubling route in InGaAsP laser diodes and quasiperiodicity route in AlGaAs self pulsating semiconductor lasers.

The possible methods for controlling chaos in directly modulated InGaAsP semiconductor lasers have been considered. Due to the practical considerations, delay feedback methods have been selected for the investigations. The effects of two different delayed optoelectronic feedback schemes on the laser have been numerically studied. The control scheme based on the Pyragas method has been found to be successful in controlling chaos in the laser diode. However, it cannot suppress the double peak structure. Directly delayed optoelectronic feedback with proper delay and strength is shown to be efficient in suppressing chaos, period doubling and the double peaks structure of the pulses.

The effects of these delay feedback techniques on the directly modulated self pulsating semiconductor lasers have also been studied. Such lasers commonly follow the quasiperiodicity route to chaos. The delayed optoelectronic feedback based on Pyragas method has been shown to be inefficient in controlling chaos in self pulsating lasers. The direct delayed optoelectronic feedback method has been found to be successful in suppressing both chaos and quasiperiodicity in such lasers.

The hystereris effect and bistability observed in the directly modulated InGaAsP lasers

have been demonstrated numerically. The effect of a direct delayed optoelectronic feedback on the bistable laser has been investigated numerically. It is found that such a feedback can be used to eliminate hysteresis and bistability in directly modulated laser diodes.

The synchronization of two unidirectionally coupled directly modulated self pulsating laser has been studied. The lasers are assumed to be separated by certain distance and the effect of phase mismatches and delay has been investigated numerically and shown that such effects cause loss of synchronization. The synchronization can be retained by exactly compensating for these effects by each other. However, in the presence of detuning, synchronization loses completely. We have verified these results for a general model of two remote unidirectionally coupled chaotic oscillators. The results show that the synchronization of remote non-autonomous chaotic system is practically impossible with conventional coupling method

7.2 Future prospects

The directly modulated semiconductor lasers with delayed feedback belong to the category of the infinite dimensional systems since their dynamics is described by the delay differential equations. In addition to showing the suppression of chaos and other instabilities, our numerical investigations done on these delay systems have revealed many interesting dynamical features such as different kinds of reverse bifurcations. It is useful to do analytical studies of these problems for determining the stability of periodic orbits of the controlled lasers. In general, chaotic systems cannot be solved analytically. However, analytical approaches can determine the stability of periodic states and different bifurcation phenomena.

The random fluctuations are known to be very much significant in the dynamics of chaotic systems. Hence it is useful study the effects of noise in the chaotic and periodic states of the laser system with delay feedback since different types of noise sources are associated with the laser diodes. Such investigations may give a more realistic picture of the dynamics of the laser system.

The delay feedback method investigated here is relatively simple and easy to implement experimentally. The main components in the necessary infrastructure are the high speed modulating sources, photodiodes, high-bandwidth digital oscilloscopes and spectrum analyzers. The experimental realization of the control schemes may have considerable importance in laser physics and photonics.

The difficulty of controlling chaos in modulated self pulsating laser diodes show the necessity of a clear understanding of the structure and divergence properties of the unstable periodic orbits (UPO) existing in the phase space of lasers. The studies in this direction

are useful for designing control setups for stabilizing the UPOs of lasers.

It is useful to study analytically the mechanism behind the suppression of bistability in directly modulated lasers when a very weak delayed negative feedback is applied. The role of the delay in the elimination of bistability is also a topic of further investigations.

The synchronization of chaos in remote modulated driven laser diodes is possible only if the phases of the independent driving sources are matched properly. Thus the development of a phase matching technique working in the GHz frequency domain is an important task in the implementation of chaotic secure communication schemes based on modulated semiconductor lasers. The practical issues such as security, noise-tolerance and bit rate of transmission can also be studied both theoretically and experimentally.